Highway Development Decision-Making Under Uncertainty: Analysis, Critique and Advancement

by

Mayar El-Khatib

A thesis
presented to the University of Waterloo
in fulfillment of the
thesis requirement for the degree of
Master of Mathematics
in
Statistics and Civil Engineering

Waterloo, Ontario, Canada, 2010

Author's Declaration

I hereby declare that I am the sole author of this thesis. This is a true copy of the thesis, including any required final revisions, as accepted by my examiners.

I understand that my thesis may be made electronically available to the public.

Abstract

While decision-making under uncertainty is a major universal problem, its implications in the field of transportation systems are especially enormous; where the benefits of right decisions are tremendous, the consequences of wrong ones are potentially disastrous.

In the realm of highway systems, decisions related to the highway configuration (number of lanes, right of way, etc.) need to incorporate both the traffic demand and land price uncertainties. In the literature, these uncertainties have generally been modeled using the Geometric Brownian Motion (GBM) process, which has been used extensively in modeling many other real life phenomena. But few scholars, including those who used the GBM in highway configuration decisions, have offered any rigorous justification for the use of this model.

This thesis attempts to offer a detailed analysis of various aspects of transportation systems in relation to decision-making. It reveals some general insights as well as a new concept that extends the notion of opportunity cost to situations where wrong decisions could be made. Claiming deficiency of the GBM model, it also introduces a new formulation that utilizes a large and flexible parametric family of jump models (i.e., Lévy processes). To validate this claim, data related to traffic demand and land prices were collected and analyzed to reveal that their distributions, heavy-tailed and asymmetric, do not match well with the GBM model. As a remedy, this research used the Merton, Kou, and negative inverse Gaussian Lévy processes as possible alternatives.

Though the results show indifference in relation to final decisions among the models, mathematically, they improve the precision of uncertainty models and the decision-making process. This furthers the quest for optimality in highway projects and beyond.

Acknowledgment

"In the Name of Allah, The Beneficent, Most Merciful. All Praise is due to Allah, The Rabb (Lord and Master, Ruler and Sovereign, Facilitator of development of inherent aptitudes, Sustainer, Provider, Cherisher, Nourisher, and Guardian) of all the worlds. The Beneficent, Most Merciful, The Ultimate Authority on the Day of Requital. Thee alone do we worship. And Thee Alone (O Allah), Do We Beseech For Help. Guide us (on to) the Right Path, the path of those on whom You have bestowed Your favor. (Let us) not (be) of those who incur Your Wrath, nor of those who go astray."[1]

First and last and everywhere else in between lies a testimony of my thankfulness and gratitude to the Almighty Allah (SWT)[2], the Creator and Sustainer of the whole universe, the Most Beneficent and the Most Merciful, for His guidance and countless bounties, especially for granting me knowledge, patience, perseverance and health to accomplish this research and for destining my life to encompass the following individuals to whom I am eternally grateful; "[h]e [or she] *who does not thank people does not thank Allah.*"[3]

I would like to thank my supervisors, Dr. Adam Kolkiewicz (Statistics and Actuarial Science) and Dr. Tarek Hegazi (Civil Engineering), for proposing the topic area of my joint degree thesis and for their unending understanding, patience, and support. I offer my special appreciation to Dr. Kolkiewicz for offering his guidance, for sharing his knowledge, and for being constantly available.

Thanks also to the following individuals who assisted in the process of data collection: from the Ontario Ministry of Government Services, Randy Reese (Manager of Business Improvements), and from the different regional branches of the Ontario Ministry of Transportation, Les Dzbik (Head of Traffic Planning and Information Services Section), Cheryl Ahmed (Head of Property Section), and Susan McKay (Land Management and Marketing Supervisor).

In the preparation of this thesis, thanks are also due to Sue Weare and Rashid Ahmed for their help with editing. Particular acknowledgment is owed to Sue for enduring the agony of going through this thesis word for word several times.

---

[1] Translation of Chapter 1 of The Quran (The Opening)
http://www.muslimbridges.org/content/view/565/84/

[2] Abbreviation to "Subhanahu wa-ta'ala": an Islamic Arabic phrase meaning glorious and exalted is He.

[3] Authentic quote by Prophet Mohammad (blessing and peace be upon him) - related by Abu Dawood (no. 4177), at-Tirmidhee (no. 1877) and declared authentic by Imam al-Albanee in as-Saheehah (no. 417)

Dedication

To My Parents

Faisal and Inayah

And

My Siblings

Hazar, Afnan, Rawan, Alia, and Ahmed

To Canada

And

To Palestine

Table of Contents

List of Figures

List of Tables

1 Introduction

Decision-making under uncertainty in highway systems is a non-trivial task that can yield great benefits with optimal decisions, but also potentially large and multifaceted cost implications with wrong ones. The reasons behind this, many of which may apply to other transportation systems or other public projects, are related to highway systems' massive size, cost and sphere of impact. As a result, the impact of decisions made on these systems have a long duration and are semi-irreversible. Further, decision optimality is a very challenging endeavor due to the overall system complexity and modeling inadequacies.

1.1 Research Motivation

The difficulty in realizing optimality in decision-making under uncertainty in transportation systems stems from the imbedded multi-dimensional system complexities. Analyzing and addressing these complexities, which constitute the cost of decisions' optimality, are significantly motivating this work. However, the bulk of this work is motivated by advancing the shortcomings of one of these complexities: the mathematical modeling of uncertainties.

1.1.1 A Context Worthy of a Thorough Analysis

In the quest for decision optimality it is crucial to rigorously analyze the intricate cost-benefit aspects of transportation projects. By studying the characteristics of transportation systems, as well as locating the potential optimality loci and subsequently advancing them, the ultimate goal of establishing a global stochastic model framework for realizing decision optimality in highway systems can be advanced.

To tackle the complexities involved in the decision-making process, a comprehensive global analysis of the various aspects of transportation systems and the decision-making under uncertainty process in highway systems needs to be undertaken.

1.1.2 Unquantifiable Assumptions in Uncertainty Modeling

These complexities essentially stem from factors that include the large number of decisions and uncertainties, their correlations, as well as the identification of the optimization approach and the modeling of the uncertainties.

There exist many optimization techniques in literature, but one technique that does not neglect the value of managerial flexibility is the real options technique. An application of this valuation technique in the realm of decision-making in highway development projects is presented in Zhao et al. (2004).

The real options technique is derived from financial options. For a specific price, a financial option gives its holder the right, but not the obligation, to purchase (call option) or sell (put option) an underlying asset for a specific price at a specific time (European option) or during a specific period (American option). The prices of these options, determined using Black-Scholes formulas for pricing European call and put options, are unique values that would prevent investors from making riskless profits (i.e., arbitrage-free prices) by simultaneously buying or selling the options and their underlying assets in certain combinations. In determining the arbitrage-free option price, the Black-Scholes formulas assume that the underlying asset (stock price) follows the lognormal Geometric Brownian Motion (GBM) process. This is a widely accepted model that Hull (2000), a

2

well-recognized authority in the field of financial derivatives industry, refers to as "the model for stock prices" (as cited in Marathe & Ryan, 2005).

However, in contrast to those of financial options, the underlying assets in real options refer to real quantities; they could be natural resource prices or growth in demand for products or services. And while the GBM process is widely accepted as a valid model for the growth of a stock price over time, it does not necessarily apply to all cases involving real assets such as physical infrastructure projects (highways). Regardless, as Marathe and Ryan (2005) explain, many GBM models have been used in research related to physical assets. Likewise, in the real options application of Zhao et al. (2004), the two uncertainties related to traffic demand and land price are unjustifiably assumed to follow the GBM model.

Like all other models, the GBM process does not come without assumptions, and unless at least some of these assumptions are empirically satisfied, this model choice cannot be mathematically justified on any level beyond that of mere convenience. The seemingly automatic adoption of the GBM model gives rise to numerous questions. What if the uncertainties that are assumed to follow the GBM dynamics fail the normality criterion? What if their distributions also possess heavy tails and have various patterns? If so, would there be alternatives to the GBM model? What about jump processes? Would they be mathematically justified? How about qualitatively? Are these jump processes flexible enough to cope with possibly different distributional patterns? These are some of the kinds of questions that may arise from works like that of Zhao et al. (2004). The authors of this paper offer a multistage real options stochastic model for decision-making in highway systems that incorporates the GBM process in modeling the evolution of two

3

uncertainties (traffic demand and land price), but also fail to offer grounds for this model choice.

In this literature, we investigate the queries posed earlier with reference to Zhao et al. (2004) by analyzing data collected in Canada. The analysis shows that the GBM notion is not supported, at least not from the normality of the log-ratios perspective.

1.2 Research Objectives and Scope

The ultimate objective of this work is to advance the quest for optimality in decision-making under uncertainty in highway development projects. Where the primary contribution of this work occurs mathematically at a micro level, a macro analysis is still offered to better understand the problem, establish value, and place the significance of the mathematical treatment offered in its proper relative dimension, thus aiding and motivating further research on this topic. Consequently, the macro expedition also reveals further insights and contributions on different levels. More specifically, below is a detailed list of the objectives of this study:

1. Conduct a comprehensive global analysis on decision-making in highway systems by:

    a. highlighting the value of right actions and the costs of making wrong decisions within the transportation systems domain;

    b. expanding, within the above framework of highlighting the cost of wrong decisions, the concepts of economic profit and opportunity cost to include potential wrong decisions.

    c. analyzing the challenges involved in the development of optimal decision-making systems with respect to the scope and relative importance of the decisions, the uncertainty factors, and the optimality techniques, as well as the accuracy of the uncertainty models.

2. Study, summarize, and critique the multi-stage stochastic model treatment of Zhao et al. (2004) in the context of the findings of the aforementioned analysis, and define accordingly the scope of the mathematical analysis portion of this research.

3. Verify the mathematical assumptions of Zhao et al. (2004).

a. Conduct data collection for the traffic demand and land acquisition price uncertainty factors.

b. Explore areas where data for traffic demand and land acquisition could be obtained and comment on data availability and its mathematical consequences.

c. Verify the inadequacy of the current GBM assumption.

d. Validate the presence of jumps in the uncertainty processes.

4. Propose a rich and flexible alternative class of models (Lévy jump processes) to the GBM model in capturing the dynamics of the continuous-time uncertainties.

5. Provide a mathematical review of the GBM model, Lévy processes in general, and particularly Merton, Kou, and negative inverse Gaussian models, in addition to a review of the parameter calibration method.

6. Develop a decision-making algorithm similar to that of Zhao et al. (2004) and identify areas of similarity and disparity.

7. Develop codes to generate the appropriate random processes applicable to the different models and integrate them, individually, into the decision-making algorithm.

8. Calibrate and implement all four models

In essence, the research claims on statistical and factual grounds that there exist other feasible alternatives to the GBM process that can be more accurate representations for these uncertainty processes. The research proposes Lévy processes as an alternative class of model that is capable of generating more accurate distributions. The research numerically validates this claim by implementing three models of Lévy processes: two from the finite activity subclass (Merton and Kou models) and one from the infinite

activity subclass (negative inverse Gaussian model). This research applies to any decision-making problem that involves multiple uncertainty factors, which can be represented in continuous time using GBM processes.

1.3 Research Methodology

The qualitative problem analysis portion of this work was supported by research from sources including journal papers, books, and reports, as well as public and private sector organization's web pages and online materials; references to all of which are provided in the references section of this thesis. The conceptual and mathematical extension of the opportunity cost notion was the author's own novel work.

In light of this analysis, we studied, summarized, and critiqued the model treatment of Zhao et al. (2004). To verify the inadequacy of the GBM model used in Zhao et al. (2004) and to investigate the appropriateness of jump processes as alternatives, data needed to be collected. Research was conducted in order to obtain data regarding land price for Canada and traffic demand for Ontario.

Generally speaking, we found that traffic demand data is readily available but not in sufficiently large numbers, given the yearly time scale adopted in the decision-making algorithm. On the other hand, the land related statistics, unlike those of traffic volumes, are outright challenging to collect. The full outcome of the data collection effort, including the data used herein, was presented and referenced.

To investigate the validity of the GBM model, we verified, using the available data, the normality of the log ratios of the annual traffic volume and land price data by constructing Quantile Quantile Plots (Q-Q plots) for samples of both uncertainties.

As for jumps, mathematically speaking, the heaviness of the uncertainty distributions tails was used as an indicator to the presence of jumps. This check was performed by

calculating the probabilities, based on the normal law, of the maximum and minimum changes in the values of the observed uncertainties over the study period. As a measure of the very likelihood of jumps, we considered an uncertainty increment occurring with a probability of as little as 1% to represent a jump.

Given the results of the above tests, we proposed three Lévy processes, two from the finite activity subclass (Merton and Kou models) and one from the infinite activity subclass (negative inverse Gaussian model) as possible alternatives to the GBM model.

For comparability, the three proposed model parameters were calibrated, as opposed to being estimated, due to scarcity of data. The calibration process, which was performed based on the GBM model using the method of moments, was outlined for each model.

With some exceptions that were also be highlighted, a decision-making algorithm similar to that of Zhao et al. (2004) was developed to test the models from a case study used in Zhao et al. (2004) in selecting design alternative. The decision-making system was developed in Matlab code and simulations with 10,000 iterations were performed for each model. For verification purposes, a detailed simple illustrative example of the core algorithm regression calculations as well as a full sample output were included in the text and the appendices, respectively.

1.4   Thesis Organization

The entire qualitative analysis portion of this thesis occupies most of the contents of Chapter 2, where in subsection 2.2, we shed some light on the infrastructure and the complexity of transportation systems. The development and maintenance of these transportation systems have certain constraints that require important decisions to be made on a continuous basis over the lifecycle of these systems. These constraints are presented in subsection 2.3. The complexities of the decision-making process is elaborated in subsection 2.4, where we discuss the cost of wrong decisions in the first sub-subsection, the cost of inaction in the second, and the price of making the right decisions in the third. The extension of the opportunity cost concept is hosted within the first part of the first sub-section. In subsections 2.5 and 2.6, we introduce the concept of real options and jump processes. Finally, we summarize our findings in Section 2.7.

In the first section of Chapter 3, we present the assumptions, the case study, and the solution algorithm of Zhao et al. (2004), as we adopt the same settings and a similar algorithm in our model implementations in Chapter 6. In the next section, we list some of the limitations of Zhao et al. (2004) in light of the findings of Chapter 2. Finally, we define the scope of our mathematical contribution in the third section.

Zhao et al. (2004) assumes that the highway traffic volume and the land price uncertainties follow the geometric Brownian motion model. In order to test this assumption, one needs to collect real data on traffic demand and land acquisition costs.

In Section 4.1, we look into means of collecting such data and in Section 4.2 we analyze the collected data. In subsection 4.2.1, we test the validity of this statistical assumption and draw some general conclusions on the distributional properties of the collected data. This leads to subsection 4.2.2, where we investigate the presence of jumps in the empirical processes.

In chapter 5, we provide, using modern probability theory, a detailed theoretical background on Lévy processes and the proposed three of its subclass models: Merton, Kou, and NIG. Also included is an outline of the Rydberg Algorithm used in simulating the NIG process and results of a test implementation performed to verify the accuracy of this algorithm. The above, which occupies several sections, is preceded by a recap of the mathematics of the uncertainties used in Zhao et al. (2004) (Section 5.1) and a brief derivation of the geometric Brownian motion model (Section 5.2), as it will be used later in the simulation and in the calibration of the proposed models.

Finally, given that the numeric calibration method in Matlab requires initial parameter guesses, the chapter concludes with outlines of the methods used herein to arrive at these initial estimates for each of the individual models.

Chapter 6 is where model implementation, testing, and analysis of the core and proposed models take place. In the first section, we outline our version of the decision-making system algorithm by highlighting its key distinguishing features. Subsequently, in Section 6.2, we present the case study on which the testing of the models is implemented. To facilitate model comparability and establish a baseline, we calculate the moments of the base GBM model in Section 6.3, where we further show a sample detailed decision system output and reveal the simulation results of the GBM model as a baseline. Sections

6.4 through 6.6 unveil the calibration calculations and the simulation results for the proposed Merton, Kou, and NIG models. Analysis and discussion follow in Section 6.7 and final conclusions are communicated in Section 6.8.

Chapter 7 is dedicated to summarizing the thesis in its entirety.

2 Background, Analysis, and Literature Review

2.1 Introduction

Transportation is essential to the personal and to the social development of people; it is necessary to the linkage and the advancement of communities, and it is vital to the growth of the local, the regional and the overall national and global economies. The necessity of developing an efficient transportation system stems from the very basic need for people to move and travel, and the need for businesses to deliver services and to transport labor, materials, equipments, livestock, crops, and other goods.

To meet these needs, several complex transportation systems of different types and infrastructures were developed over time. In subsection 2.2, we shed some light on the infrastructure and the complexity of these systems, putting the highway system network in its relative magnitude on the map of transportation systems.

In the process of developing and maintaining these transportation systems, it is crucial for the transportation authorities to ensure that certain constraints are met. These constraints are presented in subsection 2.3.

The process of developing and maintaining transportation systems with the set of criteria listed in subsection 2.3 requires important decisions to be made on a continuous basis over the lifecycle of these transportation systems. The complexity of this decision-making process is geared by certain characteristic factors of the transportation systems that we elaborate on in subsection 2.4. Listing some relevant factors and challenges, we

discuss the cost of wrong decisions in the first sub-subsection, the cost of inaction in the second, and in the third, the price of making the right decisions.

As a technique to attaining optimality, in subsection 2.5 we introduce the concept of real options and in subsection 2.6, we present jump processes as a means of improving the uncertainty models. Finally, paving the way to the mathematical treatment, in section 2.7 we summarize our findings in chapter 2.

2.2 *Highway System in Context: Complexity and Relative Importance*

Transportation systems can be broadly classified into land, marine, and air transportation systems. However, the land transportation system can be regarded as the core of all transportation systems. It not only provides the medium through which most of the transportation traffic is served, but it also forms a necessary complementary system to the marine and air transportation systems that generates and terminates traffic from their origins to their final destinations.

Unlike the other two system infrastructures, the land transportation infrastructure is not focused only at the endpoints (airports and seaports) but rather it lays its infrastructure along the entire trip paths. Serving large areas of varying mesh densities of origin-destination links and/or stretching over vast distances and possibly across multitudes of terrains as well as other material and space restrictions, the land transportation system, with all its subsystem networks, is significantly more complex than the other two systems.

The land transportation system is composed of intricately and harmoniously interlinked networks, including networks of highways and interchanges, heavy vehicle routes, railways, transit system (subway, bus, and streetcars systems), light rapid transit system (sky trains), in addition to a vast network of roads, which may be superimposed by networks of High Occupancy Vehicle (HOV) and bicycle lanes, as well as sidewalks.

Of all the subsystems, the highway system represents a major and a fundamental component of the land transportation system. According to the American Road & Transportation Builders Association's (ARTBA) report, *Monthly Value of Transportation Construction Put in Place Report of May of 2005*, out of $7.9 billion USD value of construction work performed on transportation projects in the United States in May 2005, $5.7 billion USD were spent on highways and bridges, which amounts to 72.15% of the total value of transportation construction work (Buechner, 2005).

2.3   Transportation System Development Constraints

In the process of developing and maintaining transportation systems, it is crucial for the transportation authorities to ensure that these systems are safe for commuters, friendly to the environment, and efficient to all the stakeholders involved (e.g., commuters, government, and local inhabitants in the system vicinity). This involves ensuring that the transportation systems are convenient, reliable, and economical to the commuters; economical and sustainable to the government to construct, to operate, and to maintain; and balanced with respect to the public benefits versus the private distresses to the local residents.

2.4 *Characteristics of Transportation Systems in relation to Decision-making*

In this section, we will outline some features of the transportation system as they pertain to the need for and the complexities of the decision-making process.

2.4.1 The Cost of Wrong Decisions: *The Factors Involved*

Making non-optimal decisions in transportation projects can lead to enormous and multifaceted costs. This stems from several characteristics of transportation systems; below are some of these factors.

2.4.1.1 The Size Factor

One common feature of transportation systems is the size factor, whether it is in the enormity of size or the vastness of space requirements of their infrastructures. Collectively, the infrastructure of the land transport systems includes: terminals (rail, bus, and transit), road and highway pavements (including streets; road intersections; carpool, transit commuter, and commercial parking lots; as well as pedestrian sidewalks.) Moreover, the land transport system infrastructure also includes bridges, highway interchanges, tunnels, gutters, culverts, retaining walls, water drainage and sewer systems, lighting systems, traffic lighting and signaling systems, toll facilities, and rest facilities, as well as vehicle service buildings, which include bus garages, service facilities, maintenance buildings, equipment storage buildings and wash facilities.

Similarly, the infrastructure of the air transportation system includes terminals, runways and others structures like hangars, maintenance buildings, aircraft storage facilities,

stand-alone air traffic towers, and space facilities; whereas the marine transportation system includes terminals, docks, piers, wharves, and other facilities.

Most of these infrastructures require a substantial amount of land space. One immediate consequence of wrong decisions in transportation systems is the enormous wastage of materials and land space.

2.4.1.2 The Cost Factor

Given the huge infrastructure noted in the previous section, transportation system development projects, like many other civil infrastructure projects, typically require large sums of investments. For instance, in 2004, Translink, the Greater Vancouver Transportation Authority, approved a comprehensive strategy, *2005 - 2007 Three-Year Plan & Ten-Year Outlook*, to invest $4.0 billion in roads and transit. In 2005, the Ontario Ministry of Transportation announced the *Northern Ontario Highways Strategy*, a record $1.8-billion five-year plan for highway improvements and expansion in Northern Ontario. Another example is the 407 Electronic Toll Route (ETR) for which, when it opened in 1997, the construction cost was roughly $1.6 billion (Leatherdale, 2005).

With reference to total annual transportation expenditure statistics, the Ontario Ministry of Finance's *Annual Report and Consolidated Financial Statements 2006–2007* states that during this period the value of government expenditure in transportation related infrastructure amounted to $3.1 billion, which represented 48% of the total government investment in all capital assets ($6.4 billion). Additionally, in the United States, according to an ARTBA report, the value of construction work performed on

transportation projects in the United States in May 2005 totaled to US $7.9 billion, amounting to 8.3% of all construction work performed in the country (Buechner, 2005).

When an optimal decision with reference to a transportation development project is made, the overall monetary cost of transportation system would be the total costs of the land acquisition and the system construction, operation, maintenance, rehabilitation, and future expansion. These costs, as high as they are, can be justified by the derived merits of the transportation system efficient operation. However, when the realized system operates inefficiently as a result of a non-optimal decision, the monetary cost of the decision would not only include the above costs but also the cost of time wasted, lost revenues, and the cost of any corrective measures taken to remedy the deficiencies. Therefore, when the monetary cost of transportation projects is of the above magnitudes, reason and prudence need to be exercised in the decision making process.

2.4.1.3 The Foregone Opportunity Factor

Because choosing between various possible alternatives is inevitable, and because the consequences of these decisions are immense, a rigorous decision-making process is crucial. In such a process where the most optimal decision is sought, opportunity cost analysis can play a vital role. But this analysis does not consider the possibility of the decision faltering upon implementation; it does not account for possible delays or additional costs, neither does it consider their forgone opportunities. If taken into account, the resulting extended opportunity cost analysis may result in better decisions. On the other hand, if a wrong decision is made, the opportunity cost factor adds another dimension to resulting losses.

2.4.1.3.1 Opportunity Cost: A Brief Review

Transportation infrastructure projects are predominantly financed by governments through tax revenues. Having other important areas of expenditure (e.g., health; education, postsecondary education and training; children's and social services; and possibly others), governments have to make decisions about their budget allocations in these areas and among different options within each area. Given the fact that budgets are limited, trade-offs among these expenditure options are inevitable. Therefore, depending on the government's priorities, a decision to spend a dollar on the highest-valued option means a dollar not spent on next best one. The value of this forgone option is what is known as the opportunity cost. It does not necessarily have to have a monetary value; the option having the greatest expected utility[4] is chosen, and it may include the do-nothing/ inaction option (e.g. money invested at the risk-free interest rate). While opportunity cost is not treated as an actual cost in any financial statement, opportunity cost analysis is an important part of the decision-making processes. (InvestorWords.com, 2010).

However, opportunity cost decision analysis does not consider the possibility of the decision faltering and costing substantial delay and additional expenses. Do not these costs have opportunity costs? Would not the total cost (including remedial expenses and value of wasted time) consumed on an implemented decision have possibly allowed for more expensive and rewarding decision alternatives, in retrospect? And, therefore, would extending the concept of opportunity cost to model such scenarios provide more accurate

---

[4] Utility is defined here as the monetary equivalence of the level of satisfaction or benefit (monetary or otherwise) that would be realized from exercising or implementing an option.

evaluations and better decisions? Addressing these queries leads us to introduce the concept of opportunity cost of wrong decisions.

2.4.1.3.2 *Opportunity Cost of Wrong Decisions*

If the realized utility of an exercised option turns out to be less than what was initially expected (i.e., if the utility were mis-estimated) and consequently the decision were deemed to be non-optimal in view of the realized scenario, the decision-maker may have to take other actions to remedy the situation, which could incur substantial additional expenses and take extra time than already planned. Modeling this possibility in opportunity cost decision analysis by extending the concepts of opportunity cost and economic cost may reap better decisions.

Therefore, where the opportunity cost of any decision to invest a certain amount of money in an option is the forgone value (utility) that would be realized from investing the same amount of money in the second-highest-valued option, we define the opportunity cost of wrong decision (OCWD) as: the forgone value that would be realized during the same period of time from investing in the second-highest-valued option, the sum of the original amount of investment in addition to the expected remedial expenses and the money value of wasted time or delay. Furthermore, in parallel with the concept of economic cost (EC) of a decision, which is defined as the cost incurred in implementing the decision plus its opportunity cost, we define the concept of economic cost of a non-optimal/ wrong decision (ECWD) to be the economic cost of the decision plus the economic cost of mis-estimation or setbacks (ECME), which is the cost of the remedial expenses and that of delay plus their opportunity costs.

Alternatively, ECWD can be defined as total expected total cost (i.e., including cost of mis-estimation) plus OCWD. The former dentition assumes that the utility of decision option as well as its opportunity cost can be partitioned between the cost of the decision option and that of the mis-estimation. Whereas the latter deals with the expected cost and its utility in totality.

ECWD of a decision option when subtracted from decision's expected utility yields the economic profit of wrong decision, EPWD. This value can be used as a criteria for decision-making, where the decision option having the maximum EPWD value is chosen.

When incorporating the possibility of setbacks in decision-making through including cost of setbacks in the total expected cost and opportunity cost, more accurate assessments and consequently better decisions may arise. On the contrary, if this possibility is not taken into consideration and a wrong decision materializes, then given the scale of the negative consequences, the forgone opportunity factor multiplies the loss. This effect is felt the most when an implemented expensive decision option becomes increasingly more costly (due to remedial expenses, wasted time, and lost revenues) and yet never yields any of the sought utility; it becomes like a double loss: the wasted resources and the forgone opportunity. A real mega-scale project example of this (Montréal-Mirabel International Airport) is presented in subsection 2.4.1.10.1.

Wrong decisions in transportation project can not only significantly increase the costs of the implemented decisions but also the values of their forgone opportunities. In addition

to the added costs, the forgone opportunity factor is another reason for seeking optimality in decision-making in transportation infrastructure projects.

2.4.1.4 The Profitability Factor: Private Sector Involvement

As mentioned earlier, due to the large cost and limited government resources, it has become increasingly more common to find the involvement of the private sector in transportation systems development through what are called public-private partnerships.

One example of interest is the 407 Express Toll Route (ETR). For the sake of a more speedy construction and to save much needed provincial funds, the Ontario government resorted to a public-private partnership to facilitate the development of the highway. Other examples include the Viva bus rapid transit network in York Region, Ontario (Koole, 2006), the Confederation Bridge construction in Prince Edward Island (Transport Canada, 2005), and the Canada Line automated rapid transit service in Greater Vancouver, British Columbia (The Canada Line).

While for the government some non optimal decisions may be justified on the basis of some non monetary or long term benefits, or because the money is eventually recoverable through future taxation, these decisions would be absolutely intolerable to the private sector, where the sole motive behind any venture is the monetary gain and where the resources are much more limited. Therefore, rigorous and comprehensive analysis becomes imperative to ascertain the viability and profitability of projects.

There is a compounded sense of necessity for making right decisions when the private sector is involved. This requires an accurate project assessment and valuation, which

according to Zhao, Sundararajan, and Tseng (2004), "demands a prudent approach in sharing the commercial, financial, and development risk among the different agencies".

2.4.1.5 The Human Factor

Construction of new transportation systems, including highways, or the expansion of existing ones can have many implications on people on different levels. Perhaps some of the most directly and immediately affected individuals are those who are located on or in near proximity to these projects. The effects of their disturbances can be economical, personal, and/or social in nature.

Naturally, one prerequisite to undertaking any new construction or expansion of an existing highway is the procurement of the land or the right-of-way. In Canada, when such projects are deemed necessary and/ or in the public interest, the appropriate authority (e.g. the provincial ministry of transportation), through enacting legal procedures embedded in the Canadian Expropriation Act[5] (1985), can take possession of the land areas that are "required by the Crown[6] for a public work or other public purpose."

The expropriation process may inflict numerous damages on the landowners that include cases where: an owner is required to give up their occupations, a specially designed building is erected on the land, or the land is being used for residence. However, the landowner is still entitled to object to these damages.

---

[5] or similar provincial versions.
[6] "*Crown*" means Her Majesty in right of Canada

A landowner, choosing to exercise the right to object to the *notice of intention*[7] to

expropriate the interest in land[8], may get engaged in a lengthy and potentially taxing

process, which involves serving on the Minister an objection[9] to the notice of intention to

expropriate the interest; attending public hearings[10] or retaining counsel[11] to present the

nature and the grounds of the objections; and, where the effect is not given to the

objection, requesting a copy of the public hearing report[12].

The landowners, having almost no choice but to sell, would, however, be entitled to

compensations, as per Section 25 of the Canadian Expropriation Act.

While the landowners are entitled to receive compensations for losses that are

subsequently endured as result of the land expropriations, they and all those who choose

to object to the notice of intention, may have to go through several other lengthy

procedures that can include attending court hearings regarding determination of titles[13] of

---

[7] "***notice of intention***": Whenever, in the opinion of the Minister, any interest in land is required by the Crown for a public work or other public purpose, the Minister may request the Attorney General of Canada to register **a notice of intention** to expropriate the interest, signed by the Minister.

[8] "***land***" includes buildings, structures and other things in the nature of fixtures and mines and minerals whether precious or base, on, above or below the surface.

[9] Section **9** of the Expropriation Act, grants the landowner the right to object to the notice of intention, within thirty days after the day the notice is given, by serving on the Minister an objection in writing.

[10] Subsection **10**.(1) of the Expropriation Act states that the Minister shall, if the Minister has been served with an objection under section 9, order that a public hearing be conducted with respect to the objection and any other objection to the intended expropriation that has been or may be served on the Minister

[11] Subsection **10**.(6) of the Expropriation Act grants any person who may be heard at a public hearing under section **10** the right to be represented by counsel at the hearing.

[12] As per Section **13,** in the event where effect was not given by the Minister to the objection to the notice of intention, the landowner can request a copy of the public hearing report with a statement of the reasons that the Minister had for not giving the effect.

[13] As per Section **18,** where the Attorney General of Canada, at any time after the registration of a notice of confirmation, is in doubt as to the persons who had any right, estate or interest in the land to which the notice relates or as to the nature or extent thereof, the Attorney General of Canada may apply to the Court to make a determination respecting the state of the title to the land or any part thereof immediately before the registration of the notice, and to adjudge who had a right, estate or interest in the land at that time, and the nature and extent thereof.

the land, hiring land appraisal agencies (Section 29), accepting or rejecting compensation offers[14], negotiating[15] compensation settlements, or filing lawsuits[16].

Aside from the economical losses and the expropriation hassles, there are other disturbances to the landowners of the expropriated lands that may not have a monetary value. These include lifestyle losses such as loss of sentimental values, changes in life habits, and social disconnections due to resettlement, as well as life quality losses to nearby inhabitants of the transportation system in terms of increased air pollution and noise levels, loss of greeneries, reduced child safety, etc.

Decisions to build or expand transportation systems can have great benefits, but they can also have enormous consequences on people, not all of which are compensable. With correct decisions, the greater public good may justify the cost paid by local inhabitants. But because wrong decisions can translate into little public benefits and result in people making unnecessary sacrifices, then extreme care must be taken in the decision-making process.

---

[14] As per paragraph **16**.(1)(*b*), following issuance of a notice of confirmation of intention (Section **14**), where the interest would, thereby, be confirmed to be expropriated becomes absolutely vested in the Crown (Section **15**), the Minister shall, within a certain period of time, make an offer in writing of compensation in an amount estimated by the Minister to be equal to the compensation to which that person is then entitled.
[15] As per Subsection **30.**(1) where, after an offer of compensation in respect of an expropriated interest has been made under section 16 to any person, the owner and the Minister are unable to agree on the amount of compensation to which the owner is then entitled, either the owner or the Minister may, within sixty days after the making of the offer, serve on the other a notice to negotiate settlement of the compensation to which the owner is then entitled.
[16] as specified under Section **31** of the Expropriation Act.

2.4.1.6 The Environmental Factor

Given the physical nature of large-scale transportation systems, the erection of a new system or a major expansion of an existing one is likely to cause significant adverse environmental effects, which according to the Canadian Environmental Assessment (CEA) Act (1992) would necessitate the conduct of a comprehensive environmental assessment study prior to approving the project. Some of the projects that would require such an assessment, as identified by the Comprehensive Study List Regulations of the CEA Act (Ibid.), include:

> The proposed construction of
>
> (a) a railway line more than 32 km in length on a new right-of-way;
>
> (b) an all-season public highway that will be more than 50 km in length and either will be located on a new right-of-way or will lead to a community that lacks all-season public highway access; or
>
> (c) a railway line designed for trains that have an average speed of more than 200 km/h.

Therefore, projects relevant to this study would certainly need to undergo a comprehensive environmental assessment. The CEA Act stipulates a variety of factors to be considered in the assessment such as "measures that are technically and economically feasible and that would mitigate any significant adverse environmental effects of the project" and "alternative means of carrying out the project that are technically and economically feasible and the environmental effects of any such alternative means".

Yet despite incorporating mitigation measures into the design of the project, some level of adverse environmental effects will be irreparable, which is justified if the merits of the

project materialize. However, if they do not, it is this irreparable damage that is the environmental cost of wrong decisions.

2.4.1.7 The Irreversibility Factor

For our purposes, irreversibility here refers to scenarios that range from the inherent difficulty of transforming a reality to cases of complete irreversibility of actions that result from poor decisions.

Unlike the previous cost factors, which are cumulative, the irreversibility factor has a multiplicative effect, on top of the cumulative cost effect. The cumulative cost effect of the irreversibility factor is attributed to the cost of transforming the system into a useful one, whereas the multiplicative effect refers to its scaling (magnifying) effect on those previous factors mentioned (i.e. human, environmental, etc.). The cumulative cost effect of the irreversibility factor, having a monetary value, is already included in the cost and the opportunity cost of wrong decision factors. Therefore, the emphasis here will be placed on the scaling effect.

Irreversibility is a common property of several elements of transportation projects. The first element relates to the size factor (Section 2.4.1.1) or the structural irreversibility. The reason behind the irreversibility of this element is twofold.

Being composed of large structures and/or spanning over vast areas makes the transportation system infrastructure virtually irreversible once erected. As a matter of fact, these infrastructures, once built, are expected, with maintenance, rehabilitation and expansion, to last for many decades, if not centuries. The massive structures erected,

whether they are airports, seaports, bridges, bus terminal, subways, or highways, consume enormous amount of materials, equipments, space, etc. Meaning that demolishing them, beyond being costly, is completely wasteful. On the other hand, the unique nature of the structural elements of these systems applies to the difficulty side of the irreversibility spectrum in that, while doable, it is typically costly and time consuming to transform them into other types of structures. Also, the decision to transform the system is usually taken only after exhausting all other feasible options to rectify the system.

The other aspect of the irreversibility of the size factor pertains to the expropriated lands and any existing structures on these lands, which would be permanently lost if the project proceeds, and would not normally be returned (at least not easily) even if the project is suspended or abandoned.

The second element of the scaling effects of the irreversibility factor relates to the cost factor, where the cost paid in establishing or transforming the system is completely irrecoverable except by the amount of revenues and/or benefits realized in the operation of the system. Therefore, the system loss or the non-recovered portion of the cost (including the opportunity cost of wrong decision) resulting from the poor decision is irreversible.

The third refers to the impact on the private sector of the irreversibility in mitigating losses.

The fourth relates, to various degrees, to the human factor, where the irreversibility of the disruptions to the lifestyles and of the reduction of life quality endured by the landowners and local residents as a result of the decision makes the cost of wrong decisions higher.

Last but not least, the fifth element involves the environmental factor; the irreversibility of the damage (again to various degrees) caused to environment also makes cost of wrong decisions higher.

2.4.1.8 The Time Factor

The time factor and the irreversibility factor (discussed in the previous section) are related. We have made an analytical distinction between these two factors in that the latter refers to the degree of irreversibility of actions resulting from non-optimal decisions. In this section we discuss the time factor and its implication on the actions that are not completely irreversible.

The process of establishing or expanding a transportation system does not start with a decision; what usually precedes this is a lengthy feasibility study involving traffic demand analysis and forecasting that leads to the recognition or prediction of a need for a corrective action. As discussed in Section 2.4.3.4.2 below, this is usually construction of new or expansion of current system. In between making the decision and the actual construction of the system are actions like proposing different alternative solutions and locations, assessing the environmental impacts, estimating costs, selecting the preferred design proposal, possibly conducting public hearings, and/or dealing with possible public outcry/ political opposition, possibly revising design, deferring or even abandoning the project altogether, procuring the land, possibly engaging in legal land expropriation

proceedings, and bidding and selecting construction companies. Following that come the detailed design and the actual construction of the system, and upon construction completion starts an ongoing process of monitoring, rehabilitation and expansion that continues over the lifespan of the system. The monitoring process includes observing the highway service quality for rehabilitation needs and traffic counts for forecasting the system traffic demand growth, in order to take the right actions to meet the needs of the future.

To varying degrees, one common feature of many of the above and other aspects of the transportation infrastructure developments is the long time-span drag. Some sporadic examples of this on different phases of existing highways are: from the time the need for Highway 407 was identified and land procurement began in the 1950s, it took about thirty years for the Ontario government to announce the construction of the highway in 1986 (Mylvaganam and Bornis, 2004); a span of around 30 years passed between the first section and the final section of Hwy 401 were completed (Marshall, 2006); Hwy 407 was sold in 1999 through an unprecedented long lease lasting 99 years (Mylvaganam and Bornis, 2005); and still existent to-date, the first portion of the QEW officially opened on June 7, 1939 (Marshall, 2006). The long time span fact has a big effect on the different factors of the transportation system related to cost of wrong decisions.

When it comes to non-optimal decisions, the time factor is much related to the concept of irreversibility in its relation to the first six factors; the time needed to remedy the effect of a wrong decision on an aspect of the transportation system is positively correlated to its level of irreversibility, and so is the relationship between the time and its effect on the cost of wrong decisions. The aspects of the transportation system (listed in the previous

section) at best require long durations (for those that are not completely irreversible), which in turn translate into a proportional level of magnification of cost. And at most (for the case of complete irreversibility), the scaling (or proportionality constant) would be equal to the inverse of the interest rate in the case where the cost can be represented as a constant perpetuity, or the inverse of the difference of the interest rate and the growth rate in the case where the representation is a growing perpetuity. This is assuming that in both cases, total cost can be represented in monetary terms.

In summary, for a decision to establish or expand a transportation system, the first six cost factors are the unavoidable price that could be justifiably paid in return for the sought merits of the system. However, if this decision is poorly made and these merits never materialize partially or completely, the price of this poorly made decision would to some degree translate into a loss. The effect of the irreversibility factor on this loss would be to extend it for a proportional period of time, where the most conservative values of these time durations are fairly long. The irreversibility and time factors thus magnify the value of the cost.

2.4.1.9 The Public and Political Factor

Concerns arising from any combination of the size, the cost, the forgone opportunity cost, the human, the environmental, the irreversibility, or the time factors to decisions to construct or expand a transportation system can induce public opposition even prior to their establishments. Promises are made, or at least expected, when projects are undertaken. For example, the website for Translink, the South Coast British Columbia Transportation Authority, states that they "will invest the public's transportation dollars

wisely to ensure that the system is sustainable in the long-term". However, when the promises made cannot be kept and the benefits of the system do not sufficiently materialize, the effect of these factors becomes more intense (proportional to the level of deficiency) and are propagated even further by the increased costs (remedial costs, wasted time, and cost of wrong decision). This would further result in public fury that may also lead to political backlashes.

The public-political factor is a very likely consequence of wrong decisions; its value is proportional to the total magnitude of all the above costs of wrong decisions and itself is another cost of wrong decision that behooves for making optimal decisions.

2.4.1.10   Can it really go that wrong?

Above, we have presented some costs of wrong decisions in transportation projects. While these costs may appear uncommon and theoretical in nature they do, however, occur and when they do they can, depending on their magnitude of deficiency, have enormous real-life consequences. Below we present few case studies that demonstrate some of these costs of wrong decisions.

2.4.1.10.1   Montréal-Mirabel International Airport

It was supposed to be "a project for the 21st century"[17], "the airport of the future"[18], the "tool to help Montreal develop into a cultural and financial magnet" (Krauss, 2004), "the facility, which was meant to be the central gateway for much of Canada's international air travel, …, [that would] take flying to new heights of luxury and efficiency", but instead it metamorphosed from an ambitious supermodern airport into a giant white elephant that only made "an ignominious landing in history's dustbin" (Toronto Star, 2004).

It is the Montreal-Mirabel International Airport (commonly known as Mirabel), which was "revolutionary in its design, with a railroad station in its basement and a road tunnel under the runways to take drivers right to its international terminal" (Krauss, 2004). According to Transport Canada's website, when inaugurated on November 29, 1975, it was the world's largest airport in terms of property area. With 97,000 acres (393 square kilometers) of right-of-way (an area more than six times the size of Manhattan (Simon, 1996)). it was envisioned to ultimately have six onsite terminal buildings and handle up to 50 million passengers a year (Toronto Star, 2004) and yet, "the airport - which cost more than $1 billion [more precisely $1.6 billion according to Maclean's (Branswell, 1997)] to build… never handled more than 3 million travellers a year" (Toronto Star, 2004), displaced some 3,500 farming families off their land (Ibid.), and ended up using only 16 square kilometers of the expropriated land (The Record, 2004). Financially, Mirabel was a disaster, as well; "…at the end [it] was running an operating deficit of $20 million a year" (Delean, 2006).

---

[17] As it was labeled in the late 1960's by the Canadian Prime Minister Pierre Trudeau (Krauss, 2004).
[18] A quote from a former employee at Mirabel-Montreal International Airport (Branswell, 1997)

In desperate attempts to resuscitate it, the Mirabel airport underwent several amputation surgeries, none of which landed far away from failure. "International commercial flights coming into Mirabel were transferred back to Dorval (now Pierre Elliott Trudeau) airport in 1997, leaving Mirabel to handle only charter and cargo traffic" (Krauss, 2004). Later, on October 31, 2004, it was reduced further to be used exclusively for cargo flights (Ibid.) and some light industry (CBC News, 2004). The death of Montreal Mirabel Airport passenger terminal was officially pronounced on February 21, 2006 when Aeroports de Montreal, the non-profit authority that runs both the Mirabel and the Pierre Elliott Trudeau airports, announced an agreement with an international consortium to transform the airport into a theme park. Despite that, the terms of the agreement state that "the terminal and adjacent buildings and property would be rented to the consortium for 25 years, with provision for two five-year extensions" (Delean, 2006); thus, preserving the option/right of resurrecting the airport once again one day in the future. However, "the Trudeau expansion, which should provide passenger capacity for Montreal for the next 35 or 40 years, makes a return to Mirabel a very poor bet" (Toronto Star, 2004). And if and when done so, it would be too outdated to be considered a viable option; it would be 70 years old! (Ibid.)

Many reasons were attributed to the Mirabel airport's failure; some are presented below:

1. *Poor passenger demand volume prediction:
   a. The "erroneous predictions of passenger volumes that were based on the astronomical increases recorded in the 1960s" (Ibid.), which were due to "the glow of the Expo '67 world fair and [the anticipation for] the 1976 summer Olympics" (Simon, 1996);

b. The economic shift marking "…the decline of Montreal as a business and financial centre" in favour of Toronto (Ibid.);

c. "[T]he '70s oil crisis that peaked during Mirabel's construction" (Toronto Star, 2004);

d. "[T]he flight of some 200,000 anglophones from Montreal after the 1976 election of the separatist Parti Quebecois [PQ]" (Ibid.).

2. *Technological ill-prognostications:

a. The creation of quieter, runway-space-efficient, and environmentally friendly airplanes abrogated most if not all the benefits of airport remoteness from the centre of Montreal City;

b. The development of fuel-efficient airplanes eliminated the necessity of landing at Mirabel for refueling.

3. Ill-advised choice of location:

a. "The airport's location, near the community of Mirabel… was … a big mistake, the result of a fundamentally flawed compromise between the federal [wanting it East of Montreal- close to Ottawa] and Quebec governments [wanting it to the West- close to Quebec city] that satisfied no one in the end". In essence, "Mirabel was a compromise that really didn't work for anybody" (Ibid.);

b. "The airport's distance (55 km) from the central city as well as from connecting flights at far-off Trudeau Airport have been crippling

deterrents to Mirabel's success from the time it opened in the fall of 1975"

(Ibid.);

c. The long and costly trips (30 minute-$60 taxi ride (Simon, 1996)), in

addition to the absence of adequate land transportation infrastructure from

Montreal to Mirabel made Mirabel very inconvenient to travelers.

However, this "crippling remoteness from the city could have been

mitigated by the promised road and rail infrastructure, which, for both

political [election of the PQ government in 1976] and economic reasons,

never materialized" (Toronto Star, 2004);

d. *Furthermore, "a decision in the early 1980s to split air traffic between the

city's two airports would prove "fatal" to Mirabel" as "it killed any transfer

business…with the 3 1/2-to four-hour [transfer-time] gaps between

Mirabel [international] and Dorval [Domestic] flights" (Ibid.).

Items marked with (*) can be interpreted as unexpected jumps.

Monetary Cost of Wrong Decisions

The Mirabel airport, being a mega-project failure, is an excellent example to illustrate the

enormous cost consequences of the wrong decisions taken. The first aspect of this cost is

the enormous size of land and structures wasted, which could have otherwise been used

more effectively. The opportunity cost of wrong decision for the airport, which when

opened in 1975 cost $1.6 billion, is another aspect (Branswell, 1997).

In Section 2.4.1.3.2, we indicated that the economic cost of wrong decision is:

$$\text{ECWD} = A + C^{\text{Delay}} + C^{\text{Remedial}} + \text{OCWD}$$

The present value of the initial construction cost (A) plus the present value of the cost of

delay (C^{Delay}) since 1975 plus the present value of all running operating deficits

(C^{Remedial}), which includes $20 million per year since 1997 (Delean, 2006) and that of all

other remedial costs (including the $200 million transformation cost (Ibid.) and of more

than $9 million in farming-resumption programs (as stated at Transport Canada's

website) plus the utility of investing all the pervious amounts in the next-highest-valued

option (OCWD) is altogether the total monetary cost of the wrong decision of

establishing the Mirabel airport. The magnitude of the opportunity cost of wrong decision

(OCWD) should at least be the return that would have been earned from investing the

first three amounts at the risk-free interest rate. Loosely speaking, however, for an idea of

a potential value of the OCWD figure, it is noteworthy to observe that when highway 407

was first opened in 1997 it cost $1.6 billion; the OCWD value could have been of the

magnitude of the present value of the 407 ETR had this option been the second-highest-

alternative investment, for example.

Human Cost

The following passages of an article in Maclean's published on September 8, 1997

vividly illustrate a sample of the human dimension of the mistakes in Mirabel.

> In 1969, the federal government began expropriating 360 square kilometres -- an
>
> area equivalent to almost three-quarters the size of the Island of Montreal. About
>
> 8,000 rural residents were affected -- many were forced to become tenants on land

they had once owned. Others, like Lafond, had to move and became embroiled in bitter and lengthy land disputes (in the end, less than 10 per cent of the expropriated terrItôry [sic] was used).

After losing his dairy farm in Ste-Scholastique in 1970, Lafond, now 64, moved his family to a smaller farm in nearby Bellefeuille. He eventually agreed to a $ 100,000 out-ofcourt [sic] settlement with the federal government. Now, standing near his redbrick bungalow as cows graze on a nearby slope, his eyes well with tears as he recalls those years. But his sadness is quickly replaced by a flash of anger -- after all the havoc the airport wreaked on their lives, Lafond and other farmers who had their land expropriated want Mirabel to survive. He complains that his land was sacrificed to "save Montreal" from noise pollution, and now the flights are returning there to save the city's economy. "They're doing it for nothing," Lafond says. "One day or another they'll have to return to Mirabel."

… Hubert Meilleur, the mayor of the nearby city of Mirabel, predicts that more than 1,000 jobs will be lost in the area as a result of scaling back flights to Mirabel. He lambastes the decision, saying it was taken to "please businessmen" and hurts two generations of people -- those who endured the expropriations, and their children, who benefited economically from the airport and could now lose their means of making a living. (Branswell, 1997)

Environmental Cost

According to the book "Structure and dynamics of land use", by Peter Brooke Clibbon, over the five year period between 1966 and 1971, and notably after 1969 when the site of the airport was selected and its official boundaries of Mirabel Airport were set, massive changes in the land use took place in the villages where the airport was constructed. During this period, the right-of-way for Mirabel airport was being expropriated and the construction was well under way.

Attributed mainly to the airport, the area of urban and para-urban land use increased between 1966 and 1971 from 1,755.8 to 4,952.0 acres (182% increase), where in 1971, this presented 5.3% of the expropriated area. The agricultural area dropped from 59,814.6 (62% of the expropriated land in 1966) to 48,053.4 acres (51.0% of the expropriated land in 1971) for a total loss of 11,761.2 acres (19.7% decrease). The shrinking of the cultivated land is explained by the withdrawal of several thousands of acres from farming in the operational area, and also by the massive abandonment, which occurred almost everywhere else in the territory even in those sectors not immediately threatened by construction projects. During this period, the area of abandoned land rose dramatically, specifically from 7,367.1 to 15,579.4 acres, for an increase of 111.5%. By 1971, the area in derelict farmland occupied 16.5% of the expropriated area, compared with 7.7% in 1966. Finally, in what amounts to a 3.6% reduction, the area of woodland declined by 955.6 acres (from 25,899.2 to 24,943.6 acres) between 1966 and 1971. In 1971, forest represented 26.5% of the expropriated land. Other land uses, which include peat bogs, swamps and marshes, bare sand and clay, and water, occupied only 701.6 acres in 1971, or 0.7% of the expropriated area.

For our purposes, the period of interest is that spanning from the commencement of the land expropriation in 1969 to the end of the airport construction or the opening of the airport in 1975. The time period of the above statistics (1966-1971) does not exactly overlap with that of our interest (1969-1975). Regardless, the above statistics, overlapping only in the first two years (1969-1971) of the six-year period, loosely illustrate the severe level of impact the establishment decision of Mirabel airport had on the land use and the environment.

Irreversibility and Time Effects

The structural irreversibility of Mirabel lies on the side of "the difficulty of undoing actions" on the scale of irreversibility that was introduced in Section 2.4.1.7. The terminal complex, which includes a 5,000-space car park, a 355-room hotel and an eight-storey office building (CBC News, 2004), would take a few years to be renovated and transformed into a theme park, and is expected to cost $200 million (Delean, 2006). It took more than three decades of option exhaustion for this decision to be made.

It was not until July of 1981 (more than a decade since the Mirabel land expropriation commenced) that the initial forecasts were revealed to be inaccurate. As a result, 80,000 acres of Mirabel Airport right-of-way (97,000 acres) were deemed excess land. And, according to Transport Canada's website, it took nearly another decade, filled with public and political turmoil, for 1,400 properties to be eventually sold back (between 1985 and 1989), at which point 11,000 acres were still kept as airport reserve land. Rightly labeled "correcting a historical injustice" (CBC News, 2006), a final move that took another two decades to be undertaken was announced in December of 2006. According to Transport

Canada's website, the federal government was to return the reserved 11,112 acres (4,450 hectares) of farmland that was expropriated almost 40 years earlier.

As painful and frustrating as this was to the inhabitants of the expropriated land, it could have been worse; their sufferings, still materializing, could have been dragged out by decades of inaction, as we shall see next.

2.4.1.10.2   *Pickering Airport: A déjà vu of Mirabel?*

In 1972, 18,600 acres of Grade A farmland (Lem, 2007) were expropriated in Pickering, Ontario for the construction of a reliever airport to the Pearson International Airport in Toronto. Due to "public opposition and the Ontario government's withdrawal of support for the project", it has been put on hold since September of 1975 (Facts on File World News Digest, 1975). Between the claim of the inability of Pearson International Airport to cope with projected future aviation demand on one hand and questions about the need for the airport, debate on Pickering airport kept resurfacing every few years (Boyle, 2007).

It is currently believed by proponents of the airport that Pearson International Airport "will meet its capacity of 50 million (passengers) by 2025-2027" (Lem, 2007). However, opponents of the project question, in part, the accuracy of these estimates, citing previous estimation flaws. Pickering airport may become a reality as soon as 2012, however, a final decision is not expected to be made until 2009 (Ibid.).

It is clear that there is a legitimate claim of serious deficiencies in estimating aviation demand, thus the value of and the need for the airport is questionable. One thing that is certainly known is that without rigorous analysis and reliable demand projection, the

construction of the Pickering airport may very well be a Mirabel-like white elephant in the making. If it is any different, it is that the cost of a wrong decision could be even bigger given the longer period of inaction.

2.4.1.10.3   Highway 407

Another colossal error of decision-making that is closer to our area of interest is the sale of the 407 Electronic Toll Road (ETR). Unlike Mirabel, the 407 ETR transpired to be a very successful enterprise. Despite that, highway 407, like Mirabel, had its share of controversy; the common fault-denominator between the two undoubtedly encompasses poor demand estimation and project valuation.

According to the 407 ETR website, "Highway 407, which extends 108 kilometres east-west, just north of Toronto" was meant to be a reliever highway to the congested highway 401, but instead the 407 ETR turned into a luxurious highway monopoly or an "Extreme Toll Ripoff" (Leatherdale, 2005).

Due to economic and political reasons, highway 407 was sold, in a competitive bid, to a consortium of private companies in 1999. The poor terms of sale, giving the consortium full ownership of the highway for 99 years with an unlimited control over the highway and its tolls, and the grave underestimation of the highway's worth were the main causes of the controversy. The $3.1 billion (Government of Ontario, 2006) privatization in 1999 was worth $13 billion, in 2005 (Mylvaganam and Borins, 2005). Since 1999, tolls have risen more than 250% (Leatherdale, 2005). The situation could have been avoided with accurate traffic and revenue forecasts and with careful project valuation analysis.

2.4.2 The Cost of Inaction

In Section 2.4.1, we discussed the high and myriad costs of making a decision to establish a transportation system and those of making non-optimal decisions, but what are the costs of not making any decisions or of inaction in general?

There are two areas of inaction; one in addressing the need for a transportation system and the other is the inaction in remedying the effects of non-optimal decisions. In Section 2.1, we have briefly mentioned the value and the benefits of transportation systems; the lack of attainment of these benefits is the cost of inaction in establishing the system. On the other hand, the continuation of losses, as well as the lost opportunities, resulting from poorly made decisions is the cost of inaction of remedying the system where possible.

The great magnitude of these costs eliminates inaction as a practicable option and therefore the quest for optimal decisions, as costly as it may be, is the *only* viable option.

2.4.3 The Price of Making Right Decisions: The Factors and Challenges Involved

Previously in Section 2.4.1, we have listed, among other details, the transportation system factors that can be attributed to the costs of wrong decisions and/or to the inaccurate valuation of transportation projects. This was done by listing the impacts of these decisions on the different stakeholders involved. Moreover, the examples in that section were presented to illustrate the real possibility of making very poor decisions and their devastating consequences.

In the effort of attaining the benefits of transportation in Section 2.1, a rigorous decision-making process is required, if not for optimizing the resources available, then at least to avoid paying the potentially massive costs resulting from the wrong decisions.

This section is devoted to exploring ways of reaching optimality in the decision-making process in transportation system development projects. In our discussion on some of the requisites and challenges faced in attaining optimal decisions, we continue studying other factors of the transportation systems that are operational in nature and that need to be addressed in the decision-making process to arrive at optimal decisions. These factors, among others, jointly make the quest for optimality a very challenging exercise that eventually necessitates making significant simplifying assumptions.

Although much of what follows may be applicable to the other modes of the land transportation system, for the sake of preciseness and focus, the discussion henceforth will be directed primarily towards highway systems.

2.4.3.1 The Need for a Rigorous Decision-making System

The Montréal-Mirabel International Airport case study, presented in Section 2.4.1.10.1, is predominantly an example of a poor decision in the planning phase, whereas the 407 ETR case in Section 2.4.1.10.3 is an example of poor decision in the operational phase resulting from poor uncertainty prediction and project valuation. While these are examples of failures on a mega-project scale, others, due to similar reasons, occur repeatedly in highway development projects. According to Zhao, T., Sundararajan, S. K., and Tseng C. L. (2004), "[o]ngoing operation decisions about capacity expansion, maintenance/rehabilitation, and regular maintenance have been based merely on

experience or perceived urgency of failure," and that, "[v]ery often, key decisions during the planning and design phases, […] are made without considering the underlying uncertainties […]".

There is a need for a rigorous multistage stochastic decision-making system in the highway system development, operation, expansion, and rehabilitation phases that is capable of accurately modeling the various uncertainties and valuating the system at its various development phases under different uncertain scenarios. It is combating the challenges in the process of attainment of such a decision-making system that constitutes the price of making optimal decisions.

2.4.3.2 Objectives of the Decision-making System

In Section 2.3, we listed the broad constraints of a healthy transportation system. Meeting these transportation system constraints (speed/ time, convenience, reliability, economy, and sustainability) collectively become the broad objectives of the decision making process. In this respect, the object focus of this work relates directly to the efficiency constraints, and not those related to the environment and the safety, which are beyond the scope of this work. As such, if the benefits of the land transportation or highway system lie in the efficient and smooth movement of traffic, then the decision-making process needs to address certain operational factors to ensure the highway system traffic is running in a smooth and efficient manner.

2.4.3.3 The Complexity Factor

Arriving at an optimal decision-making system for highway systems is a nontrivial endeavour. Modeling the highway system involves many challenges and complexities, some of which are elaborated on in the following sections.

Naturally, the decision-making system needs to make optimal decisions in such a way that the total value of the highway system is maximized. These decisions need to be made continually and on a timely basis throughout the life-cycle of the highway. One challenge that lies in this process is the large number of decisions that need to be made. Given the infeasibility of considering them in their entirety, the decision-making system needs to include only the most important decisions. Not necessarily independent of one another, these decisions also need to be modeled in the decision-making system in a way that reflects these interdependencies.

The value of the project and the outcomes of these decisions are contingent on the realization of the relevant underlying uncertainties that are imbedded in the highway system. Perhaps more of a challenge is addressing this uncertainty factor. Not only are they numberless, these uncertainties are highly correlated, have unknown stochastic dynamics, and require vigorous data analysis and tedious data collection efforts such that modeling them is at best nontrivial.

A third challenge is relating in an optimization technique the decisions, the modeled uncertainties and other highway parameters in a way that closely resembles reality and that yields the optimal results sought.

In the following three sections, we elaborate on these challenges.

2.4.3.4 Scope of Decisions: The First Challenge

When attempting to develop an optimal decision-making system that deals with the different phases of the life-cycle of the highway system, one immediate constraint is the infeasibility of optimizing the large number of complicated decisions that need to be made during the life-cycle of the highway in absolution. These include many decisions within various processes taking place at the different phases of the highway life-cycle; some of these processes are listed below.

- **Planning phase**: determining the needs for and the benefits of the highway project as well as the constraints to the highway users and economy (as illustrated previously in Sections 2.1 and 2.3 respectively), studying the character of the area, selecting the path of the highway, and acquiring the land.
- **Design phase** (preliminary and final): designing of the highway parameters such as geometric shape and vertical alignment, design speed, number of lanes, width of right-of-way, drainage, and highway interchanges.
- **Development phase**: construction of the highway.
- **Operation phase**: highway maintenance, rehabilitation, and expansion.

Naturally, the efficiency of the decision-making system lies in the optimality of its decisions. However, given the wide spectrum of decisions, optimality lies in making optimal decisions of the most important types of decisions. Below are some of these important decisions that arise as a direct result of meeting the main objective of the highway system in this work: the efficiency objective.

2.4.3.4.1 System Quality: The Rehabilitation Decision

One factor that directly affects the efficiency of the highway system (meaning the smoothness of traffic, convenience, reliability and economy of the system) is the system traffic flow capacity. This depends on the highway service quality, where the higher the service quality of the system, the higher the system traffic flow capacity.

Whether due to environmental reasons and/ or traffic use, deterioration in highway systems is inevitable, as is the need to maintain and to rehabilitate its infrastructure.

Furthermore, rehabilitation is costly. Being so, there is a tradeoff between the cost of rehabilitation and the benefits gained. Thus, the modeling of the highway deterioration process and the timing of the rehabilitation decision become of the essence.

The rehabilitation of the system is an important decision that needs to be made, where the decision making system needs to determine the optimal timing of these decisions to ensure its sustainability.

2.4.3.4.2 Congestion Mitigation: The Expansion Decision

The highway traffic flow efficiency also depends on the traffic demand on the highway as traffic congestion can severely hinder the efficiency of the system. In the long run, chronic traffic congestion on highway systems arises due to two main reasons: deterioration in the transportation system quality condition (as discussed earlier) and/or growth in the traffic volume to a level where the traffic demand approaches or exceeds the highway capacity. Therefore, the time analysis of the traffic demand is also needed in the transportation decision-making system with regard to the determination of the optimal

time to exercise a corrective decision option. But what are the corrective decision options that can be made to maintain system efficiency and alleviate congestions?

Many strategies can be adopted to alleviate traffic congestion. They include system infrastructure management strategies such as highway rehabilitation and/or expansion, and traffic reduction strategies such as promoting the use of transit systems and carpools, as well as encouraging multi-occupant vehicle through the provision of restricted high occupancy vehicle (HOV) lanes[19], promoting the notion of flexible work hours to reduce rush hour congestions, or taking punitive measures such as increasing fuel taxes and/or public parking fares.

While traffic reduction strategies are being used in practice, they seem to be effective only when the transport system reaches absolute maximum expansion capacity and/or the cost (in time and money) becomes too excessive (e.g. Downtown Toronto or some sections of highway 401 during peak travel periods). Moreover, some of these strategies depend on the availability of well developed and convenient alternative transportation systems. Therefore, the system infrastructure management strategies remain the predominant set of options adopted to alleviate traffic congestion, thereby qualifying the adoption of this particular mitigation approach as a corrective or a preemptive optimizing decision in the decision-making process.

Again, highway expansion is costly (more so than rehabilitation) and depends on the number of expansion lanes. In addition to the need to determine the timing of the

---

[19] High occupancy vehicle lanes (HOV) are lanes that are designated only to vehicles that carry at least two people.

expansion, the decision-making system also needs to determine the optimal number of lanes to be expanded.

2.4.3.4.3 The Space Factor: The Land Acquisition Decision

In sub-subsection 2.4.1.1, we elaborated on the massive sizes and the vastness of the land space requirements of the land transportation systems. Prior to the implementation of the expansion decisions, land on which the highway is to be constructed needs to be secured by the proper authorities. Land, especially in urban areas, is mostly owned by the private sector. Thus, land expropriation is inevitable. Moreover, the cost of the land acquisition constitutes a major portion of the overall highway development cost.

The size of the land expropriated is dependent upon the geometric design (number of lanes to be built) and the outcome of the expropriation process where, for example, damages to the landowner may dictate that the entire land parcel be expropriated. Beyond being a prerequisite to highway construction or expansion, land acquisition also acts as an insurance against future variability in prices and in availability when acquired in excess of the current or the foreseen needs. It also grants the decision-maker the option of flexibly expanding the highway when deemed worthwhile, as the magnitude of this flexibility is confined by the size of land acquired.

Land acquisition cost is enormous and, as noted in Section 2.4.1.3, government budgets are limited. Thus, there is a tradeoff between the cost of land to be acquired and the security and benefits sought. Consequently, there is a need to optimize the width of the right-of-way to be acquired in size and time.

2.4.3.5 The Uncertainty Factor: The Second Challenge

A rigorous decision-making system rests on the accurate valuation of uncertain alternatives. The highway systems alternatives and states are embedded with myriad correlated uncertainties. And the uncertainties, themselves, can follow unknown distributions. The second challenge in developing a robust decision-making system lies in the treatment of the uncertainty factor, more specifically, the infeasibility of a full containment of all the uncertainties and their correlations and in mathematically capturing their dynamics. Therefore, in order to optimize decisions, one first needs to examine the different uncertainties involved and choose the most important ones to model. One also needs to ensure that the selected uncertainties indeed reflect the most feasibly accurate approximations of the valuation variables.

Uncertainty is a common feature of many aspects of highway development projects, such as system cost, traffic demand, revenue, highway service condition, and user benefits. Below are some of these uncertainties and their correlations, as they relate to three important stochastic valuation variables in the decision-making process (highway development cost, traffic demand, and highway service quality):

1) **Highway development cost**

    a) *Land acquisition cost (Expropriation cost)*

        i) Land price

            (1) Area of the expropriated land

                (a) Highway design

                (b) Exact size of expropriated land given damages to landowners

(2) Time

(3) State of economy

(4) Location

    (a) Urban

    (b) Rural

(5) Public/ private investments

(6) Government decisions: e.g. Landfills

ii) Damages to the owner

(1) Loss in business/ occupation

(2) Lost properties (homes, specialized building, etc…)

(3) Relocation

iii) Amount of decrease in the value of the remaining property

iv) Legal costs

b) *Construction/Rehabilitation Cost*

i) Material cost

(1) Fuel price

(2) Labor cost

(3) Raw material cost

ii) Labor cost

(1) Inflation

iii) Equipment rental & operational costs

iv) Oil price

v) Transportation cost

vi) Running costs

c) *Operational cost*

d) *Inflation*

e) *Foreign exchange rates*

2) **Traffic demand**

a) *Fuel price*

b) *Population growth*

c) *State of Economy*

d) *Highway service quality level*

e) *Highway location*

f) *Seasonal changes*

g) *Traffic shifts due to higher capacity (new highways or expansions) or shifts from other forms of transportation*

h) *Government interventions: HOV and other traffic reduction incentive initiatives*

i) *Private/public investment decisions*

i) New major enterprise

ii) Political decisions (Hosting Olympics, foreign trade or partnership agreements, decisions to invest in regional industrial production or regional infrastructure development)

3) Highway service quality (deterioration)

   a) Traffic demand

   b) Type of traffic

   c) Time/age (material degradation)

   d) Environmental conditions and disasters

   e) Chemical spills

   f) Structural failure

In the next few subsections, we analyze these major valuation variables and highlight some of their embedded uncertainties and suggest ways to model them.

2.4.3.5.1 Highway Development Cost in relation to Land Acquisition Cost

Due to the significant weight of the cost factor, as indicated in Section 2.4.1.2 above, there is a need to accurately model the dynamics of the highway development cost uncertainty.

For a government, the total highway development cost includes the cost of land acquisition, in addition to those of the system construction, operation, maintenance, rehabilitation, and expansion. As alluded to in Section 2.4.3.4.3 above, the first cost item is significant; in fact, it could be manifolds that of the latter ones. For example, where the construction cost of Highway 407, when opened in 1997, was roughly $1.6 billion, estimates of the amount of money spent since the 1970s in acquiring the land on which the highway sits range from $104-107 billion dollars as of March 31, 1998 (Ontario, Legislative Assembly, 1998).

Therefore, when modeling the total highway development cost, attaining an accurate representation of the cost process of the land acquisition (being potentially more than 65 times of the construction cost) should certainly supersede that of the highway construction. Traditionally, however, the cost of the right-of-way acquisition has been modeled simply through models of land price variability which, as seen above, involves a great level of simplification.

In Section 2.4.1.5, we explained the process of land acquisition illustrating the grievance and losses that the landowner may endure as a result of the expropriation process. There we stated that the landowner, having almost no choice but to sell, would nonetheless be entitled to compensations as per Section 25 of the Canadian Expropriation Act. Here, we elaborate on this clause of the Act, which states:

> **25.** (1) Compensation shall be paid by the Crown to each person who, immediately before the registration of a notice of confirmation[20], was the owner of a right, estate or interest in the land to which the notice relates, to the extent of his expropriated interest, the amount of which compensation shall be equal to the aggregate of
>
> (a) the value of the expropriated interest at the time of its taking, and
>
> (b) the amount of any decrease in value of the remaining property of the owner, determined as provided in Section **27**.

---

[20] "***notice of confirmation***" is a notice issued following a request by the Minister to the Attorney General of Canada to register a notice confirming the intention to expropriate an interest in land

[Where] the value of an expropriated interest is the market value thereof, that is to say, the amount that would have been paid for the interest if, at the time of its taking, it had been sold in the open market by a willing seller to a willing buyer.

This value, as stated in **25**.(1)(*a*) and determined in accordance with Section **26**, is assessed differently for different expropriation scenarios, such as those where the owner is required to give up an occupation, where the Crown has taken physical possession of land, where specially designed building is erected on the land, or where the land is being used for residence. Therefore, compensation (or expropriation price) is composed of the sum of the market price of the expropriated land, the amount of decrease in the value of the remaining property, and other damages to the owner.

$$\text{Land expropriation price} = \text{Market price of expropriated land} + \text{decrease in the value of remaining property} + \text{other damages to the owner} \qquad (2.1)$$

This is a far more realistic representation of the actual cost being paid by the government than that resulting from the sole consideration of the unit market land price. After all, this is the cost that is being incurred to obtain the right-of-way on which the highway is to be built, and it can be considerably larger than the mere market price of the expropriated land.

From the mathematical modeling perspective, the dynamics of the land acquisition cost may substantially differ from that of the land price (being only one segment of the land acquisition cost), as the land price is one of many other widely uncertain factors. One of the land acquisition cost components is time dependent, whereas the other is location

dependent. The component of the dynamics of the land acquisition cost process that is time dependent is the unit land price; whereas, the other expenses relating to the landowner compensations are time independent, applying only at the time of expropriation, and depend on the location and the unique circumstances of the landowner.

In order to conduct a thorough mathematical analysis to study the factors behind the different uncertainties in the land acquisition cost (e.g. damages to landowners or cost in urban vs. rural areas), one needs to collect a detailed breakdown of the statistics on the land acquisition cost values directly from the expropriating agency as well as collecting time varying statistics on unit market land prices.

One simple way of modeling the cost of land acquisition is by analyzing the highway system section-wise and adding for each highway section an appropriate average unit expropriation cost term and the land price. Another way to model land acquisition cost process is to model it as a two-dimensional jump process:

- Land price: time-variant process
- Compensation cost: space-variant process

Despite the above analysis and suggestions, and as stated in the scope of this work, for simplicity, the land acquisition cost will be based on a time-variant unit land price.

2.4.3.5.2 Construction Cost in relation to Material Cost

Following the land acquisition cost, the next considerable item in highway development cost is the construction cost. Construction cost is composed of materials cost, labor cost, equipment rental and operational costs, as well as other running costs. Out of them all, the cost of construction material is the most substantial component.

According to the May of 2005 ARTBA report *Value of Transportation Construction Put in Place,* "[m]aterials comprise just under half of highway and bridge construction costs [,…]" (Buechner, 2005). Noting an increase of 6.7% in the total value of highway and bridge construction work performed for the first 5 months of 2005 as compared to the same period in 2004, the ARTBA report also states that

> [s]ome of the increase in the value of construction on highways and bridges this year [2005] may simply represent higher material costs. During 2004, steel, fuel and cement prices all increased significantly, raising the cost of highway and bridge construction materials by 8.5%, according to data from the Bureau of Labor Statistics. So far in 2005, prices for aggregates, ready-mix cement and asphalt paving mixtures have risen significantly. (Ibid.)

This indicates a potentially volatile nature for the construction material cost.

In dollar value, the total value of construction work performed on highway and bridge projects in the US during that period of time totaled to $5.7 billion; this is still a significant component of the total cost in the absolute sense.

Its substantial proportion of the cost and its seemingly volatile nature may make modeling the materials cost as a stochastic process (as opposed to a constant variable) a fruitful measure, as it may capture the dynamics of the construction cost process more accurately.

Despite the above, for the sake of simplicity, the consideration of material cost will not be part of the scope of this work.

2.4.3.5.3 Oil Price

Metaphorically speaking, if the economy in general is a physical body, then the transportation system would be its nervous system and oil would be its blood stream. Oil price is directly and indirectly a sub-factor of many other uncertain variables, the accurate representation of which may rely heavily on that of the dynamics of oil prices.

The inclusion of the oil sub-factor in the modeling of the other factors, while it may be beneficial, can complicate the modeling and analysis of the decision-making system.

Oil price process appears to have a very volatile dynamics, with an upward trend that seems to exhibit sudden big jumps. However, a thorough incorporation of this uncertainty is very challenging; therefore, this uncertainty will not be considered in this paper.

2.4.3.5.4 Traffic Demand

Traffic demand is an important valuation variable because it is a measure of a primary objective of the transportation system: the efficiency of the highway system. This could be measured by the congestion level of the highway, which is directly proportional to the traffic demand level past reaching the highway traffic capacity.

Traffic demand is very volatile, and its volatility is time-scale dependent. The traffic demand behaviour varies on an hour-to-hour scale, on a day-to-day scale, on a month-to-month scale, and on that of a year-to-year scale. The different time scales capture different traffic variation patterns that may not be readily noticeable at other time scales, if detectible at all. For example, at the hour-to-hour scale, one would expect a large increase in traffic counts on certain highways during rush hours and a drop during the night hours on most highways. The weekday-weekend effect where traffic counts may increase or decrease during the weekends is mostly observable at the day-to-day scale. Other patterns may occur at the margin of two time scales, as in the case of some highways where traffic increases in the evening hours prior to the start of the first weekday and after the end of the last weekday. From a longer time-scale perspective, an effect that is revealed on the month-to-month scale could be that of the vacation season, where large peaks of traffic take place on certain highways during the months of summer or that where traffic substantially declines in the months of winter.

Finally there is the year-to-year scale, which captures a wide spectrum of factor effects. There are many factors that drive the fluctuations in traffic demand at this time scale, perhaps the most significant ones being those leading to large increases: the long term increase due to growth in traffic demand or economic reasons and the big spontaneous jumps. These jumps may occur due to many factors such as: big jumps in fuel prices, seasonal/ environmental changes, traffic shifts due to higher traffic capacity (new highway or expansion) or shifts from other modes of transportation. Other factors include government traffic interventions such as adding HOV lanes or other traffic reduction

incentives, private/ public investment decisions such as building a new plant, and international events such as hosting the Olympics.

Given that our interest is in a decision-making system that runs over the lifecycle of the highway system (many decades), that the shorter time scale variations could be aggregated in a single point (i.e. the average annual daily traffic (AADT) parameter), and that the most significant traffic fluctuations occur at the yearly time scale, the yearly time scale is the one that will be adopted. To model this uncertainty variable, one could also use a suitable stochastic model with jumps.

2.4.3.5.5 *Highway Service Quality*

In subsection 2.4.3.4.1, we have shown that rehabilitation is an important decision, the timing of which needs to be optimized. When attempting to do so, it becomes imperative to model the highway deterioration time process to know when the rehabilitation ought to be undertaken. Thus, highway deterioration or highway service quality level is another important valuation variable. It can be modeled through subjective discrete indices, such as the discrete-time Markov chain.

2.4.3.6 The Path towards Optimality: The Third Challenge

The complexity of the decision-making process, arising from the many interrelated decisions and the innumerable correlated uncertainties, has brought about voluminous research literature on topics related to decision-making under uncertainty. Techniques like Monte Carlo simulation and artificial intelligence techniques (such as artificial neural networks, knowledge-based expert systems, genetic algorithms, fuzzy logic, and hybrid systems thereof) were all developed in an attempt to facilitate optimal decision-making.

For many decades, researchers and practitioners have continued to apply these techniques to a wide spectrum of engineering applications. Another major challenge in attaining optimality lies in determining the best path towards optimality (meaning the most optimal optimization technique).

One rather recent technique of interest, called real options, is based on financial mathematics. In valuing decision options, it incorporates the value of the very real flexibility that the decision-maker possesses and exercises throughout the lifecycle of a project, in terms of exploiting opportunities by changing the course of decisions depending on the unfolding of the embedded uncertainties. Thus, unlike traditional techniques, where the uncertainty has been typically portrayed as a risk that needs to be mitigated and managed[21], the real options technique strategically manages uncertainties to exploit opportunities that maximize the project value; it offers a more realistic project assessment and consequently may constitute a more reliable decision-making tool than the traditional ones.

For the purpose of this work, the real options optimization technique adopted is adapted from Zhao et al. (2004). It incorporates Monte Carlo simulation and least-squares regression integrated with backward dynamic programming steps. While, in this work, we are interested in improving on this real options technique, we do not claim that this is necessarily the most optimal technique.

---

[21] Uncertainty is prevalently perceived as a negative factor that can only generate losses. This is reflected in the four general methods of risk mitigation, namely: "avoidance, reduction, shifting or transfer, and assumption (CII, 1989)" (Ford et al., 2002).

2.5   Real Options

Ford et al. (2002) provide the following concise literature review of real options:

> Real options theory is based on the approach developed to value and analyse
> options on financial assets (Black and Scholes, 1973; Cox *et al.*, 1979; Bookstaber,
> 1982). Methods for valuing options specifically on real assets have since been
> developed and analysed (Kemna and Vorst, 1990; Trigeorgis, 1993, 1995; Dixit
> and Pindyck, 1994; Brealey and Meyers, 2000), applied to engineering (Baldwin
> and Clark, 2000; Park and Herath, 2000; Benaroch, 2001), and promoted as a
> strategic planning aid by both academics (Kensinger, 1988; Biernlan and Smidt,
> 1992; Amram and Kulatilaka, 1999b; Miller and Lessard, 2000) and practitioners
> (Leslie and Michaels, 1997). The real options approach has been adapted to
> financial strategy (*Myers, 1984*; *Trigeorgis, 1993*). The real options approach has
> been adapted to financial strategy (Myers, 1984; Trigeorgis, 1993). Real options
> have been used to capture latent value in many domains, including natural
> resources, research and development, technology, real estate, and product
> development (Kemna, 1993; Dixit and Pindyck, 1994; Trigeorgis, 1995; Amram
> and Kulatilaka, 1999a; Brennan and Trigeorgis, 2000; Benaroch, 2001).

Real options valuation is based on financial options. In finance, an option is defined as
the right, but not the obligation, to buy or sell an asset (instrument) under specified terms
(Zhao et al., 2004). For example, an option that gives the right to purchase an asset is
called a call option, whereas an option that gives the right to sell an asset is called a put
option. Usually, there is a specified price (called the exercise price) at which the

underlying asset can be purchased or sold upon exercise of the option and a specified period of time over which the option is valid. There are two primary conventions regarding the acceptable exercise dates before expiration: an American-style option allows exercise at any time before and including the expiration date, whereas a European-style option allows exercise only on the expiration date. (Zhao et al., 2004)

As applied to physical assets, real options valuation refers to the options embedded in real operational processes, activities, or investment opportunities that are not financial instruments (Zhao et al., 2004). It is a right without an obligation to take specific future actions depending on how uncertain conditions evolve (Amram and Kulatilaka, 1999). Thus, the value of the option lies in the asymmetry of the right to capture the upside without the obligation to bear the downside (Ng and Björnsson, 2004.) Therefore, the central premise of real options theory is that when the future conditions are uncertain and the managerial strategy may later produce substantial losses/opportunities pending the outcome of these conditions, having flexible strategies, whereby decisions could be delayed until such times as the uncertain conditions are revealed, may reduce a loss or yield a latent value (i.e. be in the money) and thereby should have a price (i.e. option price). This is contrary to the traditional approaches where making/evaluating all strategic decisions invariably occurs at the preliminary planning phase. Essentially,

> [r]eal options theory attempts to answer the questions: what are the future alternative actions; when should we choose between these actions to maximize value based on the evolution of conditions; and how much is the right to choose an alternative worth at any given time (Ford et al., 2001).

In Section 2.4.3.4, we have listed some possible decisions that need to be taken throughout the life cycle of the highway system. Any of these decision alternatives translate into flexibility (a real option), the consideration of which in the analysis can turn the associated uncertainties from risks into opportunities. Of course, the trade-off between the number of real options considered and analysis complexity remains a very significant limitation.

2.6 Jump Processes

The accuracy of any decision-making system involving uncertainty rests on its ability to model the uncertain factors. For example, the case studies presented in Section 2.4.1.10 clearly illustrate how the inaccurate projection of passenger volume and traffic demand contributed to grave shortcomings in Mirabel and the 407 ETR.

An analyst wishing to accurately capture the dynamics of uncertainties should not neglect how certain events, decisions and other factors, such as those marked with (*) in the list of reasons behind the failure to project the passenger volumes of Mirabel Airport, can result in unpredictable major jumps and result in devastating consequences. Modeling this phenomenon of uncertainties dynamics (the jumps) has, so far, been mostly neglected. Yet it is clear that even without any rigorous analysis, it would not be unreasonable to assume the likelihood of spontaneous, possibly correlated, jumps in dynamics of the uncertainty processes.

2.7 *Summary and Conclusions*

In the first few sections of chapter 2, we have emphasized the value of transportation and the need for developing transportation systems. Presenting the complexity of current transportation systems, we showed the relative importance of the highway system and listed some constraints that need to be met by the transportation systems. Later, in Section 2.4, we tackled the topic of decision-making under uncertainty in transportation systems. We showed, in the first subsection (2.4.1), the enormous cost of wrong decisions on various aspects; there, we introduced the new concept of the opportunity cost of wrong decisions as well as the irreversibility as a scaling cost factor. Subsequently, we presented a few real life case studies illustrating the real possibility of errors in decisions on mega-scales. In the second subsection (2.4.2), we claimed that inaction is not a viable option, and stated the reasons for that.

The third subsection (2.4.3) addressed the price of making optimal decisions; listed there were three challenges faced in the development of an optimal decision-making system: the choice of decisions, uncertainties, and optimization technique. Addressing the first challenge (2.4.3.4), we, in accordance with the implementation in Zhao et al. (2004), highlighted the rehabilitation of the system as an important decision that needs to be made, one where the decision making system needs to determine the optimal timing of these decisions. The second decision relates to system expansion, where the system needs to determine the timing of the expansion and the optimal number of lanes to be expanded. Finally, a prerequisite to expansion is land acquisition. Consequently, the third decision is in regards to acquiring the land; in making this decision the system needs to optimize the width of the right-of-way to be acquired in size and time.

The second challenge (2.4.3.5) relates to the underlying uncertainties; not only are they numberless, they are highly correlated, have unknown stochastic dynamics, and consequently require vigorous data analysis and tedious data collection efforts to model. In this segment, we illustrated the numerousness and the high correlation of the underlying uncertainties. Furthermore, we extensively examined some of the most important ones. There, we asserted that in modeling the total highway development cost process, the land acquisition cost, being possibly manifold that of construction, supersedes construction cost in importance. The land acquisition cost is in fact the expropriation price paid to landowners, in which the land price is only one component. Therefore, modeling it solely as land price process involves a great level of simplification.

We also stated that in the highway construction cost, which is still significant, material cost makes up a sizeable part; modeling the volatile material price process may be useful in better capturing that of the construction cost and ultimately the highway development cost process. Other important uncertainties presented were oil price, traffic demand, highway service quality.

The last challenge discussed (2.4.3.6) was the choice of the optimization algorithm, which led to Section 2.5 where we introduced the real options optimization technique adopted in this paper. Subsequently in Section 2.6, we presented jump processes as a means of improving the uncertainty models.

The following chapters will be devoted to the computational aspect of this paper. Despite many of the analytical findings presented thus far, and as stated previously, our computational treatment will mostly follow Zhao et al. (2004) assumptions.

3 Proposed Framework for Highway Decision Analysis

So far, we have analyzed the context of the problem at hand, where we justified the need for and explored the challenges involved in developing an optimal decision-making system. Skimming through different techniques in the field of decision-making under uncertainty, we focused our attention on the real options technique and expressed our interest in advancing the real options algorithm presented in Zhao et al. (2004). In the next few chapters, we will attempt to advance the algorithm by improving on some of its mathematical assumptions.

In first section of this chapter, we will present the assumptions, the case study, and the solution algorithm of Zhao et al. (2004), as we will adopt the same settings and a similar algorithm in our implementation. Then in the next section, we will list some of the limitations of the Zhao et al. (2004) in light of the findings of chapter 2, and finally we will define the scope of our mathematical contribution in the third section.

3.1 *Highway Development under Uncertainty: A Real Options Approach*

Optimality, which is to be sought at all phases of the life of the highway system, can be achieved through the maximization of the overall highway system value (which can be subjective) among the different possible scenarios by simulating the evolution of uncertainties and the corresponding timely exercitation of the different decision options. The different scenarios are generated by altering the various conceivable combinations of decision options available.

In Zhao et al. (2004), a multistage stochastic model for decision making in highway development, operation, expansion, and rehabilitation is developed. Accounting for the evolution of three uncertainties (traffic demand, land price, and highway service quality index), the algorithm applies the real options approach through the incorporation of Monte Carlo simulation and least-squares regression integrated with backward dynamic programming steps. In the algorithm, the modeled decisions options are the exercitation options regarding the size of land acquisition as well as the number of lanes to be expanded or rehabilitated. The method introduced not only can select the optimal design alternative in the design phase but also can provide timely decisions on additional right-of-way acquisition and highway expansion and rehabilitation during the operation phase. Below is a more detailed description of the algorithm.

3.1.1 Embedded Real Options

Beginning from the early planning phase to the design, and the construction all the way to the operation phase, there are many complicated decisions that ought to be made throughout the life-cycle of the highway system (as alluded to in 2.4.3.4). Each decision may provide a different level of flexibility and therefore can potentially be modeled as a real option. The real options embedded in the life-cycle of the highway systems refer to the decision options that may provide flexibility for future decision making or those that may be flexibly exercised to cope with the revealed uncertainty. Being exercisable at any time (discrete) during the highway service life, these real options are of the American-style. Consistent with Zhao et al. (2004), the three real options considered here are:

- **Right-of-way Acquisition**: According to Zhao et al. (2004), "A right-of-way contract is apparently a real option of expansion. Acquiring the required right-of-way is needed for every highway expansion (widening) process. Acquiring additional right-of-way width beyond the immediate need may be viewed as reserving land. This may reduce the risk associated with land availability and price fluctuation in future highway expansion". Exercising this real option involves the determination of the optimal time and the width of land to be acquired.

- **Highway Expansion**: "With an acquired right-of-way, the DM [decision maker] may exercise the expansion real option. The decision making regarding exercising this real option involves the determination of the optimal timing and the number of expansion lanes at different stages in the life cycle" (Ibid.).

- **Rehabilitation Decisions**: "These decisions may be viewed as real options because they can be made flexibly to cope with highway deterioration ... the focus is on the exercise timing and the opportunity profit due to proper exercise of the option" (Ibid.).

3.1.2 Underlying Uncertainties

There are many uncertainties that a highway system is subjected to over time, such as changing requirements of users in terms of traffic demand, changing social and economic environment, changes in technology, and deterioration of the highway. These can be broken up into internal and external uncertainties. The internal uncertainties refer to those integral to the advancement of the highway, such as aging and deterioration. The

external uncertainties correspond to the variability in the external environment that may affect decision-making, such as land price, labour cost, traffic demand, political and socio-economic environment, land availability, and natural hazards such as earthquakes, hurricanes, and floods. Again, the underlying uncertainties that will be modeled will be those in Zhao et al. (2004).

Traffic Demand

The fundamental measure of traffic volume is the annual average daily traffic (ADT), which is defined as the number of vehicles that pass a particular point on a roadway during a period of 24 consecutive hours, averaged over a period of 365 days. ADT values can be converted to other measures of traffic, such as peak hourly volumes using empirical relations. The demand for traffic volume, denoted by Q, is represented by the ADT values. For toll roads in particular, being able to forecast the demand for traffic volume is an important task for economic reasons. There are potential pitfalls in forecasting traffic demand including data quality and model accuracy, system stability over time, land use, travel behaviour, value of time, etc. Other pitfalls could include development of competing facilities and changes in political and economic environment. These pitfalls worsen the accuracy in forecasting traffic demand and eventually become an underlined uncertainty for the highway system over its life-cycle. Because of the wide variability of traffic flow over time, the demand Q was modeled in Zhao et al. (2004) as the following stochastic process:

$$\frac{dQ}{Q} = \mu_Q(Q,t)\,dt + \sigma_Q dz_Q,$$ (3.1)

where z_Q is a Wiener process. In particular, $\mu_Q(Q,t)$ is called the drift function, and

σ_Q is the volatility. Without the noise z_Q, the demand pattern can be obtained by

solving the following differential equation:

$$\frac{dQ}{Q} = \mu_Q(Q,t)\,dt$$ (3.2)

A positive drift term means the uncertainty tends to drift up over time and the greater the

volatility, the more volatile the uncertainty evolution.

Land Price

Land prices vary over time and are dependent on land use, which is used as an input to

forecast traffic demand. One should always estimate the market value of land at its best

use. Land appraisal is usually implemented by one of the following three approaches:

cost, sales comparison, and income capitalization. Land price, denoted by P, was

assumed in Zhao et al. (2004) to follow the below stochastic process:

$$\frac{dP}{P} = \mu_P(P,t)\,dt + \sigma_P dz_P,$$ (3.3)

where z_P is a Wiener process, and $\mu_P(P,t)$ and σ_P are the drift function and volatility

of land price, respectively.

Highway Service Quality

The highway service quality is the degree to which the highway serves users and fulfills

the purpose that it was built for. It can be represented by a condition index, on a scale of

1 to 5, corresponding to the condition of very poor, poor, fair, good and excellent,

respectively. The condition index at time t is denoted as I_t, and $\{I_t, t = 0, 1, 2, \cdots\}$ is a

(discrete-time) Markov chain, that takes value in $\{1, 2, 3, 4, 5\}$ and $\{I_t\}$ decreases over

time. The stochastic process $\{I_t\}$ can be seen as the deterioration process of the highway

if no maintenance is done to the highway. The factors that cause this physical

deterioration are load, environment, construction quality, and material degradation.

Interdependency of the Uncertainties

There are well-pronounced interdependencies existing among uncertainties, such as

demand, land price and service quality. Improved service quality on a highway system

increases the "induced traffic", while improved economic conditions increase the

"developed traffic". Both induced and developed traffic improve the region's social and

economic situation which will result in an increase in land use and price. Moreover,

traffic demand and land price may be positively correlated due to regional development.

To model this, a correlation can be imposed to the two Wiener processes that control the

uncertainty evolutions, e.g.,

$$\mathrm{cov}\left(z_Q,\ z_P\right) = \rho_{QP}, \tag{3.4}$$

where ρ_{QP} is a constant. It is also possible that an increase in highway demand would

accelerate the deterioration of the highway and reduce service quality. The state transition

probabilities of the Markov chain can be modeled in such a way that they are dependent on μ_Q and σ_Q; however, this will not be considered.

3.1.3   Multistage Stochastic Model

The standard notations Q_t, P_t, and I_t are traffic demand, land price, and highway condition index at time t, respectively.

t = index for time $(t = 0, \cdots, T)$ in years, where T= length of the planning horizon over the life cycle of the highway system. n_t = state variable indicating the number of lanes of the highway at time t, where $n_t \in \{2,4,6,8\}$. Δn_t = decision variable indicating the number of lanes of the highway to be expanded at time t, where $\Delta n_t \in \{2,4,6\}$. w_t = state variable indicating the right-of-way width at time t. Assume that the width of right of way along the highway is uniform and $w_t \in \{150,175,200\}$ (ft). Δw_t = decision variable indicating the width of the right of way to be acquired at time t, $\Delta w_t \geq 0$. $h_t \in \{0,1\}$ is a decision variable for rehabilitation. v_t = a vector (collection) of the decision state variables at time t, where $v_t = (n_t, w_t)$. u_t = a vector (collection) of decision variables at time t, where $u_t = (\Delta n_t, \Delta w_t, h_t)$. X_t = a vector (collection) of underlying uncertainties at time t, $X_t = (Q_t, P_t, I_t)$. $f_t(v_t; X_t)$ = revenue function of the highway system in time period t under state v_t, conditioned on the uncertainty realization of X_t at time t. (Note the semicolon (;) distinguishes variables from parameters. In this case, X_t is a parameter.) $c_t(u_t, v_t)$ = cost incurred for making decision u_t under state v_t at time t.

Assume at state v_t at time t, the uncertainty vector X_t is revealed. Upon observing X_t, the DM [decision-maker] (i) must realize the current system revenue $f_t(v_t; X_t)$ and (ii) strategically utilize the available flexibility [decision options] by making decisions u_t with a cost of $c_t(u_t, v_t)$ incurred (Ibid.).

$F_t(v_t, X_t)$ is the total value (expected profit) of the system for the remaining period at state v_t at time t. Given the above, the problem can then be formulated by the following recursive relation:

$$F_t(v_t, X_t) = f_t(v_t, X_t) + \max_{u_t}\left\{e^{-r}E_t\left[F_{t+1}(v_{t+1}, X_{t+1})\right] - c_t(u_t, v_t)\right\}$$ (3.5)

where r = risk-adjusted discount rate over one year, E_t = expectation operator, and subscript t = expectation based on the available information for the uncertainty X_t at time t, and $t \in [0, T-1]$ (Ibid.). The expectation in Eq. (3.5) is constrained by the following:

State Transition Constraints:

$$n_{t+1} = n_t + \Delta n_t \leq 8 \quad \forall t$$ (3.6)

$$w_{t+1} = w_t + \Delta w_t \leq 200 \ (\text{ft}) \quad \forall t$$ (3.7)

Expansion Constraints:

$$n_t \omega \leq w_t \quad \forall t$$ (3.8)

where ω = lane width

Rehabilitation Constraints:

$$h_t = 1 \ \text{ if } \ I_t = 1$$ (3.9)

$$I_{t+1} = 5 \quad \text{if} \quad h_t = 1 \tag{3.10}$$

$$h_t \in \{0,1\} \quad \forall t \tag{3.11}$$

Initial Conditions:

$$\text{At } t = 0, \; v_0 = \tilde{v}_0, \; X_0 = \tilde{X}_0$$

Revenue Function:

$$f_t(v_t; X_t) = \text{Revenue from traffic flow} + \text{Revenue from land} \tag{3.12}$$

$$\text{Revenue from traffic flow} = \gamma \min\left[\alpha.n_t\, x\left(I_t\right), Q_t\right] \tag{3.13}$$

where γ = average yearly revenue per vehicle; α = lane capacity of ADT (Annual Average Daily Traffic); $x\left(I_t\right)$ = weighing factor of the revenue in terms of the highway service level.

$$x\left(I_t\right) = \beta^{5-I_t}, \quad \beta \in (0,1) \tag{3.14}$$

$$\text{Revenue from land} = \ell\left(w_t - \omega n_t\right)d \tag{3.15}$$

where d = total distance of the highway and ℓ = per mile revenue that the highway owner may obtain from the land use such as planting crops, parking lots, or other commercial developments.

Cost Function:

$$
\begin{aligned}
c_t(u_t, v_t) &= \text{expansion cost} + \text{right-of-way acquisition cost} + \text{rehabilation cost} \\
&= d\left(c_n \Delta n_t + P_t \Delta w_t + c_m n_t h_t\right)
\end{aligned} \tag{3.16}
$$

where c_n = construction cost and c_m = rehabilitation cost; both measured per lane and per mile. Note: at time t, $c_t(\cdot)$ is known with certainty only at time t.

Algorithm Development:

Define:

$$\pi_t(X_t; u_t, v_t) = E_t\left[F_{t+1}(v_{t+1}; X_{t+1})\right] \qquad (3.17)$$

where u_t and v_t = parameters.

If $\pi_t(\cdot)$ is known for all the different realizations (u_t, v_t) at time t when X_t is revealed, then the decision-maker would know the expected system value at time $t+1$ and consequently make the optimal decision. From (3.5), the optimal system profit at time $= t$ at state v_t becomes:

$$F_t(v_t, X_t) = f_t(v_t, X_t) + \max_{u_t}\left\{e^{-r}\pi_t(X_t; u_t, v_t) - c_t(u_t, v_t)\right\} \qquad (3.18)$$

The difficulty, however, arises when trying to evaluate $\pi_t(\cdot)$ given the nonexistence of or at least the difficulty of obtaining an analytic form for $\pi_t(\cdot)$. To tackle this problem Zhao et al. (2004) employs numerical methods based on Monte Carlo simulation and least-square regression integrated with backward dynamic programming steps to approximate $\pi_t(\cdot)$; this is done as described below.

To approximate $\pi_t(X_t; u_t, v_t) = E_t\left[F_{t+1}(v_{t+1}; X_{t+1})\right]$ in Eq. (3.17), N data samples $\left(X_t^{(i)}, X_{t+1}^{(i)}\right)$, $i = 1, \cdots, N$ are generated based on the uncertainty model of X_t. For a given (u_t, v_t), $F^{(i)} = F_{t+1}\left(v_{t+1}; X_{t+1}^{(i)}\right)$ in Eq. (3.5) are calculated for $i = 1, \cdots, N$. Subsequently,

the values and the functional forms of $\pi_t \left(X_t ; u_t , v_t \right)$ are simultaneously estimated by the

best function that regresses $F^{(i)}$ on $X_t^{(i)}$ for $i = 1, \cdots, N$.

For each given decision $\left(\Delta n_t , \Delta w_t , h_t \right)$ under each state, v_t, and highway quality

index, I_t, the functional form used in the regression is assumed to take the form below:

$$\pi_t \left(\cdot \right) = a_1 + a_2 P_t + a_3 Q_t + a_4 Q_t^2 + a_5 Q_t^3 + a_6 Q_t^4 \tag{3.19}$$

The above represents the Monte Carlo and the regression segments of the algorithm. The

backward dynamic programming component of the algorithm (that is based on Bellman's

principle of optimality) calculates $\pi_t \left(\cdot \right)$ backward in time from $t = T$ by letting at this

time step,

$$\pi_T \left(X_T ; u_T , v_T \right) = 0, \qquad \forall u_T , v_T , X_T \tag{3.20}$$

and determining $\pi_{t-1} \left(X_{t-1} ; u_{t-1} , v_{t-1} \right)$ from $\pi_t \left(X_t ; u_t , v_t \right)$, as illustrated in the following

algorithm.

Algorithm: Obtaining $\pi_{t-1} \left(X_{t-1} ; u_{t-1} , v_{t-1} \right)$ with $\pi_t \left(X_t ; u_t , v_t \right)$ known for all u_t , v_t.

Data: u_{t-1} and v_{t-1} are given.

- Step 0: Set $i \leftarrow 0, F^{(i)} \leftarrow 0$

- Step 1: If $i > N$, go to step 4. Otherwise, generate a random vector $X_{t-1}^{(i)}$.

- Step 2: Evaluate $F^{(i)} = f_t \left(v_t , X_t^{(i)} \right) + \max\limits_{u_t} \left\{ e^{-r} \pi_t \left(X_t^{(i)} ; u_t , v_t \right) - c_t \left(u_t , v_t \right) \right\}$

- Step 3: Update $i \leftarrow i + 1$ and $F^{(i)} \leftarrow 0$, then go to step 1.

- Step 4: Regress $F^{(i)}$ on $X_{t-1}^{(i)}$ to obtain $\pi_{t-1} \left(X_{t-1} ; u_{t-1} , v_{t-1} \right)$

At $t = 0$, setting $u_0 = \bar{u}_0$, $v_0 = \tilde{v}_0$, and $X_0 = \tilde{X}_0$, the maximization in step 2 gives the optimal decision that yields the maximal expected system profit.

The above was essentially the model proposed in Zhao et al. (2004); for other model details and descriptions, algorithm development and challenges, the reader is encouraged to refer back to the original paper (Zhao et al., 2004), where most of the content of this section was obtained.

3.2   Some Limitations of the Paper

Some of the limitations of Zhao et al. (2004) are presented in the paper itself; the numerous limitations essentially stem from the simplified assumptions made in the paper. A few of these are that:

1. only three uncertainties and three decisions/ real options are considered;

2. the uncertainties considered are independent of the decision-maker's decisions;

3. the highway quality index uncertainty is independent on traffic demand;

4. highway expansion does not improve highway quality

5. the continuous state uncertainties follow geometric Brownian motion;

6. the width of right-of-way along the highway is assumed to be uniform; and

7. the expectation operator in Eq. (3.5) is not measured in risk-neutral framework.

However, in view of our analysis in Chapter 2, there exist additional noteworthy limitations, part of which will be the centre of our mathematical contribution.

We have shown in 2.4.1.5 and 2.4.3.5.1 that material cost is highly volatile and that it represents just under half of the total highway construction cost. Thus, the volatility of material cost should directly lead to a positively correlated level of volatility in the cost of expansion and rehabilitation. However, in Eq. (3.16), the total cost function $c_t\left(u_t, v_t\right)$ assumes that c_n and c_m to be constant. This assumption of certainty of these unit costs in the value of total cost may, therefore, constitute a significant oversimplification.

Also in 2.4.1.5 and 2.4.3.5.1, the land acquisition cost was shown to be the sum of the land price, the amount of decrease in the value of the remaining property, and other

damages to the landowner(s). What is modeled in Eq. (3.16), however, is simply the land price, $d\left(P_t \Delta w_t\right)$, which accounts for only one segment of the actual land acquisition cost. Because the other two costs items are relatively massive and volatile, considering the quantity $d\left(P_t \Delta w_t\right)$ alone can be a grave underestimation of the true land acquisition cost. Moreover, it was shown in subsection 2.4.3.4.3 that even the size of the land (or its width, Δw_t) to be eventually acquired can vary substantially, and thus to assume the width to be uniform introduces some error as well.

To remedy this deficiency, the other two segments could be modeled individually and incremented to the land price, where the land price can be modeled as time-varying stochastic process; the damages components of the land acquisition cost, on the other hand, are time-invariant uncertainties that are applicable only at the very last point of the land price trajectory. To be able to model them individually, one would need to collect detailed statistics on land acquisition costs.

Uncertainty models represent the building blocks of the decision-making system at hand. Inaccurate representation of the uncertainty models may lead to erroneous decisions bearing potentially enormous monetary, human and other consequences; accurate modeling, on the other hand, involves great challenges, one aspect of which is determining the true distribution of these uncertainties.

Another limitation in Zhao et al. (2004) relates to the uncertainty model assumptions; lacking any justification, the geometric Brownian motion model seems to be adopted out of mere mathematical convenience.

Furthermore, in light of our discussion in Section 2.6, another limitation is the lack of consideration of jumps. The incorporation of jumps can be a means to account for the time-invariant components of the cost uncertainty above as well as many other explainable and unexplainable patterns in the dynamics of uncertainty processes in general.

While previously in this chapter, we presented as background the general backbone of the decision-making system adopted, the one that is actually implemented is presented in Chapter 6. There, further critiquing will take place as we present the decision-making algorithm implemented.

3.3 Scope of Mathematical Contributions

Having studied the anatomy of the highway systems and having diagnosed many of their challenges and limitations, we now move on to problem treatment. Our treatment efforts will be mainly mathematical-computational in form and will centre on some aspects of the uncertainty factor.

In Zhao et al. (2004) the continuous-time[22] uncertainties, the land price and the traffic demand, were modeled as correlated geometric Brownian motions. In what follows, we will verify the validity of this normality assumption and investigate the presence of jumps. Subsequently, we will propose a class of models that incorporates jumps and implement and analyze certain models of this class. These models, applied to X_t in step 1 of the solution algorithm above, can improve the uncertainty models and may alleviate some of the deficiencies presented earlier.

---

[22] While modeled as continuous time processes, they are sampled at discrete times.

4 Testing the Validity of the Assumptions of Normality & Lack of Jumps

If, for a decision optimization system, choosing the right set of uncertainties makes option valuation more accurate, correctly modeling these uncertainties makes it more precise. Accurate modeling and simulation of the uncertainties is essential for an accurate analysis and correct decisions: garbage in-garbage out.

Zhao et al. (2004) assumes that the highway traffic volume and the land price uncertainties follow the geometric Brownian motion model. In order to test this assumption, one needs to collect real data on traffic demand and land acquisition costs.

In the following section we will look into means of collecting data and in Section 4.2, we will, in subsection 4.2.1, test the validity of this statistical assumption and draw some general conclusions on the distributional properties of the collected data. This leads to subsection 4.2.2, where we investigate the presence of jumps.

4.1 Data Availability

In this section, we will explore some venues where highway traffic volume as well as both unit land price and total land acquisition cost data could be obtained in Ontario, Canada.

4.1.1 Traffic Volumes

As seen in chapter 3 above, to calculate the highway system revenues of the different decision options, traffic volumes need to be simulated. Therefore, to better understand the distributional properties of the traffic demand uncertainty and test the normality assumption in Zhao et al. (2004), data needs to be collected. Generally speaking, this data is easily available but, unfortunately, not in sufficiently large numbers, given the yearly time scale adopted. Below are two sources of traffic demand data.

4.1.1.1 GTA Regional Traffic Demand Statistics

Traffic volume data can be obtained from the Traffic Planning and Information Services Sections (TPISS) of various Regional Traffic Offices of the Ontario Ministry of Transportation in the Greater Toronto Area (GTA). Traffic data such as volume, occupancy and average speed, collected through Vehicle Detector Systems (VDS) installed along Highway 401 and sections of the QEW across the GTA, are stored in the Freeway Traffic Management System (FTMS) Data Warehouse Systems (DWS). The TPISS, having access to this system, extracts 24x7 volume data in a standard three season inventory cycles (spring, summer & fall) on yearly basis, subject to available/ functional VDS stations.

We have been able to collect from the Central Region Traffic Office traffic volume

counts for QEW–Burlington corridor for the five year period (2001-2005). However, our

interest is in Annual Average Daily Traffic (AADT[23]) counts. Therefore, while seemingly

abundant, after mathematical massaging, the data collected would translate into only 5

points, which is a very small sample size. A sample traffic volume data is available in

Appendix 1.

4.1.1.2 Ontario Traffic Demand Statistics

Another readily available source of traffic volume statistics is the Provincial Highways

Traffic Volumes 1988-2003 Manual available online on the Ontario Ministry of

Transportation (MTO) website (Ontario Ministry of Transportation, 2006). The report

lists, among other averaged traffic volume information, the Average Annual Daily Traffic

(AADT) for each section of the highways under the jurisdiction of MTO.

The statistics contained in the report, having a bigger sample size (15 as opposed to 5),

being readily available in the sought AADT time scale, and being "obtained from sources

considered to be reliable" are to be used in analysis (Ontario Ministry of Transportation,

2006)[24]. A sample traffic volume data is available in Appendix 2.

---

[23] AADT: Average 24-hour, two way traffic for the period January 1 to December 31.
[24] It should be noted that although the Ministry of Transportation asserts that this data is accurate, it also
states that "[t]he Ministry makes no representation or warranty, expressed or implied with respect to [the
data's] accuracy or completeness".

4.1.2 Land Acquisition Cost

The multistage stochastic model of Zhao et al. (2004) presented in chapter 3 also includes the land price as one of three cost components of the total highway development cost function (Equation (3.16)); the other two components being the highway expansion costs and the cost of rehabilitation.

It was shown in 2.4.3.5.1 that the land expropriation cost may represent more than 65 times the construction cost, and that the rehabilitation cost is relatively less significant. Hence, accurate modeling of the land acquisition cost uncertainty in any decision-making system involving highway development is of paramount importance. In addition, the section also revealed that land acquisition cost is in fact the expropriation price paid by the government, which is composed, for a given expropriated land, of the sum of the market price of the expropriated land, the amount of decrease in the value of the remaining property and other damages to the landowner. The former component is time-dependent, while the latter two are case-specific. Therefore, ideally, the cost data that needs to be collected, analyzed, modeled and then simulated are: 1. historic unit land prices extending to the time of expropriation, and 2. the actual cost that is being incurred by the government at the time of expropriation in acquiring the land (expropriation price). Here, the expropriation price is the combination of the very last data point (that at the time of expropriation) of the land price trajectory in 1 and the compensation payment to damages sustained by landowners as a result of the expropriation.

In general, land related statistics, unlike those of traffic volumes, are challenging to collect. In the next two subsections, we will explore some areas where it is possible to collect historic land prices and actual land acquisition costs in Ontario.

4.1.2.1 Historic Land Sale Prices

4.1.2.1.1 Land Registry Offices

In Ontario, the Ministry of Government Services keeps physical records of all patented lands in 54 Land Registry Offices (LRO) located in 53 locations across Ontario. One manual method to obtain various land-related statistics is possible by directly contacting, for a specific land parcel, the appropriate Land Registry Office[25]. On April 24, 2006, Randy Reese, Manager of Business Improvements at the Ontario Ministry of Government Services, stated in an email to the author of this paper that, "if the land is patented and the government purchased the lands, the Transfer/Deed[26] of Land would be recorded on title to the property". However, the purchase price may or may not be included in the document. Even if included, a breakdown of the expropriation price in terms of Eq. (2.1) would not be available (i.e., the land price and the landowner compensation segment of the expropriation price would be irretrievable).

Moreover, apart from expropriation costs, other historic sale prices, if recorded, would only be available when a Transfer/Deed of Land would have occurred and that for a particular land parcel would not normally be frequent enough for a rigorous statistical

---

[25] On April 24, 2006, Randy Reese also stated that, "You need to know which Land Registry Office the land is in based on the County/District or Regional Municipality of the land. You also need the Property Identification Number (PIN) of the property. This can be obtained by various search methods such as search by name or search by address or on-site in the specific land registry office by lot/plan number".

[26] A deed is the document that legalizes a transfer of ownership of a real estate, which contains the names of the old and new owners, as well as a legal description of the property.

analysis. This indicates that average regional annual unit land sale prices should be sought instead. However, the task of extracting historic sale prices from physical records is very laborious and eventually the quality of results depends on the number of sale prices actually recorded. Such an endeavour is beyond the scope of this work.

4.1.2.1.2 Province of Ontario Land Registration and Information System: POLARIS

With the Province of Ontario Land Registration and Information System (POLARIS), "[t]he Province of Ontario is the first jurisdiction in the world to provide electronic registration of land-related documents" (Government of Ontario, 2007). The government of Ontario website explains that, "POLARIS consists of two databases: the title database with its abstracts of title information; and a database of maps". The records contained in the system are accessible commercially through a private gateway software, Teraview Software[27]. Having access to Ontario's land registry information, the online service GeoWarehouse can also be valuable tool; "[i]ts database contains over 4 million properties from the automated land registry database and delivers the data [one needs] in convenient reports" (Teranet, 2006). Two reports that GeoWarehouse generates that could be of use for undertakings such ours are:

- "The Sales History Report [, which] provides historical ownership and sale price information for subject properties [and;]

- The Neighbourhood Sales Report [, which] delivers accurate sales information within a geographic radius and for a time period that [one specifies]" (Ibid.)

---

[27] For more information about Teraview Software, please visit their website at http://www.teranet.ca/services/gov.html.

However, according to Randy Reese,

> The POLARIS records do not contain a complete historical record of the lands. They are complete with all outstanding encumbrances and interests as to a specific date forward which is the date of automation. The date of automation varies between Land Registry Offices and within each Land Registry Office since the records physically could not all be automated on the same day. The title prior to the automated records is obtained in the specific Land Registry Office.

The title data contained in the commercial (GeoWarehouse) database is delivered directly from the POLARIS database. Therefore, while convenient, the commercial database would not contain additional land price information to that available on POLARIS and consequently that at the land registry offices. Therefore, any scarcity of historic land prices existing at the source would only be translated in the commercial database reports. Despite that, the POLARIS Neighbourhood Sales Reports may still be useful in obtaining historic data on unit land prices in the neighborhood of the highway, although this was not attempted in this work.

4.1.2.1.3 Other Sources of Historical Land Prices

Even if historic sale prices of lands are not recorded at the LROs or POLARIS, there are other ways to arrive at this data, which are perhaps difficult but not impossible. Some of these, which are useful in land appraisal, are listed in the article "Sources of Historical Data for Appraisal Reports" by Chris Dumfries (2002) of the Appraisal Institute of Canada. These sources include historical archives, the Department of Indian and Northern Affairs Canada (e.g. land leases and bylaws), the knowledge of band members, and data

from Revenue Canada. For more details, the reader is advised to refer to the original article.

4.1.2.2 Land Acquisition and Landowner Compensation Costs

Ideally, the land acquisition cost is the quantity that should be modeled and not merely the sub-cost, the land price. Where the land price component of the land acquisition cost is time-dependent, the other component, the landowner damages, is time-independent and case-specific.

To be able to model the landowner compensation cost portion of the land acquisition cost, real cost data of expropriated lands needs to be collected. A natural place to seek such data is the expropriating government agency itself (i.e. the Ministry of Transportation). Land acquisition cost data could be sought for an existing highway that is to be expanded. Otherwise, for a new highway, land expropriation data from another highway in a similar region could be used, as well as land expropriation data for any other public purpose at the same or nearby sites as the new highway. The process of collecting such data, containing confidential information, falls under the Freedom of Information Act. This route was not pursued here, being beyond the scope of work.

4.1.3 Data Used

The statistics to be used in this thesis are the following: for traffic volumes, data were obtained from the Provincial Highways Traffic Volumes 1988-2003 (Ontario Ministry of Transportation, 2007). For unit land prices in urban and rural areas, data were obtained from Colliers International Industrial Land Sale Report (Colliers International, 2006) and from Farm Credit Canada (2006), respectively.

4.2   Data Analysis

Inaccurate simulation of the underlying uncertainties may lead to inaccurate valuation
and consequently may lead to poor recommendations/decisions. In turn, this may result in
such devastating consequences as we saw earlier. As the accuracy of uncertainty
simulation hinges on its underlying stochastic assumptions, we will analyze the
mathematical models of the continuous-time uncertainties in Zhao et al. (2004), the
traffic volume and the land price. In doing so, we will use the data collected to investigate
the validity of the geometric Brownian motion process assumption by exploring some
distributional properties of these uncertainties.

4.2.1   Examining the Geometric Brownian Motion Assumption

In their article, "On the Validity of the Geometric Brownian Motion Assumption",
Marathe and Ryan (2005) confirm that,

> Many recent engineering economic analyses have relied on an implicit or explicit
> assumption that some quantity that changes over time with uncertainty follows a
> geometric Brownian motion (GBM) process […] The GBM process, also
> sometimes called a lognormal growth process, has gained wide acceptance as a
> valid model for the growth in the price of a stock over time […] Under this model,
> the Black-Scholes formulas for pricing European call and put options, as well as
> their variations for a few of the more complex derivatives, provide relatively
> simple analytical evaluation of asymmetric risks.

To that extent, Marathe and Ryan (2005) further assert that "[m]any recent examples of
GBM models have arisen in real options analysis, in which the value of some 'underlying

asset' is assumed to evolve similarly to a stock price." The real options application in Zhao et al. (2004) is one such example. However, "[a]s pointed out in Thorsen (1998), the GBM process assumption must be subject to test. Where significant financial impacts may result from the decision, it is of utmost importance to verify that a time series follows the GBM process, before relying on the result of such an assumption" (Ibid.). Likewise, this also applies in the case of Zhao et al. (2004). In fact, lacking any justification, the GBM assumption perhaps had been motivated by mere mathematical convenience. In what follows, some aspects of the geometric Brownian motion assumption in modeling the traffic demand and the land price stochastic processes will be tested.

There are statistical implications to the GBM assumption, one of which is the non-stationary characteristic of the uncertainty increments. Geometric Brownian motion is a log-normal diffusion process, whose variance grows proportionally with time. Thus, in the long run, the simulated uncertainty values would tend to substantially deviate/drift away from realistic values albeit preserving the mean value. This is, to some extent, a non-issue in Zhao et al. (2004) given the yearly time scale adopted, as this assumption results in a relatively short time series. However, there are other consequences to the GBM assumption, such as the independence of the GBM process increments and the normality of the log increment ratios. While we will not delve into the independence aspect in this paper, we will test the normality consequence.

4.2.1.1 The Normality Assumption

The uncertainty dynamics, when modeled as a log-normal diffusion process implies that the increments of the logarithm of the uncertainties, or equivalently, the logarithm of the ratios of the uncertainty data (log-ratios), are normally distributed. In what follows, we will examine the validity of this normality assumption.

To investigate the validity of the normality of the log ratios of the annual traffic volume and land price data, we will construct Quantile Quantile Plots[28] (Q-Q plots) for a sample of highway sections as well as two other ones for average industrial land prices in the GTA and for national and provincial farmland prices. Results are portrayed below.

---

[28] Q-Q Plot is a graphical technique to determine whether two data sets come from populations with a common distribution; here samples quantiles of the logarithm of the data ratios will be plotted against the theoretical quantiles from a normal distribution. If the distribution of the log ratios of the traffic volume data is normal, the plot will be close to linear.
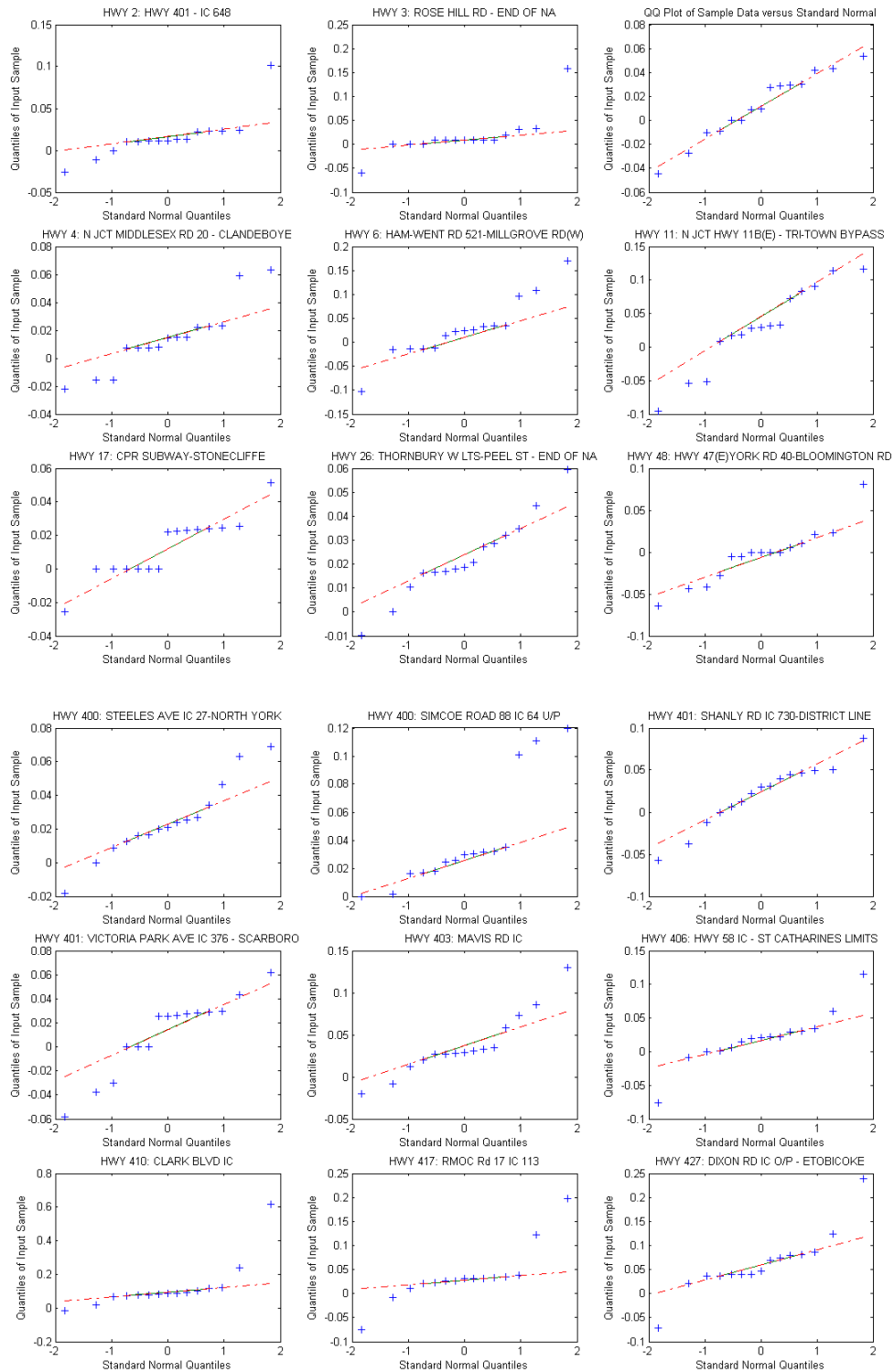
Figure 4-1: Q-Q Plots of Log-ratios of Traffic Volumes on a Sample of King's Highway Sections (1988-2003).

The Q-Q plots in Figure 4-1 above belong to samples from sections of King's highways[29]. Traffic on these sections ranges from few thousands to few hundreds of thousands of AADT. Whereas, plots presented in Figure 4-2 and Figure 4-3, below, relate to Secondary highway[30] and Tertiary road[31] sections with traffic in the range of tens to several hundreds of AADT, respectively.
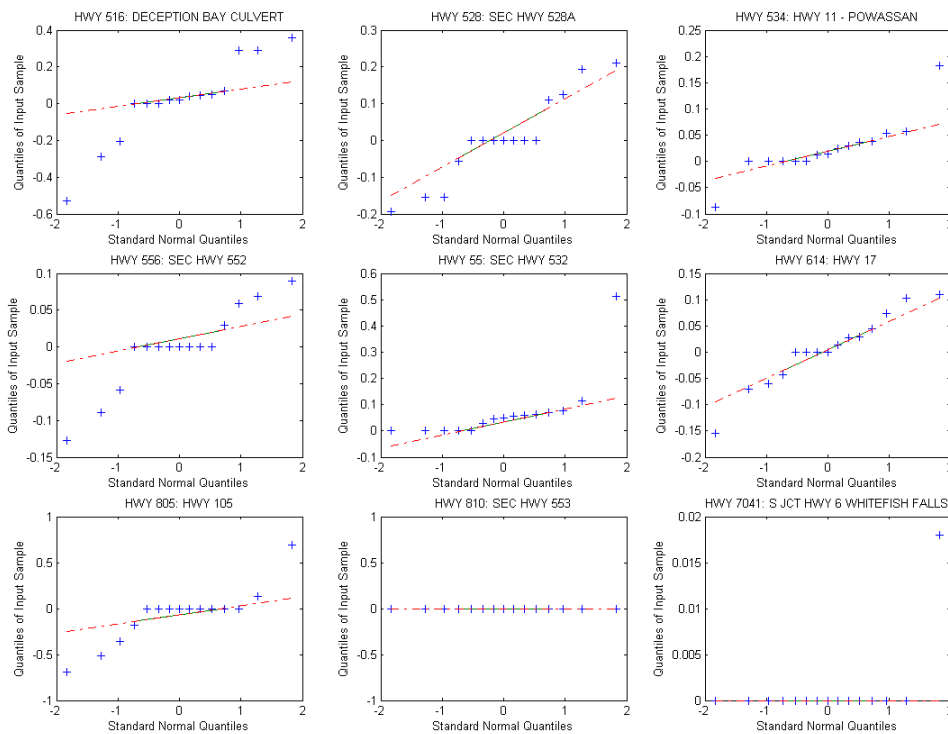
Figure 4-2: Q-Q Plots of Log-ratios of Traffic Volumes on a Sample of Secondary Highway Sections (1988-2003).

---

[29] Kings Highways include: Queen Elizabeth Way (Q.E.W.), Highway 2 to Highway 148, and the 400 series (Highway 400 to Highway 427)

[30] Secondary Highways include: Highway 502 to Highway 673

[31] Tertiary Roads include: Highway 801 to Highway 811
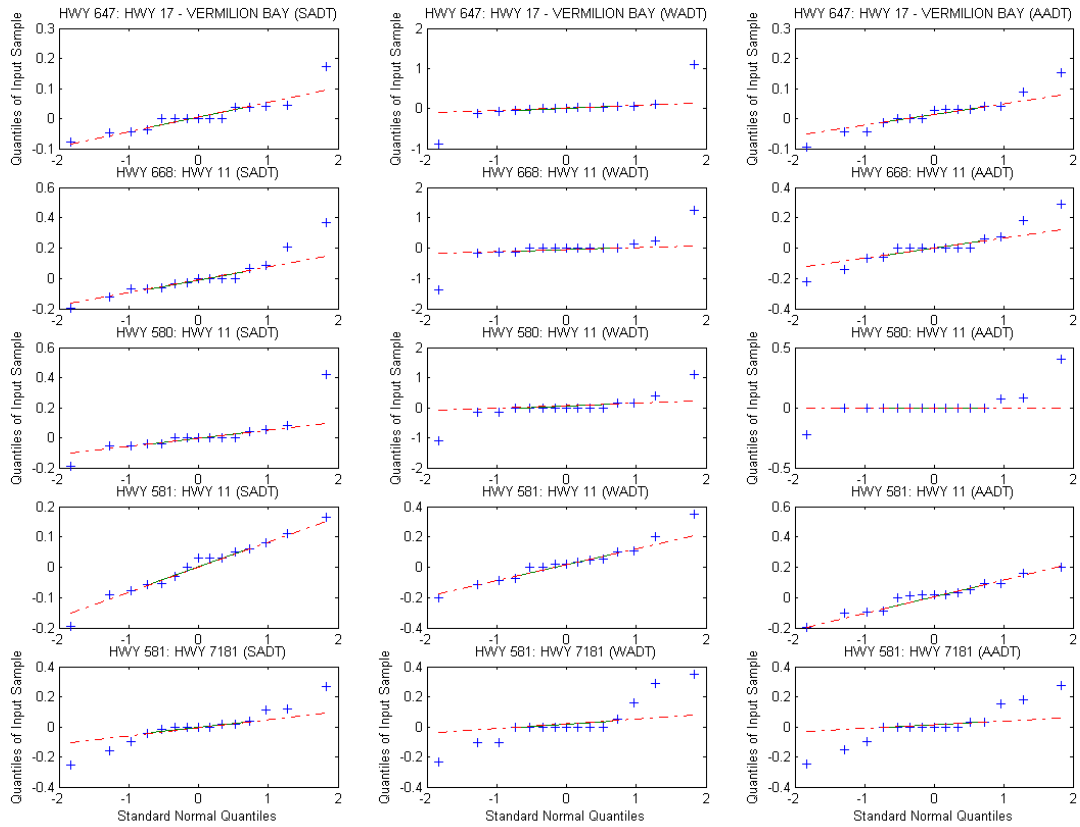
Figure 4-3: Q-Q Plots of Log-ratios of Traffic Volumes on a Sample of Tertiary Road Sections: Summer, Winter, and Average Annual Daily Traffic Counts (1988-2003).

With reference to land price statistics, the Q-Q plots in Figure 4-4 relate to industrial land prices in the Greater Toronto Area (GTA), whereas those in Figure 4-5 and Figure 4-6 relate to national and provincial farmland prices, respectively.

100
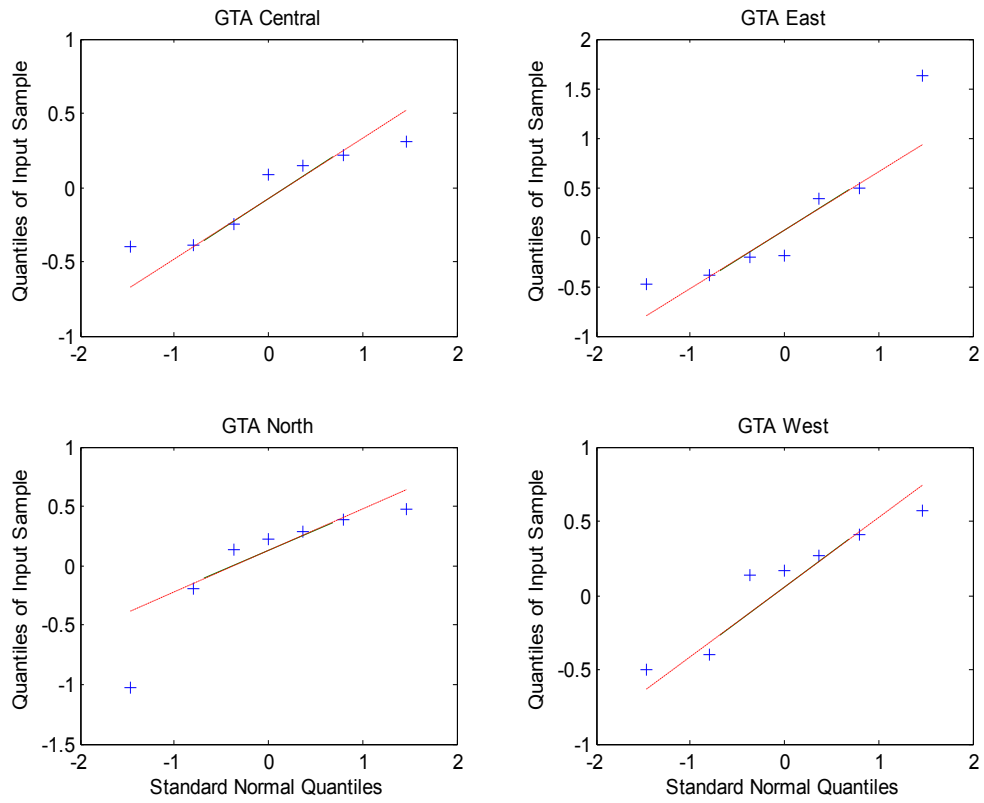
Figure 4-4: Q-Q Plots of Log-ratios of Industrial GTA Land Prices (1998-2005).
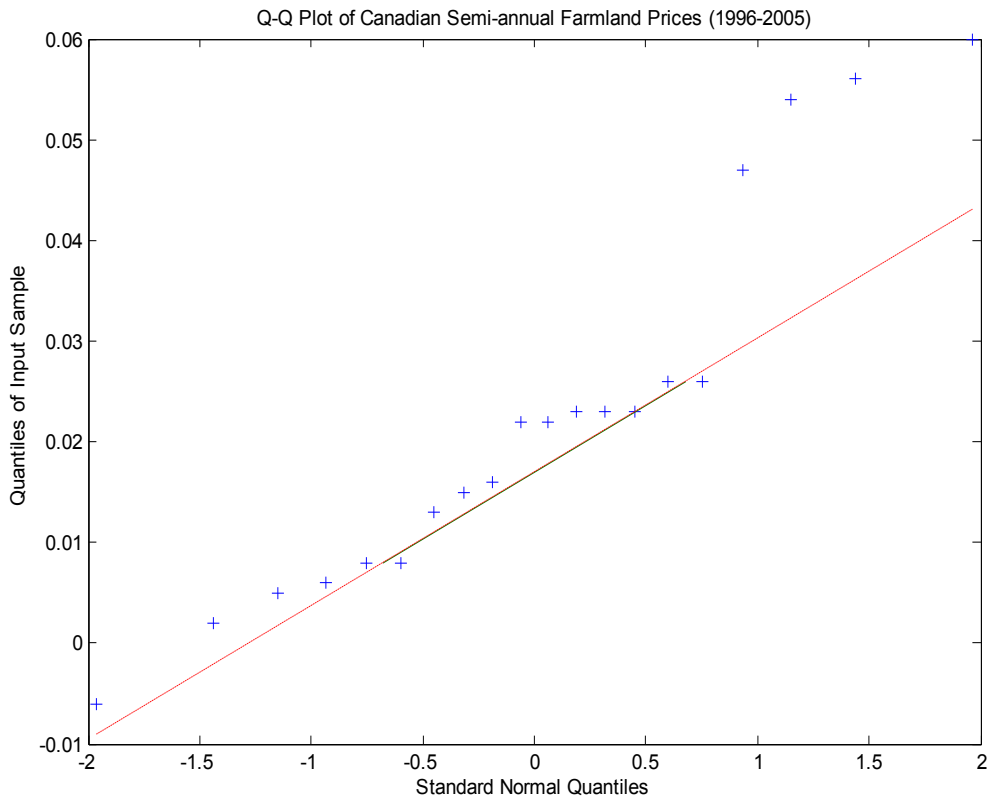
Figure 4-5: Q-Q Plot of Canadian Semi-annual Farmland Prices (1996-2005)
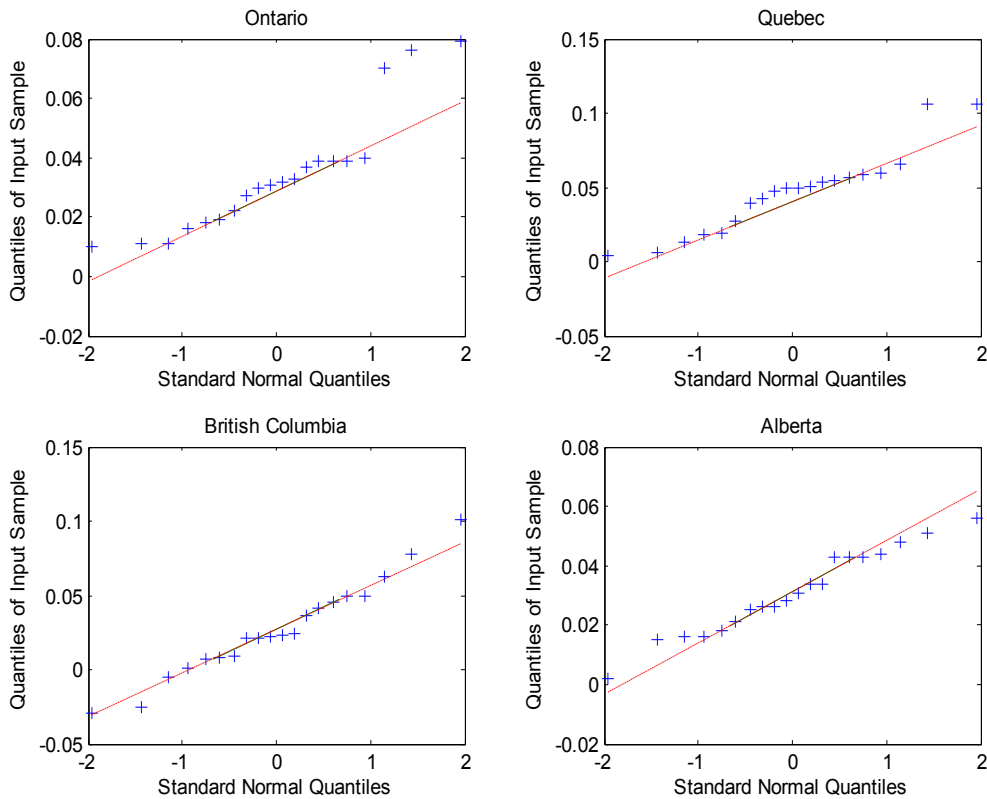
Figure 4-6: Q-Q Plot of Some Provincial Semi-annual Farmland Prices (1996-2005)

Other Q-Q plots related to the other six provinces are provided in Appendix 3.

As shown in Figure 4-1, Figure 4-2, and Figure 4-3, for the most part, the traffic volume statistics failed the normality test. In terms of land prices, Figure 4-4 and Figure 4-5 likewise portray similar patterns.

It is clear that the Q-Q plots do not support the notion of normality of the log ratios of the AADT and the land price data, thus exposing a violation to the Geometric Brownian Motion assumption. However, the Q-Q plots also fail to identify any unique pattern; for the most part, they indicate that the traffic and land price data come from heavy-tailed distributions.

4.2.1.2 Some Notes on Seasonality

Marathe and Ryan (2005) reiterate the importance of removing the seasonality effect from the time series prior to testing the GBM assumption.

It would suffice to look in Figure 4-7 at the seasonal variation traffic curves belonging to the intermediate and high variations (Recreation and Tourist) traffic curves to be convinced of the existence of high degree of seasonality in these particular traffic volume time series at the monthly and daily timescales.

However, given that the time scale of the decision-making analysis is annual and the fact that the cyclical variations of the traffic volume occurs within the year timeframe, any seasonality effects embedded within the AADT values will have no bearing on the Q-Q plots. The same applies to any seasonal variations that may exist in the average yearly land price data.
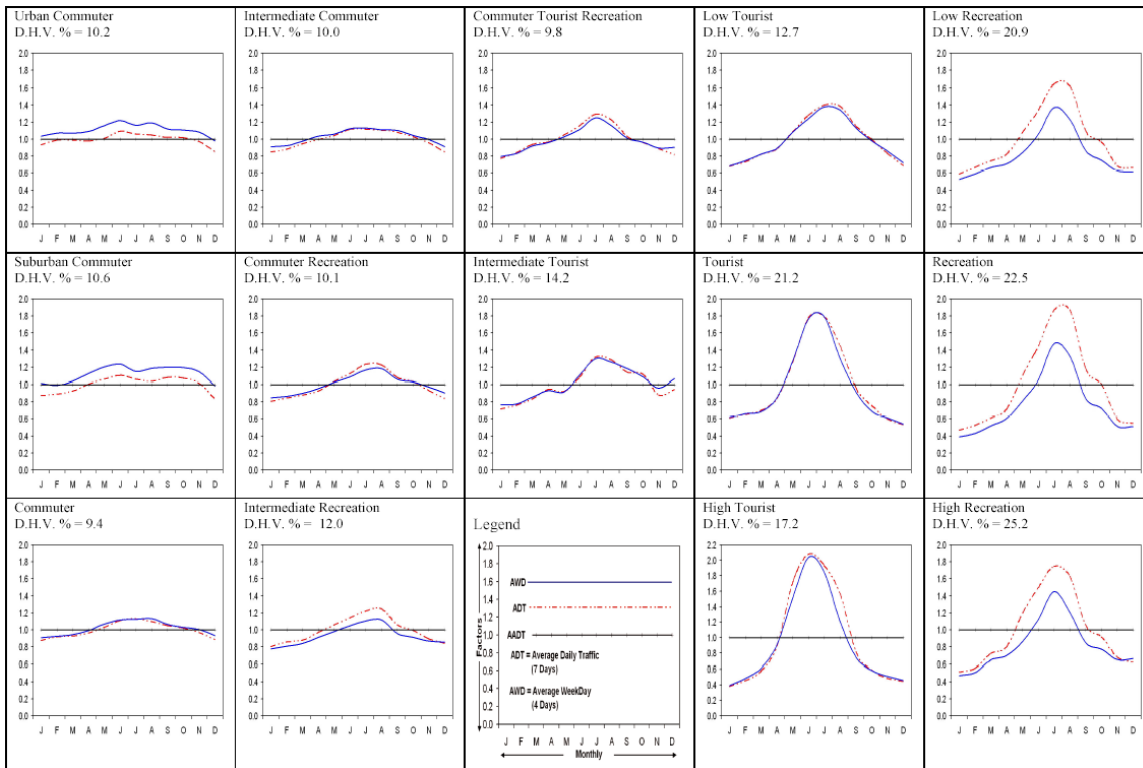
Figure 4-7: 2003 Seasonal Variation Curves (Ontario Ministry of Transportation, 2006)

Figure 4-8: Traffic Seasonal Variation Types (Ontario Ministry of Transportation, 2006)

Furthermore, traffic count statistics on highways of the high variation type may exhibit

deviations from normality that does not only occur collectively at the annual level

(AADT) but also separately at the seasonal level (SADT and WADT). For example, in Figure 4-3 above, heavy tail behaviors were observed in all the summer, winter, and average annual daily traffic counts. In that figure, highways 647, 668, and 580 are of HT type, whereas highway 581 is an HR.

4.2.2 Jumps

Heavy-tailed distributions may be attributed to presence of jumps. Jumps are essentially unexpected large changes in the value of the uncertainty. To investigate the possibility of this phenomenon we shall calculate the probabilities, based on the normal law, of the maximum and minimum changes in the values of the uncertainties over the study period as illustrated below:

$$P(X > x^{Max}) = 1 - \int_{-\infty}^{x^{Max}} \frac{1}{\sqrt{2\pi}\sigma} . e^{-\left(\frac{(x-\mu)^2}{2\sigma^2}\right)} \text{ and } P(X < x^{Min}) = \int_{-\infty}^{x^{Min}} \frac{1}{\sqrt{2\pi}\sigma} . e^{-\left(\frac{(x-\mu)^2}{2\sigma^2}\right)}$$

$$\text{where } X \in \{\Delta\text{AADT}, \Delta P\}.$$

It is a subjective measure to define how low an increment probability should be for the increment to constitute a jump. In the following subsections, we present the assumptions and the outcome of this investigation.

4.2.2.1 Traffic Volumes

To illustrate the very real possibility of jumps, we shall consider an increment of AADT with a probability $\leq 1\%$ to represent a jump. The figures and results presented below relate to three examples, of several others, of highway sections taken from a sample of

King's highways, Secondary highways, and Tertiary road sections, that met the above established jump criterion.
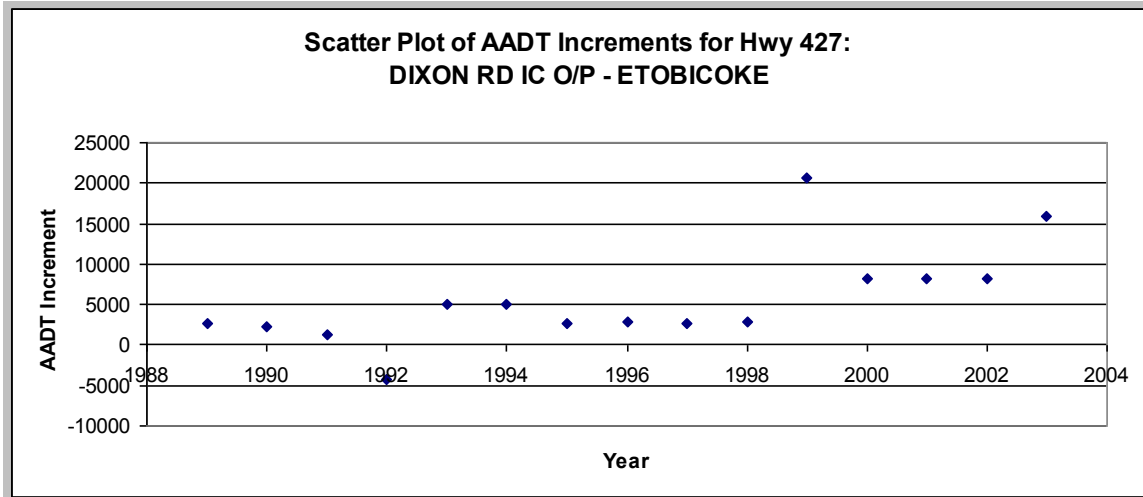
Figure 4-9: Scatter Plot of a Sample of a King's Highway Sections with Jumps.

Mean =	5613.333333	Std =	6123.476
x^{Max} =	20700 (**369 %**)	x^{Min} =	-4200 (-75 %)
$Year^{Max}$ =	**1999**	$Year^{Min}$ =	1992
P ($X>x^{Max}$) =	**0.0069**	P ($X<x^{Min}$) = 0.0545	
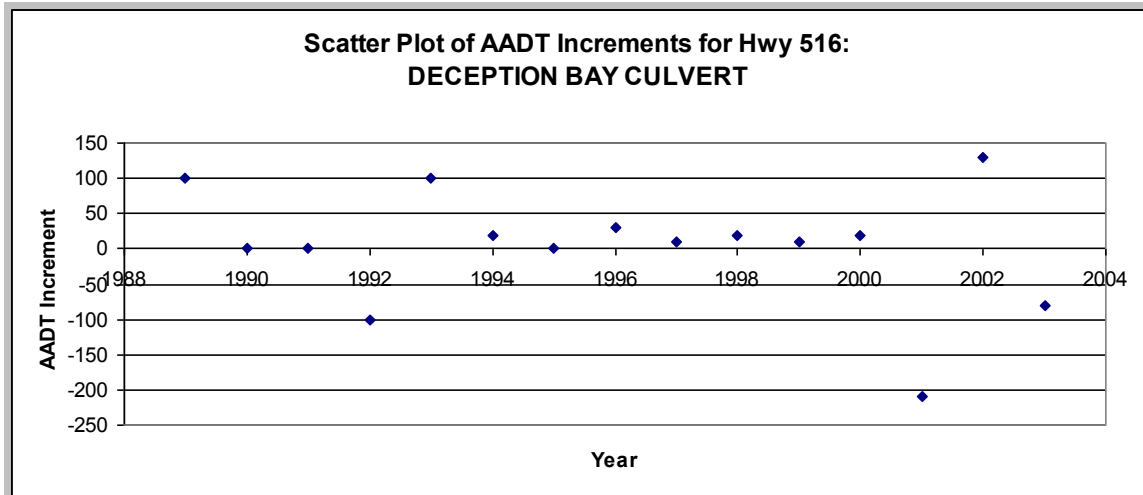
Figure 4-10: Scatter Plot of a Sample of Secondary Highway Sections with Jumps.

Mean =	3.333333333	Std =	84.31799
x^{Max} =	130 (3900 %)	x^{Min} =	-210 (**-6300** %)
$Year^{Max}$ =	2002	$Year^{Min}$ =	**2001**
P ($X>x^{Max}$) =	0.0665	P ($X<x^{Min}$) =**0.0057**	
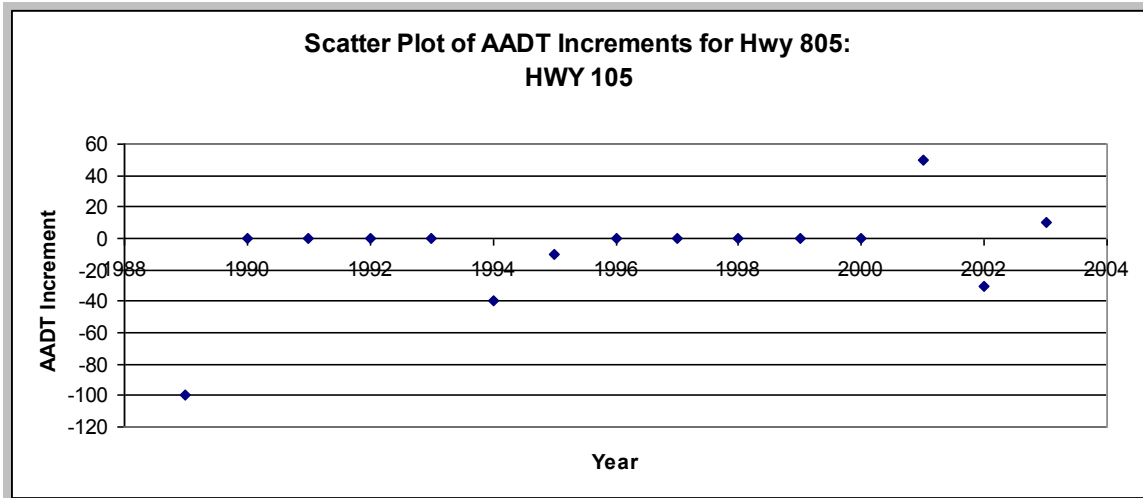
Figure 4-11: Scatter Plot of a Sample of Tertiary Road Sections with Jumps

Mean =	-8		Std =	31.89268
$x^{Max} =$	50 (-625 %)		$x^{Min} =$	-100 (**1250** %)
$Year^{Max} =$	2001		$Year^{Min} =$	**1989**
$P(X>x^{Max}) =$	0.0345		$P(X<x^{Min}) =$	**0.0020**

All the above statistics show that very large jumps are occurring when theoretically, given a normal law, these jumps are extremely unlikely. For example, Hwy 427: Dixon RD IC O/P: Etobicoke highway section contains an upward jump of size equivalent to 369% of that of the mean change with a probability of less than 0.69% as illustrated in Figure 4-9. This is consistent with the corresponding Q-Q plot in Figure 4-1, which indicates that the downward jump in 1992 is also nonconforming with the normal law.

4.2.2.2 GTA Unit Industrial Land Sale Prices

For the industrial land sale prices, we again consider an increment with a probability $\leq 1\%$ to represent a jump. The figures and results presented below relate to the four GTA regions (East, North, West, and South).
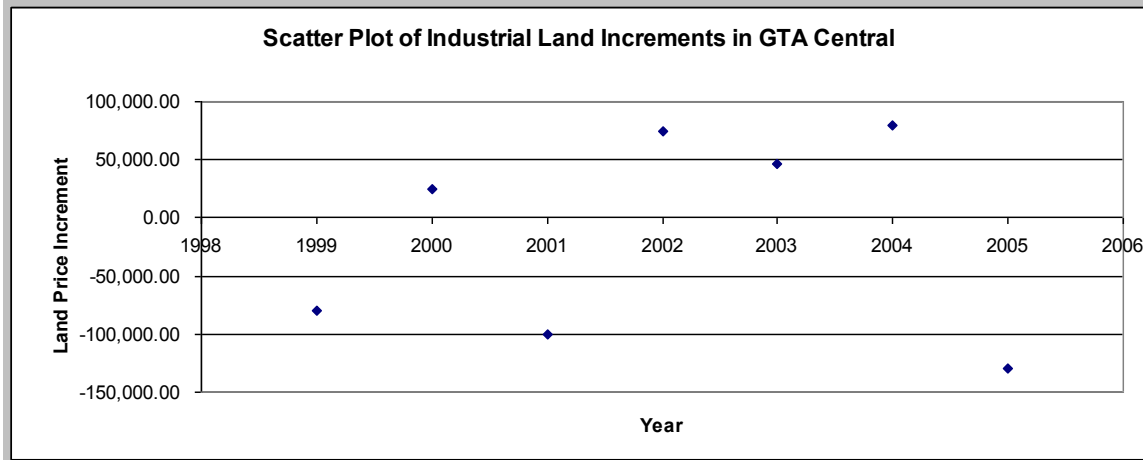
Figure 4-12: Scatter Plot of Industrial Land Increments in GTA Central.

Mean =	7,433.33	Std =	78,647.43
x^{Max} =	79,682.00 (1072 %)	x^{Min} =	-129,057.00 (-1736 %)
$Year^{Max}$ =	2004	$Year^{Min}$ =	2005
$P\,(\mathbf{X} > x^{Max}) = 0.1791$		$P\,(\mathbf{X} < x^{Min}) = 0.0413$	
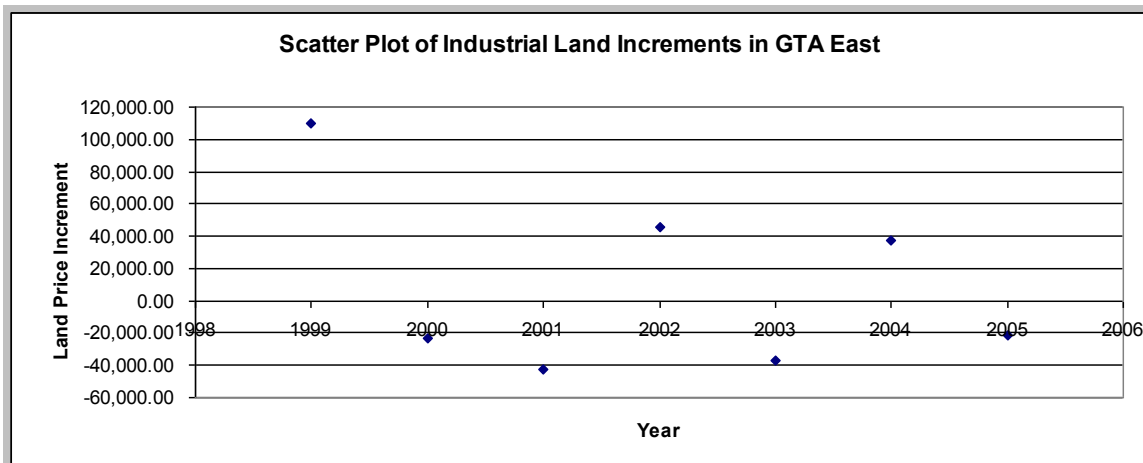
Figure 4-13: Scatter Plot of Industrial Land Increments in GTA East.

Mean =	15,025.67	Std =	59,894.31
x^{Max} =	109,823.00 (731 %)	x^{Min} =	-42,176.00 (-281 %)
$Year^{Max}$ =	1999	$Year^{Min}$ =	2001
$P\,(\mathbf{X} > x^{Max}) = 0.0567$		$P\,(\mathbf{X} < x^{Min}) = 0.1698$	
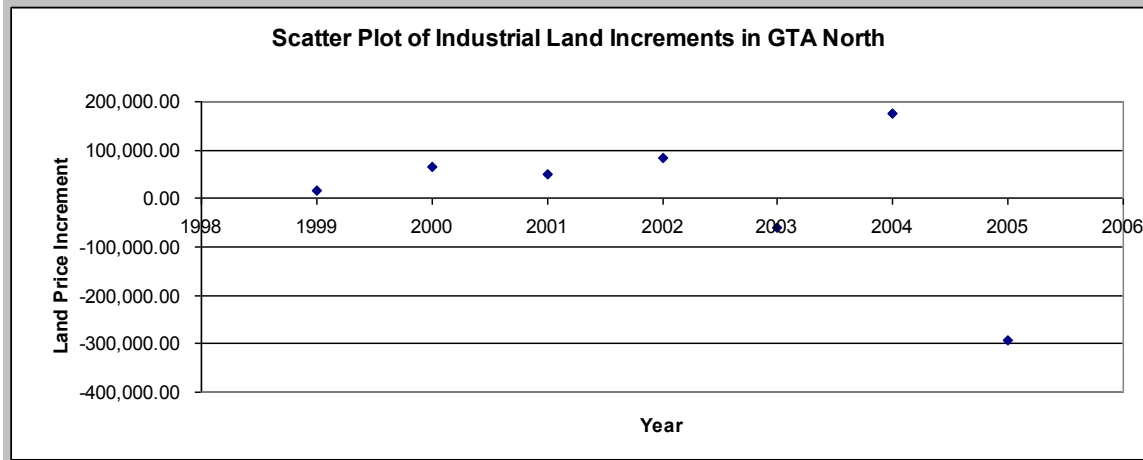
Figure 4-14: Scatter Plot of Industrial Land Increments in GTA North.

Mean =	55,569.33	Std =	77,335.15
x^{Max} =	174,738.00 (314 %)	x^{Min} =	-292,630.00 (**-527 %**)
$Year^{Max}$ =	2004	$Year^{Min}$ =	**2005**
P ($X > x^{Max}$) =	0.0617	P ($X < x^{Min}$) =	**0.0000034**
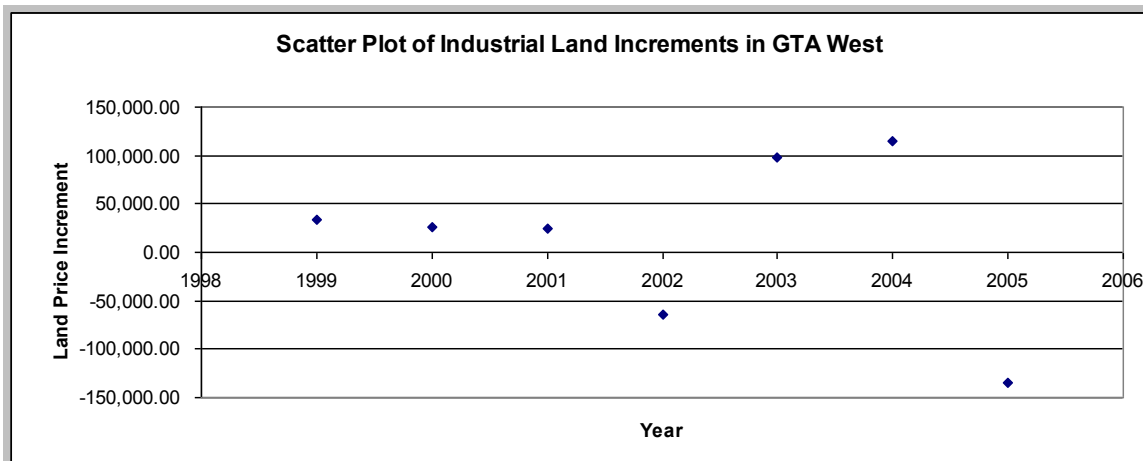
Figure 4-15: Scatter Plot of Industrial Land Increments in GTA West.

Mean =	38,761.67	Std =	63,601.55
x^{Max} =	114,875.00 (296 %)	x^{Min} =	-134,542.00 (**347 %**)
$Year^{Max}$ =	2004	$Year^{Min}$ =	**2005**
P ($X > x^{Max}$) =	0.1157	P ($X < x^{Min}$) =	**0.0032**

4.3   Conclusions

In testing the validity of the geometric Brownian motion assumption in Zhao et al. (2004), data must first be obtained. The first section of this chapter was dedicated to looking into areas where this data could be collected. The ultimate outcome of this quest was that data could be obtained but in statistically insignificant numbers. Subsequently in section 4.2, using the data collected a simple graphical test, Quantile-Quantile plots, was employed to investigate the normality of the log ratios of the sampled uncertainty increments. The plots showed significant deviation from normality that, while indicating unanimously that the data came from heavy tail distributions, failed to identify any unique distribution pattern; this motivated some further analysis.

As a possible contributing element to the heavy tail behavior, the presence of jumps was hypothesized and tested. The calculated low probabilities of the extreme values of the sampled increments supported this hypothesis.

Given the varied distributions and the established existence of jumps, one way to better model the traffic volume and the land price uncertainty processes is to adopt a wide class of mathematical models involving jump processes. One such class of models is called Lévy processes, a detailed introduction of which is provided in Chapter 5 below.

5 The Mathematics of the Uncertainty Model Representation and Calibration: A Theoretical Review

In Chapter 4 we saw that the traffic demand and the land price uncertainties do not evolve continuously; i.e. they exhibit jumps. Furthermore, the underlying distributions are not normal and are heavy (or fat) tailed. Cont and Tankov (2004) emphasize that it is especially important to specify the tail behavior correctly because "the tail behavior of the jump measure determines to a large extent the tail behavior of the probability density of the process" (p. 111).

As an alternative model, the Lévy processes provide a convenient and more adequate framework to modeling the above empirical observations. On top of their ability to generate sample paths that can have jumps and to generate distributions that can be heavy tailed, they can also generate skewed distributions and smile-shaped implied volatilities (Papapantoleon, 2005).

In this chapter we provide, using modern probability theory, some general theoretical background to Lévy processes and three of its subclass models: Merton, Kou, and NIG. This will be preceded by a recap of the uncertainties used in Zhao et al. (2004) and a brief derivation of the geometric Brownian motion theory, as it will be used later in the simulation and calibration of the three Lévy models. Finally, the chapter will conclude with a theoretical background to the calibration of the NIG models.

5.1 Underlying Uncertainties

Out of the three uncertainties modeled in Zhao et al. (2004), two (traffic demand, Q, and land price, P) are continuous state uncertainties and are assumed to follow geometric Brownian motion:

$$\frac{dS}{S} = \mu_S\left(S,t\right)dt + \sigma_S dz_S$$

where here $S \in \{Q,P\}$, z_S is a Wiener process, while $\mu_S\left(S,t\right)$ and σ_S are the drift function and the volatility of the uncertainty S, respectively. The two Wiener processes are assumed to be correlated through $\mathrm{cov}\left(z_Q, z_P\right) = \sigma_{QP}$ with σ_{QP} being constant.

The third uncertainty, the highway service quality index, I_t, is modeled as a discrete state uncertainty with five discrete values that correspond to the highway conditions of excellent (5), good (4), fair (3), poor (2), and very poor (1). The condition index at time t, denoted as $\{I_t, t = 0,1,2,...\}$, is modeled as a decreasing (discrete time) Markov chain taking values in $\{1, 2, 3, 4, 5\}$.

5.2 Geometric Brownian Motion Model

The classical diffusion model for the process S_t is

$$dS_t = \mu S_t dt + \sigma S_t dW_t$$

where W_t is a standard Wiener process, μ is the expected return and σ is the volatility (Black and Scholes, 1973; Merton, 1973). The solution for this equation is

$$\frac{dS_t}{S_t} = \mu dt + \sigma dW_t \tag{5.1}$$

where $S_t \in \{Q_t, P_t\}$.

Taking the natural logarithm of S_t and invoking Ito's lemma yields the following differential equation:

$$d \ln S_t = \left(\mu - \frac{\sigma^2}{2} \right) dt + \sigma dW_t \tag{5.2}$$

Through integration,

$$\int_0^t d \ln S_t = \int_0^t \left(\mu - \frac{\sigma^2}{2} \right) dt + \int_0^t \sigma dW_t$$

produces

$$\ln \frac{S_t}{S_0} = \left(\mu - \frac{\sigma^2}{2} \right) t + \sigma W_t \tag{5.3}$$

or its equivalent:

$$S_t = S_0 e^{\left(\mu - \frac{\sigma^2}{2} \right) t + \sigma W_t} \tag{5.4}$$

From this we can conclude that the $\ln S_t$ follows a generalized Wiener process where

$$\ln(S_t) - \ln(S_0) = \ln\left(\frac{S_t}{S_0}\right) \sim N\left(\left(\mu - \frac{\sigma^2}{2}\right)t, \sigma^2 t\right)$$

Also, equation (5.3) above can be expressed as:

$$X_t = \gamma t + \sigma W_t, \tag{5.5}$$

where $X_t = \ln\left(\dfrac{S_t}{S_0}\right)$ and $\gamma = \mu - \sigma^2/2$.

Therefore,

$$\mu_t^X = \mathrm{E}\left[X_t = \ln\left(\frac{S_t}{S_0}\right)\right] = \left(\mu - \sigma^2/2\right)t = \gamma t$$

$$\sigma_t^{2(X)} = \mathrm{Var}\left(X_t = \ln\left(\frac{S_t}{S_0}\right)\right) = \sigma^2 t \tag{5.6}$$

Furthermore,

$$\mu_t^s = \mathrm{E}\left[\frac{S_t}{S_0} = e^{X_t}\right] = \mathrm{E}\left[e^{y \cdot X_t}\right]\Big|_{y=1} = M_{X_t}(y)\Big|_{y=1}$$

$$\because X_t \sim N\left(\gamma t, \sigma^2 t\right),$$

$$\mu_t^s = \exp\left(\gamma t \cdot y + \frac{1}{2}\sigma^2 t \cdot y^2\right)\Big|_{y=1} = \exp\left(\left(\mu - \frac{\sigma^2}{2}\right)t + \frac{\sigma^2}{2}t\right)$$

$$\mu_t^s = \mathrm{E}\left[\frac{S_t}{S_0} = e^{X_t}\right] = e^{\mu t} \tag{5.7}$$

and

$$\sigma_t^{2(S)} = \mathrm{Var}\left(\frac{S_t}{S_0} = e^{X_t}\right) = \mathrm{E}\left[\left(e^{X_t}\right)^2\right] - \left(\mathrm{E}\left[e^{X_t}\right]\right)^2$$

$$= \mathrm{E}\left[e^{2X_t}\right] - \left(\mu_t^s\right)^2 = M_{X_t}(y)\Big|_{y=2} - \left(\mu_t^s\right)^2$$

$$= \exp\left(\gamma t \cdot y + \frac{1}{2}\sigma^2 t \cdot y^2\right)\Big|_{y=2} - \left(e^{\mu t}\right)^2$$

$$= \exp\left(2\left(\mu - \frac{\sigma^2}{2}\right)t + 2\sigma^2 t\right) - e^{2\mu t}$$

$$= \exp\left(2\mu t - \sigma^2 t + 2\sigma^2 t\right) - e^{2\mu t}$$

$$\sigma_t^{2(S)} = \mathrm{Var}\left(\frac{S_t}{S_0} = e^{X_t}\right) = e^{2\mu t}\left[e^{\sigma^2 t} - 1\right] \tag{5.8}$$

5.3 Lévy Processes: The Preliminaries

As defined in Rasmus et al. (2004), "[a] Lévy process is a stochastically continuous process with stationary and independent increments". More formally,

A cádlág[32] stochastic process $(X_t)_{t \geq 0}$ on [probability space] $(\Omega, \mathcal{F}, \mathbb{P})$ with values in $\mathbb{R}^d$ such that $X_0 = 0$ is called a Lévy process if it possesses the following properties:

1. Independent increments: for every increasing sequence of times $t_0 \dots t_n$, the random variables $X_{t_0}, X_{t_1} - X_{t_0}, \dots, X_{t_n} - X_{t_{n-1}}$ are independent.

2. Stationary increments: the law of $X_{t+h} - X_t$ does not depend on *t*.

3. Stochastic continuity: $\forall \varepsilon > 0, \lim_{h \to 0} \mathbb{P}(|X_{t+h} - X_t|) = 0$. (Cont and Tankov, 2004, p. 68)

Being a Lévy process, $(X_t)_{t \geq 0}$ has by definition an infinitely divisible distribution at every time *t*. While restricting the possible distributions[33] available for *X*, this condition still leaves room for a rich enough class of models for *X*.

For a Lévy process $(X_t)_{t \geq 0}$, there exists a continuous function $\psi : \mathbb{R}^d \mapsto \mathbb{R}$, which completely characterizes the law of *X* such that: $\mathrm{E}\left[e^{iz.X_t}\right] = e^{t\psi(z)}, \quad z \in \mathbb{R}^d$. ψ is called the characteristic exponent and $\mathrm{E}\left[e^{iz.X_t}\right]$ is the characteristic function of $(X_t)_{t \geq 0}$.

The characteristic function of a Lévy process $(X_t)_{t \geq 0}$ on $\mathbb{R}^d$ with a characteristic triplet (or Lévy triplet) $(\gamma, \mathbf{A}, \nu)$ is given by

---

[32] A function *f* is said to be cádlág if it is right-continuous with left limits.
[33] Some examples of infinitely divisible distributions include: the Gaussian, gamma, α – stable, Poisson, log-normal, Pareto, Student, and normal inverse Gaussian distributions.

$$\psi(z) = i\gamma.z - \frac{1}{2}z.\mathbf{A}z + \int_{\mathbb{R}^d}\left(e^{iz.x} - 1 - iz\,x\,1_{|x|<1}\right)v(dx) \qquad (5.9)$$

where $\gamma, z \in \mathbb{R}^d$, $\mathbf{A}$ is a symmetric positive n x n covariance matrix, and v is a positive

Radon measure on $\mathbb{R}^d \setminus \{0\}$ verifying the following:

$$\int_{|x|\leq 1} |x|^2 v(dx) < \infty \quad \text{and} \quad \int_{|x|\geq 1} v(dx) < \infty.$$

In one dimension (d= 1), the characteristic exponent with the triplet (γ, σ, v) becomes

$$\psi(z) = i\gamma.z - \frac{\sigma^2 z^2}{2} + \int_{\mathbb{R}}\left(e^{iz.x} - 1 - iz.x 1_{|x|<1}\right)v(dx) \qquad (5.10)$$

where $\gamma, z \in \mathbb{R}$, $\sigma \in \mathbb{R}_+$, and v a measure on $\mathbb{R} \setminus \{0\}$.

The measure v, called the Lévy measure of X, defines how jumps occur.

Lévy processes fall into different categories with respect to activity of jumps and variation of jump sizes. A Lévy process, X, is of finite activity (a.k.a. jump-diffusion model) if $v(\mathbb{R}) < \infty$, which would mean that almost all paths of X have a finite number of jumps in every compact interval. On the contrary, X is of infinite activity type if $v(\mathbb{R}) = \infty$, which would mean that X has an infinite number of jumps in every compact interval.

With respect to quadratic variation, a Lévy process, X, is of finite variation if $A = 0 (\sigma^2 = 0$ in 1d) and $\int_{|x|\leq 1} |x| v(dx) < \infty$. On the other hand, X, is of infinite variation if $A \neq 0$ or if $A = 0$ and $\int_{|x|\leq 1} |x| v(dx) = \infty$. $A = 0$ indicates the lack of a Brownian component, i.e., a pure jump process (Papapantoleon, 2005).

Whether finite or infinite in activity or in variation, "every Lévy process is a superposition of a Wiener process and a (possibly infinite) number of independent Poisson processes" (Cont and Tankov, 2004, p.67).

5.4   The Lévy and the Compound Poisson Processes

A compound Poisson process $(X_t)_{t \geq 0}$ with intensity $\lambda > 0$ and jump size distribution

$f(x)$ is a stochastic process defined as

$$X_t = \sum_{i=1}^{N_t} Y_i \qquad (5.11)$$

where jump sizes Y_i are i.i.d with distribution $f(x)$ and $(N_t)_{t \geq 0}$ is a Poisson process

with intensity λ, independent from $(Y_i)_{i \geq 1}$.

The compound Poisson process is the only Lévy process with piecewise constant function

sample paths. The fact that any cádlág function can be approximated by a piecewise

constant function makes the compound Poisson process very useful in approximating

general Lévy processes.

The characteristic function of the compound Poisson process has the following

representation:

$$\mathrm{E}\left[e^{iz.X_t} \right] = e^{t\psi(z)} = \exp\left\{ t \int_{\mathbb{R}^d} \left(e^{iz.x} - 1 \right) v(dx) \right\}, \quad \forall z \in \mathbb{R}^d \qquad (5.12)$$

where v is a Lévy measure[34] on $\mathbb{R} \setminus \{0\}$ and not a probability measure since

$\int_{\mathbb{R}} v(dx) = \int_{\mathbb{R}} f(x) dx = \lambda \neq 1$, and $f(x)$ is the jump size distribution.

---

[34] Lévy measure, $v(C)$, is the expected number (per unit of time) of jumps whose size belongs to C,

where $C \subset \mathbb{R}^d$. Jumps of sizes in set C occur as a Poisson process with an intensity parameter $\int_C v(dx)$.

The value of the compound Poisson process lies in the fact that it is also an ingredient of general Lévy processes. A Lévy process can be decomposed into 4 independent sub Lévy processes: a constant drift, a Brownian motion, a compound Poisson process, and a square integrable pure jump martingale (Papapantoleon, 2005).

More specifically, Cont and Tankov (2004) explain that, as per Lévy-Itô decomposition, for a Lévy process $(X_t)_{t \geq 0}$ on $\mathbb{R}^d$ with the following conditions:

- Lévy measure ν verifying the conditions in expression (5.9), and

- Jump measure[35] of X, denoted by J_X, as a Poisson jump measure on

    $[0, \infty[\times \mathbb{R}^d$ with intensity $\nu(dx)dt = \lambda f(dx)dt$, where λ is the intensity of a

    compound Poisson process and $f(x)$ is the jump size distribution,

there exists a vector γ and a d-dimensional Brownian motion $(B_t)_{t \geq 0}$ with an arbitrary covariance matrix $\mathbf{A}$ such that:

$$X_t = \gamma t + B_t + X_t^l + \lim_{\varepsilon \downarrow 0} \tilde{X}_t^\varepsilon, \quad \text{where}$$

$$X_t^l = \int_{|x| \geq 1, s \in [0,t]} x J_X(ds \times dx), \quad \text{and} \tag{5.13}$$

$$\tilde{X}_t^\varepsilon = \int_{\varepsilon \leq |x| < 1, s \in [0,t]} x \{ J_X(ds \times dx) - \nu(dx)ds \}.$$

The first two terms in expression (5.13) relate to a continuous Gaussian Lévy process (a Brownian motion with drift), whereas the latter two terms relate to discontinuous jump processes; X_t^l, is a finite compound Poisson process of absolute jump sizes > 1 and

---

[35] $J_X([t_1, t_2], C)$ is a jump measure that counts the number of jump times between t_1 and t_2 such that their jump sizes are in C.

$\lim\limits_{\varepsilon\downarrow0}\tilde{X}_t^{\varepsilon}$ is an infinite compensated[36] compound Poisson process of absolute jump sizes between ε and 1, where $\varepsilon>0$.

An important implication of the Lévy-Itô decomposition is that every Lévy process can be represented as a combination of a continuous Gaussian Lévy process $\left(B_t+\gamma t\right)$ as well as a possibly infinite sum of independent compound Poisson process. "This implies that every Lévy process can be approximated with arbitrary precision by a jump-diffusion process" (Cont and Tankov, 2004, p.81). While very useful in approximating Lévy processes, this result is not utilized in this work as the models are simulated exactly.

In the next two sections, we will describe a few specific models belonging to the finite and the infinite types of Lévy processes.

---

[36] Compensated, or centered, to ensure convergence of X^{ε}, as $\varepsilon\to0$.

5.5   *Finite Activity (Jump Diffusion) Models*

A Lévy process, X_t, of the jump-diffusion (finite) type takes the following form:

$$X_t = \gamma t + \sigma W_t + \sum_{i=1}^{N_t} Y_i, \qquad\qquad (5.14)$$

where $(N_t)_{t>0}$ is a Poisson process counting the jumps of X, and Y_i's are i.i.d. random variables representing the jump sizes. In the finite activity type of the Lévy processes, it is the distribution of the jump sizes, $\nu_o(x)$, that defines the particular parametric model. The following two subsections offer brief descriptions of the Gaussian and the double exponential jump processes.

5.5.1   Merton Jump Diffusion Model

In his paper, "Option Pricing When Underlying Stock Returns are Discontinuous", Merton (1976) states that,

> the Black-Scholes solution is not valid, even in the continuous limit, when the stock price [uncertainty] dynamics cannot be represented by a stochastic process with a continuous sample path [...] i.e., in a short interval of time, the stock price can only change by a small amount. (p. 2-3)

He concludes that,

> the antipathetical process to this continuous stock price motion would be a "jump" stochastic process defined in continuous time. In essence, such a process allows for a positive probability of a stock price change of extraordinary magnitude, no matter how small the time interval between successive observations. (p. 3)

Essentially, Merton introduces a stochastic model with the following dynamics:

$$\frac{dS_t}{S_t} = \mu dt + \sigma dW_t + d\left(\sum_{i=1}^{N_t}(Y_i - 1)\right) \tag{5.15}$$

where W_t is a standard Brownian motion, $(N_t)_{t \geq 0}$ is a Poisson process with rate λ, and $(Y_i)_{i \geq 1}$ is a sequence of independent identically distributed (i.i.d.) nonnegative random variables such that $\Upsilon_i = \log(Y_i)$ has a normal distribution. $(Y_i - 1)$ represents the percentage change in the value of the uncertainty due to jumps.

Solving the differential equation in (5.15) yields the following dynamics of the modeled uncertainty:

$$S_t = S_0 \exp\left\{\left(\mu - \frac{1}{2}\sigma^2\right)t + \sigma W_t\right\}\prod_{i=1}^{N_t} Y_i. \tag{5.16}$$

In the Merton jump diffusion model, the log-uncertainty process X_t in (5.14) contains 5 parameters: γ - drift, σ - diffusion volatility, λ - jump intensity, ρ - mean jump size, and δ - standard deviation of jump size. The Lévy density is

$$v(x) = \frac{\lambda}{\delta\sqrt{2\pi}}\exp\left\{-\frac{(x-\rho)^2}{2\delta^2}\right\} \tag{5.17}$$

and the characteristic exponent is given by

$$\psi(z) = i\gamma z - \frac{\sigma^2 z^2}{2} + \lambda\left\{e^{-\frac{\delta^2 z^2}{2} + i\mu z} - 1\right\} \tag{5.18}$$

The cummulants are:

$$\begin{aligned}
c_1 &= E[X_t] = t(\gamma + \lambda\rho), \\
c_2 &= \text{Var}(X_t) = t(\sigma^2 + \lambda(\delta^2 + \rho^2)), \\
c_3 &= t\lambda\rho(3\delta^2 + \rho^2), \text{ and} \\
c_4 &= t\lambda(3\delta^3 + 6\rho^2\delta^2 + \rho^4).
\end{aligned} \tag{5.19}$$

5.5.2 Kou Model

The Kou model was introduced in an effort to address two established empirical phenomena in finance, namely the asymmetric leptokurtic and the volatility smile phenomena. The leptokurtic feature means that the uncertainty distribution "is skewed to the left, and has a higher peak and two heavier tails than those of the normal distribution" (Kou, 2002, p. 1086). The volatility smile refers to the implied volatility curve resembling a "smile" (i.e., a convex curve) as opposed to being constant, as is assumed in the Black-Scholes model.

In describing the model, Kou (2002) states:

> The [proposed] model is very simple. The logarithm of the asset price is assumed to follow a Brownian motion plus a compound Poisson process with jump sizes double exponentially distributed. Because of its simplicity, the parameters in the model can be easily interpreted, and the analytical solutions for option pricing can be obtained. The explicit calculation is made possible partly because of the memoryless property of the double exponential distribution. (Ibid.p. 1087)

The model here is identical to that in (5.15) and (5.16) except that the sequence of i.i.d. nonnegative random variables $\Upsilon = \log(Y)$ has, as opposed to a normal law, an asymmetric double exponential distribution. It is given by

$$f_\Upsilon(y) = p.\lambda_+ e^{-\lambda_+ y} 1\{y \geq 0\} + (1-p).\lambda_- e^{-\lambda_- y} 1\{y < 0\},$$
$$\lambda_+ > 1,\ \lambda_- > 0 \tag{5.20}$$

where p represents the probability of upward jump. In other words,

$$\log(Y) = \Upsilon \overset{d}{=} \begin{cases} \xi^+, & \text{with probability } p \\ -\xi^-, & \text{with probability } 1-p \end{cases}, \tag{5.21}$$

where ξ^+ and ξ^- are exponential random variables with means $1/\lambda_+$ and $1/\lambda_-$, respectively. All sources of randomness, W_t, N_t, and Υs are assumed to be independent, even though this can be relaxed (Kou, 2002). Kou also states the following:

$$\text{Note that } E(\Upsilon) = \frac{p}{\lambda_+} - \frac{(1-p)}{\lambda_-}, \quad \text{Var}(\Upsilon) = p(1-p)\left(\frac{1}{\lambda_+} - \frac{1}{\lambda_-}\right)^2 + \left(\frac{p}{\lambda_+^2} - \frac{1-p}{\lambda_-^2}\right), \text{ and}$$

$$E(Y) = E(e^{\Upsilon}) = p\frac{\lambda_+}{\lambda_+ - 1} + (1-p)\frac{\lambda_-}{\lambda_- + 1}, \quad \lambda_+ > 1, \ \lambda_- > 0 \qquad (5.22)$$

The requirement $\lambda_+ > 1$ is needed to ensure that $E(Y) < \infty$ and $E(S(t)) < \infty$; it essentially means that the average upward jump cannot exceed 100% (p. 1088).

Again using the log-price process X_t in (5.14), the Kou jump diffusion model contains 6 parameters: γ - drift, σ - diffusion volatility, λ - jump intensity, λ_+, λ_-, p - parameters of the jump size distribution. The Lévy density is

$$v(x) = p\lambda\lambda_+ e^{-\lambda_+ x} 1_{x>0} + (1-p)\lambda\lambda_- e^{-\lambda_-|x|} 1_{x<0} \qquad (5.23)$$

and the characteristic exponent is given by

$$\psi(z) = i\gamma z - \frac{\sigma^2 z^2}{2} + iz\,\lambda\left\{\frac{p}{\lambda_+ - iz} - \frac{1-p}{\lambda_- + iz}\right\} \qquad (5.24)$$

The cummulants are the following:

126

$$c_1 = \mathrm{E}\left[X_t\right] = t\left(\gamma + \lambda\left\{\frac{p}{\lambda_+} - \frac{(1-p)}{\lambda_-}\right\}\right),$$

$$c_2 = \mathrm{Var}\left(X_t\right) = t\left(\sigma^2 + \lambda\left\{\frac{p}{\lambda_+^2} + \frac{(1-p)}{\lambda_-^2}\right\}\right),$$

$$c_3 = t\lambda\left(\frac{p}{\lambda_+^3} - \frac{(1-p)}{\lambda_-^3}\right), \text{and}$$ (5.25)

$$c_4 = t\lambda\left(\frac{p}{\lambda_+^4} + \frac{(1-p)}{\lambda_-^4}\right),$$

$$c_5 = t\lambda\left(\frac{p}{\lambda_+^5} - \frac{(1-p)}{\lambda_-^5}\right).$$

Finally, the semi-heavy (exponential) tails are as follows[37]: $p(x) \sim e^{-\lambda_+ x}$ as $x \to +\infty$ and

$p(x) \sim e^{-\lambda_- |x|}$ as $x \to -\infty$.

---

[37] Results obtained from Cont and Tankov (2004).

5.6 *Infinite Activity Models: Generalized Hyperbolic Model*

A Lévy process of the infinite activity type is one that has in almost all paths an infinite number of jumps on every compact interval. A large family of Lévy processes of the infinite activity type (also referred to as pure jumps processes) is the generalized hyperbolic (GH) family.

The GH model has the following parameters and domains:

$\alpha > 0$ (shape), $0 \leq |\beta| < \alpha$ (skewness), $\mu \in \mathbb{R}$ (location), $\delta > 0$ (scale), $\lambda \in \mathbb{R}$ (shape)
It has an infinitely divisible distribution with a probability density function given by the following:

$$f^{GH}(x;\lambda,\alpha,\beta,\mu,\delta) = c(\lambda,\alpha,\beta,\delta)\left(\delta^2 + (x-\mu)^2\right)^{\frac{\left(\lambda-\frac{1}{2}\right)}{2}}$$

$$\times K_{\lambda-\frac{1}{2}}\left(\alpha\sqrt{\delta^2 + (x-\mu)^2}\right)\exp\left(\beta(x-\mu)\right)$$

$$\text{where} \quad c(\lambda,\alpha,\beta,\delta) = \frac{\left(\alpha^2 - \beta^2\right)^{\lambda/2}}{\sqrt{2\pi}\alpha^{\lambda-\frac{1}{2}}\delta^{\lambda}K_{\lambda}\left(\delta\sqrt{\alpha^2 - \beta^2}\right)}, \tag{5.26}$$

$$\text{and} \quad K_{\lambda}(z) = \frac{1}{2}\int_0^{\infty} t^{\lambda-1}\exp\left(-\frac{1}{2}z\left(t+t^{-1}\right)\right)dt$$

where K_{λ} is the modified Bessel function of the third kind[38] with index λ.

The characteristic function of the GH model is

---

[38] Modified Bessel functions of the third kind can also be referred to as modified Bessel functions of the second kind. According to Eric Weisstein (2008), "[t]he modified Bessel function of the second kind is the function $K_{\lambda}(z)$ which is one of the solutions to the modified Bessel differential equation. The modified Bessel functions of the second kind are sometimes called the Basset functions, modified Bessel functions of the third kind (Spanier and Oldham 1987, p. 499), or Macdonald functions (Spanier and Oldham 1987, p. 499; Samko et al. 1993, p. 20). The modified Bessel function of the second kind is implemented in Mathematica as BesselK[nu, z] ".

$$\psi_{GH} = e^{iz\mu} \left(\frac{\alpha^2 - \beta^2}{\alpha^2 - (\beta + iz)^2} \right)^{\frac{\lambda}{2}} \frac{K_\lambda \left(\delta \sqrt{\lambda^2 - (\beta + iz)^2} \right)}{K_\lambda \left(\delta \sqrt{\alpha^2 - \beta^2} \right)} \qquad (5.27)$$

and the cummulants are as follows:

$$E[X_t] = \mu + \frac{\beta\delta}{\sqrt{\alpha^2 - \beta^2}} \frac{K_{\lambda+1}(\xi)}{K_\lambda(\xi)},$$

$$\text{var}(X_t) = \delta^2 \left(\frac{K_{\lambda+1}(\xi)}{\xi K_\lambda(\xi)} + \frac{\beta^2}{\alpha^2 - \beta^2} \left\{ \frac{K_{\lambda+2}(\xi)}{K_\lambda(\xi)} - \left(\frac{K_{\lambda+1}(\xi)}{K_\lambda(\xi)} \right)^2 \right\} \right), \qquad (5.28)$$

where $\xi = \delta\sqrt{\alpha^2 - \beta^2}$.

The tails of the Lévy density and the probability density are exponential with decay rates

$\lambda_+ = \alpha - \beta$ and $\lambda_- = \alpha + \beta$ (Cont and Tankov, 2004).

Different values of $\lambda, \alpha,$ and β yield different subclasses/shapes of the GH model:

Normal inverse Gaussian: $\lambda = -\frac{1}{2}$,

Hyperbolic: $\lambda = 1,$

Variance gamma: $\delta = 0$ and $\mu = 0,$

Student t: $\lambda < 0$ and $\alpha = \beta = \mu = 0.$

For simulation purposes, it is useful that the GH distribution can be represented as normal variance-mean mixtures with generalized inverse Gaussian distributions as mixing distributions;

$$\text{GH}(\lambda, \alpha, \beta, \mu, \delta) = N(\mu + z\beta, z) \wedge_z GIG(\lambda, \sigma^2, \alpha^2 - \beta^2) \qquad (5.29)$$

Among the different members of the GH class, the normal inverse Gaussian distribution is used herein. In the succeeding subsections, we explore some properties of the normal inverse Gaussian (NIG) distribution, outline a method of generating NIG random variables, and test the results against theoretical values.

5.6.1 Negative Inverse Gaussian Lévy Process: From GH to NIG

The normal inverse Gaussian Lévy process, X_t, is defined as a Lévy process whose increments are stationery, independent, and distributed as negative inverse Gaussian. The distribution of this increment size produces a Lévy process of the infinite activity type. The NIG distribution belongs to the class of generalized hyperbolic densities, with

$$\lambda = -\frac{1}{2}.$$

The NIG distribution has four parameters $(\alpha, \beta, \mu, \delta)$, where α is a shape or a steepness parameter whose value is proportional to the steepness of the density (or the tail heaviness), β is a skewness or an asymmetry parameter where $\beta = 0$ represents a symmetric density, μ is a location or shift parameter, and δ is a scale parameter. The characteristic triplet of the NIG Lévy process, X_t, has the following Lévy-Khinchin representation (γ, A, ν), where (Ribeiro and Webber, 2003)

$$\gamma = \mu + 2\frac{\delta\alpha}{\pi}\int_0^1 \sinh(\beta x) K_1(\alpha x) dx \qquad (5.30)$$

and $\nu(dx) = f(x) dx$ is the Lévy jump measure with a Lévy density given by (Ribeiro and Webber, 2003; Rasmus, Asmussen, and Wiktorsson, 2004):

$$f(x; \alpha, \beta, \delta) = \frac{\delta\alpha}{\pi|x|}\exp(\beta x) K_1(\alpha|x|) \qquad (5.31)$$

with a characteristic exponent given by (Rasmus, Asmussen, and Wiktorsson, 2004)

$$\psi_{NIG}(t) = \mu t + \delta\left[\left(\alpha^2 - \beta^2\right)^{\frac{1}{2}} - \left(\alpha^2 - (\beta + t)^2\right)^{\frac{1}{2}}\right] \qquad (5.32)$$

The density function is given by the following expression (Kalemanova and Werner, 2006):

$$f^{NIG}(x;\alpha,\beta,\mu,\delta) = \frac{\delta\alpha}{\pi}\exp\left(\delta\sqrt{\alpha^2-\beta^2}+\beta(x-\mu)\right)\frac{K_1(\alpha g(x))}{g(x)}$$

where $g(x) = \sqrt{\delta^2 + (x-\mu)^2}$,

$x \in \mathbb{R}, \ \mu \in \mathbb{R}, \ \alpha,\delta > 0, \ 0 \leq |\beta| \leq \alpha$, and   (5.33)

$$K_1(z) = \frac{1}{2}\int_0^{\infty}\exp\left(-\frac{1}{2}z(t+t^{-1})\right)dt$$

$K_1(z)$ is the modified Bessel function of the third kind and index 1, where here

$z = \alpha g(x)$.

The moment generating function of $X \sim \text{NIG}(\alpha,\beta,\mu,\delta)$ is (Ibid.)

$$M_X(t) = \exp(\mu t)\frac{\exp\left(\delta\sqrt{\alpha^2-\beta^2}\right)}{\exp\left(\delta\sqrt{\alpha^2-(\beta+t)^2}\right)}$$ (5.34)

and its cummulant generating function with respect to β is (Rydberg, 1997)

$$\kappa(\beta) = -\delta\sqrt{\alpha^2-\beta^2} + \beta\mu$$ (5.35)

Two important properties of the NIG distribution are the scaling property and that pertaining to its closure under convolution.

For $X \sim \text{NIG}(\alpha,\beta,\mu,\delta)$ and a scalar c, cX is also NIG distributed with parameters

$$cX \sim \text{NIG}\left(\frac{\alpha}{c},\frac{\beta}{c},c\mu,c\delta\right)$$ (5.36)

131

For independent random variables $X \sim \text{NIG}(\alpha, \beta, \mu_1, \delta_1)$ and $Y \sim \text{NIG}(\alpha, \beta, \mu_2, \delta_2)$, the sum of X and Y is also NIG distributed with parameters

$$X + Y \sim \text{NIG}(\alpha, \beta, \mu_1 + \mu_2, \delta_1 + \delta_2). \tag{5.37}$$

Having its increments being distributed as NIG random variables, the NIG Lévy process, X_t, when conditioned on $X_0 = 0$, has NIG distribution with the following parameters (Ribeiro and Webber, 2003; Rydberg, 1997):

$$X_t \sim \text{NIG}(\alpha, \beta, \mu_t, \delta_t), \text{ where } \mu_t = \mu \times t \text{ and } \delta_t = \delta \times t \tag{5.38}$$

From Rydberg (1997), the first four cummulants of X_t are given by:

$$
\begin{aligned}
\kappa_1(t) &= \mu_t + \delta_t \beta \gamma^{-1}, \\
\kappa_2(t) &= \delta_t \alpha^2 \gamma^{-3}, \\
\kappa_3(t) &= 3\delta_t \beta \alpha^2 \gamma^{-5}, \\
\kappa_4(t) &= 3\delta_t \alpha^2 (\alpha^2 + 4\beta^2) \gamma^{-7}, \\
\text{where } \gamma &= (\alpha^2 - \beta^2)^{\frac{1}{2}}
\end{aligned}
\tag{5.39}
$$

Equivalently, differentiating the cummulant generating function in (5.35) with respect to β yields other equivalent expressions for the cummulants of the distribution of X_t:

$$\kappa_1(t) = \mu_t + \delta_t \beta \gamma^{-1}$$

$$\kappa_2(t) = \delta_t \beta^2 \gamma^{-3} + \delta_t \gamma^{-1}$$

$$\kappa_3(t) = 3\delta_t \beta^3 \gamma^{-5} + 3\delta_t \beta \gamma^{-3}$$

$$\kappa_4(t) = 15\delta_t \beta^4 \gamma^{-7} + 18\delta_t \beta^2 \gamma^{-5} + 3\delta_t \gamma^{-3} \qquad (5.40)$$

$$\kappa_5(t) = 105\delta_t \beta^5 \gamma^{-9} + 150\delta_t \beta^3 \gamma^{-7} + 45\delta_t \beta \gamma^{-5}$$

$$\text{where } \gamma = \left(\alpha^2 - \beta^2\right)^{\frac{1}{2}}$$

For a fixed t, the parameters $\xi_t = (1 + \delta_t \gamma)^{-\frac{1}{2}}$ and $\chi_t = \dfrac{\beta}{\alpha}\xi_t$ are invariant under location

and scale transformations.

The skewness and kurtosis are as follows:

$$\text{skewness: } \frac{\kappa_3}{\kappa_2^{3/2}} = 3\frac{\beta}{\alpha\sqrt{\delta_t \gamma}} \text{ and}$$

$$\qquad (5.41)$$

$$\text{kurtosis: } \frac{\kappa_4}{\kappa_2^2} = 3\frac{\alpha^2 + 4\beta^2}{\delta_t \alpha^2 \gamma}.$$

5.6.2   Simulation of Normal Inverse Gaussian Lévy Process

A NIG Lévy process is a Lévy process with increments distributed as NIG random

variables. Hence, to generate the NIG Lévy process we need to generate these NIG

random increments. There are different ways to do so that vary in exactness; in this

subsection, we present and test an exact method of generating NIG random variables.

5.6.2.1 The Rydberg Algorithm

By definition, the normal inverse Gaussian Lévy process, X_t, is a process whose

increments, $\Delta X_t = X_{t+1} - X_t$, are stationery, independent and distributed as *NIG* random

variables with parameters given by: $\Delta X_t \sim NIG(\alpha, \beta, \mu, \delta)$. Thus, from (5.37),

$$X_t = \sum_{t=0}^{t} \Delta X_t \Rightarrow X_t \sim NIG(\alpha, \beta, \mu t, \delta t) \qquad (5.42)$$

The stochastic process X_t which generates *NIG* distributed log ratios is given by:

$$S_t = S_o \exp(X_t) \qquad (5.43)$$

where

$$X_t = \log \frac{S_t}{S_{t-1}} = \log S_t - \log S_{t-1} = \sum_{t=0}^{t} \Delta X_t \sim NIG(\alpha, \beta, \mu t, \delta t)$$

To model the increments of the processes, $X_t = \sum_{t=0}^{t} \Delta X_t$, with $\Delta X_t \sim NIG(\alpha, \beta, \mu, \delta)$, we hereby proceed by describing a method to generate these NIG increments.

In the simulation of $NIG(\alpha, \beta, \mu, \delta)$ (or equivalently $GH(\frac{1}{2}, \alpha, \beta, \mu, \delta)$) random variables, one can utilize the fact that in (5.29) all GH distributions could be represented as normal variance-mean mixtures with generalized inverse Gaussian distributions as mixing distributions:

$$NIG(\alpha, \beta, \mu, \delta) = N(\mu + z\beta, z) \underset{z}{\wedge} GIG(\frac{1}{2}, \delta^2, \alpha^2 - \beta^2) \qquad (5.44)$$

Therefore, simulation of an $NIG(\alpha, \beta, \mu, \delta)$ random variable reduces to sampling two random variables: a normal random variable, $N(\theta, \sigma)$ (with $\theta = \mu + z\beta$ and $\sigma^2 = z$) and a generalized inverse Gaussian random variable, $GIG(\lambda, \chi, \psi)$ (with $\chi = \delta^2$ and $\psi = \alpha^2 - \beta^2$).

An algorithm[39] to generate NIG random variables that is based on Atkinson (1982) and

Michael, Schucany & Hass (1976) is presented below (Rydberg, 1997):

To generate $\Delta X \sim \text{NIG}(\alpha, \beta, \mu, \delta)$:

1. Sample Z from $GIG(\lambda, \chi, \psi)$ where $\chi = \delta^2$ and $\psi = \alpha^2 - \beta^2$, and let $\sigma^2 = Z$

   To sample Z from $GIG(\lambda, \delta^2, \alpha^2 - \beta^2)$, the following is a special approach

   for sampling from the $GIG(\lambda, \chi, \psi)$ distribution that applies only to the case

   where $\lambda = -\dfrac{1}{2}$ (NIG distribution):

   a. Sample v_0 from $\chi^2(1)$

   $$\text{if we let } \mu' = \sqrt{\frac{\chi}{\psi}} = \sqrt{\frac{\delta^2}{\alpha^2 - \beta^2}} \text{, then } V = \frac{\chi(Z - \mu')^2}{\mu'^2 Z} \sim \chi^2(1)$$

   b. Solve for Z, which yields

   $$z_1 = \mu' + \frac{\mu'^2 v_0}{2\chi} - \frac{\mu'}{2\chi}\sqrt{4\mu'\chi v_0 + \mu'^2 v_0^2} \text{, and } z_2 = \frac{\mu'^2}{z_1},$$

   where v_0 is a realization of V.

   c. Choose $Z = z_1$ with probability $\dfrac{\mu'}{\mu' + z_1}$ (or $Z = z_2$ with probability

   $\dfrac{z_1}{\mu' + z_1}$)

2. Let $\sigma^2 = Z$

3. Sample Y from N(0,1)

4. Return $\Delta X = \mu + \beta\sigma^2 + \sigma Y$

---

[39] Other methods to generate NIG random variables exist; Kalemanova and Werner (2006) present an alternative algorithm that uses Gaussian and inverse Gaussian random variables.

The algorithm presented above was used to generate at every time step, t, n independent sample points of $(\Delta X)_t^{(i)}$ with the parameters $NIG(\alpha, \beta, \mu, \delta)$.

This effectively results in a process $X_t = \sum_{t=0}^{t} \Delta X_t^{(i)}$, $1 \leq i \leq n$, such that

$X_t \sim NIG(\alpha, \beta, \mu t, \delta t)$.

Finally, using (5.43), the values of the simulated uncertainty process, S_{t_i}, are obtained forward in time by evaluating $S_{t_i} = S_{t_i-1} \exp(X_{t_i})$.

In the context of our application, the land acquisition cost and the traffic volume uncertainties are to be modeled as independent NIG Lévy processes.

5.6.2.2 Testing the Algorithm

To test the algorithm in Rydberg (1997), we implemented it in Matlab using the parameter values contained in Appendix A, *Table 2: Deutsche Bank*.

As such, the NIG process to be generated has the following parameters:

$$X_t = NIG(\alpha, \beta, \mu t, \delta t) = NIG(75.49, -4.089, 0 \times t, 0.012 \times t)$$

The process duration was arbitrarily assumed to be 10 years, with an initial value $S_0 = 0.1$ and a number of iterations (paths), NP=50,000.

The cummulants of the generated NIG process values are tabulated below against their theoretical counterparts (as defined in (5.39)).

×10⁻³ → $\times 10^{-3}$

Year	1	2	3	4	5	6	7	8	9	10
$E[X_t]$	**-0.6509**	**-1.3019**	**-1.9528**	**-2.6038**	**-3.2547**	**-3.9057**	**-4.5566**	**-5.2076**	**-5.8585**	**-6.5095**
$\overline{X}_{Exact}$	-0.6496	-1.2692	-1.9016	-2.5906	-3.2458	-3.9530	-4.5781	-5.3195	-5.8895	-6.5748
$VAR[X_t]$	**0.1597**	**0.3193**	**0.4790**	**0.6387**	**0.7983**	**0.9580**	**1.1176**	**1.2773**	**1.4370**	**1.5966**
S^2_{Exact}	0.1588	0.3194	0.4807	0.6398	0.8022	0.9597	1.1203	1.2878	1.4484	1.6202

$\times 10^{-5}$

Year	1	2	3	4	5	6	7	8	9	10
$\kappa_3(t)$	**-0.0345**	**-0.0689**	**-0.1034**	**-0.1379**	**-0.1724**	**-0.2068**	**-0.2413**	**-0.2758**	**-0.3102**	**-0.3447**
$E\left[\tilde{X}^3_{Exact}\right]$	-0.0254	-0.0612	-0.0872	-0.1157	-0.1413	-0.2020	-0.2248	-0.2909	-0.3236	-0.3728

Year	1	2	3	4	5	6	7	8	9	10
Tskew	**-0.1709**	**-0.1208**	**-0.0986**	**-0.0854**	**-0.0764**	**-0.0698**	**-0.0646**	**-0.0604**	**-0.0570**	**-0.0540**
$Sskew_{Exact}$	-0.1269	-0.1071	-0.0828	-0.0715	-0.0622	-0.0680	-0.0600	-0.0629	-0.0587	-0.0572
Tkurt	**3.3555**	**1.6777**	**1.1185**	**0.8389**	**0.6711**	**0.5592**	**0.4794**	**0.4194**	**0.3728**	**0.3355**
$Skurt_{Exact}$	6.0190	4.5502	4.0531	3.8214	3.6925	3.5704	3.4763	3.4403	3.3824	3.3879

$E[X_t] = \kappa_1(t) = \mu_t + \delta_t \beta \gamma^{-1}$ is the theoretical expected value, $\overline{X}$ is the sample average,

$VAR[X_t] = \kappa_2(t) = \delta_t \alpha^2 \gamma^{-3}$ is the theoretical variance, and S^2 is the sample variance. In

the second table, $\kappa_3(t) = 3\delta_t \beta \alpha^2 \gamma^{-5}$ is the theoretical third moment and $E\left[\tilde{X}^3\right]$ is the

sample third moment. In the third table, Tskew and Tkurt are the theoretical skewness

and kurtosis, respectively, whereas Sskew and Skurt are those of the simulated sample.

Except for those of the kurtosis, the tabulated values indicate that the exact algorithm does indeed generate NIG random variables fairly accurately; Figure 5-1 below is a graphical illustration.

histogram area = 1.0000000   pdf area   = 1.002632125
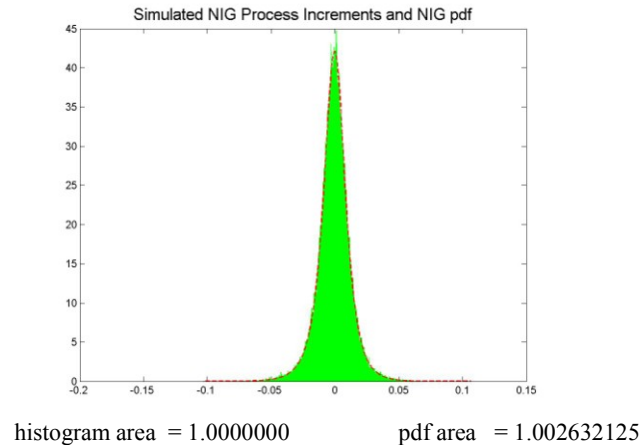
Figure 5-1: Theoretical (dotted) and Simulated (shaded) NIG Probability Distribution Function.

As stated in Figure 5-1 above, the histogram area is 1.0000000 and the probability density area is 1.002432125. The pdf area, an approximate figure, is calculated as the sum of areas of discretized bins under the NIG density function between predetermined upper and lower limits. The bin areas are evaluated at the centers of the discretization bins.

The figures below are the simulated NIG log ratios and the resulting NIG Lévy process, S_t.
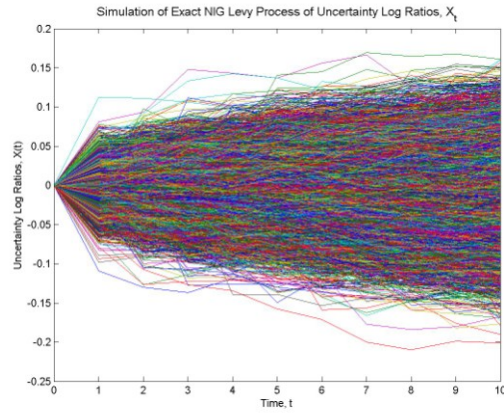
Figure 5-2: Simulated NIG Log Ratios, X_t
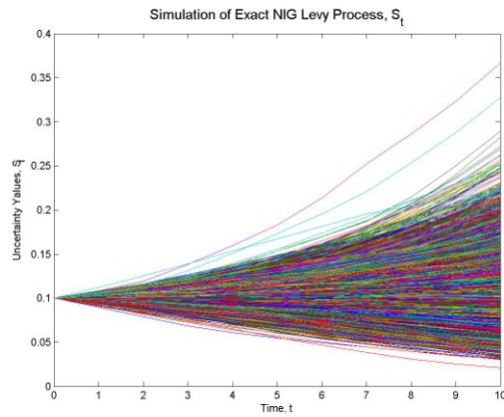
Figure 5-3: Simulated NIG Process, S_t

5.7 *Model Calibration*

The Merton, Kou and NIG models all assume different sets of parameters. The scarcity of data alluded to previously prohibits parameter estimation, which makes parameter calibration the only feasible option.

Calibration will rely on the method of moments where the moments of the proposed models are to be matched with those of the geometric Brownian motion model applied in Zhao et al. (2004); this is to make all the models comparable.

In matching the moments, the sum of squares of differences of moments of the proposed model and those of the log-normal model will be minimized. Given that all the proposed models have more parameters than those of the lognormal one, a numeric technique will be employed to minimize the following function O:

$$O=\sqrt{\sum_{i=1}^{n}\left(m_i - m_i^*\right)^2} \tag{5.45}$$

where m_i is i^{th} moment of the proposed model, whereas m_i^* is the ith moment of the base model and n is the number of moments to be matched.

In Section 5.5, we list the cummulants, $\kappa_i, \left(1 \le i \le n\right)$ of the Merton and Kou models, while in Section 5.6 those of the NIG models are listed. The moments m_i for each model can be obtained from the cummulants using the results (5.46) below:

$$m_1 = \kappa_1$$

$$m_2 = \kappa_2 + (m_1)^2$$

$$m_3 = \kappa_3 - 2(m_1)^3 + 3m_1 m_2 \tag{5.46}$$

$$m_4 = \kappa_4 + 4m_1 m_3 + 3(m_2)^2 - 12(m_1)^2 m_2 + 6(m_1)^4$$

$$m_5 = \kappa_5 + 5m_1 m_4 + 10m_2 m_3 - 10(m_1)^2 m_3 - 10m_1(m_2)^2 + 60(m_1)^3 m_2 - 24(m_1)^5$$

As for the numeric technique, the Matlab function *fminsearch* will be used to search for the model parameters that would minimize the sum of squares function O above (i.e. find the parameters in the proposed models that would best match the moments of the base model). *fminsearch* uses what is generally referred to as unconstrained nonlinear optimization to find a minimum of a scalar function of several variables, starting at an initial estimate. The initial estimates of the parameters for the proposed models will be obtained by explicitly equating the first two moments.

In the next subsection, we determine the moments of the base model and in the subsequent subsections, we present methods to obtain the initial estimates for each individual model.

5.7.1 Base Model

In Zhao et al. (2004), the traffic demand and the land price uncertainties are modeled as correlated geometric Brownian motion processes:

$$\frac{dS_t}{S_t} = \mu dt + \sigma dW_t$$

where $S_t \in \{Q_t, P_t\}$.

While the simulation of the uncertainties will be implemented as $S_t = S_0 e^{\left(\mu - \frac{\sigma^2}{2}\right)t + \sigma W_t}$, the

calibration will be performed in the log scale as $X_t = \gamma t + \sigma W_t$, where $X_t = \ln\left(\frac{S_t}{S_0}\right)$ and

$\gamma = \mu - \sigma^2/2$.

Given that $X_{t=1} \sim N(\gamma, \sigma^2)$, its moment generating function is $M_{X_t} = \exp\left(\gamma t + \sigma^2 t^2/2\right)$

and consequently the first five moments are as follows:

$$
\begin{aligned}
m_1^* &= \mathrm{E}\left[X\right] = \gamma \\
m_2^* &= \mathrm{E}\left[X^2\right] = \gamma^2 + \sigma^2 \\
m_3^* &= \mathrm{E}\left[X^3\right] = \gamma\left(\gamma^2 + 3\sigma^2\right) \\
m_4^* &= \mathrm{E}\left[X^4\right] = \gamma^4 + 6\gamma^2\sigma^2 + 3\sigma^4 \\
m_5^* &= \mathrm{E}\left[X^5\right] = \gamma\left(\gamma^4 + 10\gamma^2\sigma^2 + 15\sigma^4\right)
\end{aligned}
\tag{5.47}
$$

$$
\begin{aligned}
\mu_{X_t} &= \mathrm{E}\left[X_t = \ln\left(\frac{S_t}{S_0}\right)\right] = \left(\mu - \sigma^2/2\right)t = \gamma t \\
\sigma_{X_t}^2 &= \mathrm{Var}\left(X_t = \ln\left(\frac{S_t}{S_0}\right)\right) = \sigma^2 t
\end{aligned}
\tag{5.48}
$$

5.7.2 Merton's Model

The Merton model can be expressed as

$$X_t^{\text{Mer}} = \gamma_{\text{Mer}}t + \sigma_{\text{Mer}}W_t + \sum_{i=1}^{N_t} Y_i,$$ (5.49)

where,

$X_t^{\text{Mer}} = \ln\left(\dfrac{S_t}{S_0}\right)$, $\gamma_{\text{Mer}} = \mu_{\text{Mer}} - \sigma_{\text{Mer}}^2/2$, $(N_t)_{t \geq 0}$ is a Poisson process counting the

jumps of X_t^{Mer}, and $(Y_i)_{i \geq 1}$, representing the jump sizes, are i.i.d. random

variables such that $\Upsilon_i = \log(Y_i) \sim N(\rho, \delta^2)$ has a normal distribution. Note that

here $\gamma_{\text{Mer}} \neq \gamma$ and $\sigma_{\text{Mer}} \neq \sigma$, unless $\sum_{i=1}^{N_t} Y_i = 0$.

Merton's model is of the jump diffusion type. Here, the log-uncertainty process, X_t^{Mer} is

the superposition of two independent processes:

$$X_t^{\text{Mer}} = X_t^{\text{M\_D}} + X_t^{\text{M\_J}}$$ (5.50)

where,

$X_t^{\text{M\_D}} = \gamma_{\text{Mer}}t + \sigma_{\text{Mer}}W_t$ is a Brownian motion (diffusion) process, and

$X_t^{\text{M\_J}} = \sum_{i=1}^{N_t} Y_i$ is compound Poisson (jump) process.

From equation (5.50), and by independence,

$$\begin{aligned} \mu_{X_t^{\text{Mer}}} &= \mu_{X_t^{\text{M\_D}}} + \mu_{X_t^{\text{M\_J}}} \\ \sigma_{X_t^{\text{Mer}}}^2 &= \sigma_{X_t^{\text{M\_D}}}^2 + \sigma_{X_t^{\text{M\_J}}}^2 \end{aligned}$$ (5.51)

where

$$\mu_{X_t^{\text{Mer}}} = \text{E}\left[X_t^{\text{Mer}}\right], \mu_{X_t^{\text{M\_D}}} = \text{E}\left[X_t^{\text{M\_D}}\right] = \gamma_{\text{Mer}}t, \ \mu_{X_t^{\text{M\_J}}} = \text{E}\left[X_t^{\text{M\_J}}\right] = \lambda t \, \text{E}[Y] = \lambda t \rho,$$

$$\sigma^2_{X_t^{\mathrm{Mer}}} = \mathrm{var}\left(X_t^{\mathrm{Mer}}\right), \sigma^2_{X_t^{\mathrm{M\_D}}} = \mathrm{var}\left(X_t^{\mathrm{M\_D}}\right) = \sigma^2_{\mathrm{Mer}}, \text{ and}$$

$$\sigma^2_{X_t^{\mathrm{M\_J}}} = \mathrm{var}\left(X_t^{\mathrm{M\_J}}\right) = \lambda t \left(\mathrm{var}(Y) + \left(E[Y]\right)^2\right) = \lambda t \left(\delta^2 + \rho^2\right).$$

Thus,

$$\gamma_{\mathrm{Mer}} t = \mu_{X_t^{\mathrm{Mer}}} - \lambda t \rho$$

$$\sigma^2_{\mathrm{Mer}} t = \sigma^2_{X_t^{\mathrm{Mer}}} - \lambda t \left(\delta^2 + \rho^2\right) \qquad (5.52)$$

Given that at time $t=1$ the values $\mu_{X_1} = \gamma$ and $\sigma^2_{X_1} = \sigma^2$ from the base model, X_t, are

known, let $\mu_{X_{t=1}^{\mathrm{Mer}}} = \mu_{X_1}$ $\left(\text{i.e. } E\left[X_1^{\mathrm{Mer}}\right] = E[X_1]\right)$ and let

$$\sigma^2_{X_{t=1}^{\mathrm{Mer}}} = \sigma^2_{X_1} \left(\text{i.e. } \mathrm{var}\left(X_1^{\mathrm{Mer}}\right) = \mathrm{var}\left(X_1\right)\right).$$

Then from equations (5.48) and (5.52),

$$\gamma_{\mathrm{Mer}} = \gamma - \lambda \rho$$

$$\sigma^2_{\mathrm{Mer}} = \sigma^2 - \lambda\left(\delta^2 + \rho^2\right) \qquad (5.53)$$

Lastly, if one assumes that due to jumps the unit variance takes a percentage r of that of

the overall process unit variance (i.e. $\sigma^2_{X_{t=1}^{\mathrm{M\_J}}} = r\sigma^2$ and $\sigma^2_{X_{t=1}^{\mathrm{M\_D}}} = (1-r)\sigma^2$, $0 \le r \le 1$), and

that the jump event arrival rate, λ, as well as the mean jump size, ρ, are known, then the

initial values for the parameters of the Merton model in (5.49) can be explicitly calibrated

as shown in Figure 5-4:

<div style="border: 1px solid black; padding: 20px;">

Initial Parameters for Merton Model

- $t = 1$,

- $\gamma, \sigma, \text{ and } \sigma_{\varepsilon_1, \varepsilon_2}$ (from the base model)

- $r = r_{Mer}, 0 \leq r \leq 1$

- λ (jump event arrival rate)

- ρ such that $\left(\rho < \sqrt{\dfrac{p \cdot r \cdot \sigma^2}{\lambda}} \right)$, (mean jump size)

- $\delta = \sqrt{\dfrac{r\sigma^2}{\lambda} - \rho^2}$ (volatility of jump size)

- $\gamma_{Mer} = \gamma - \lambda\rho$ (drift of diffusion process)

- $\sigma_{Mer} = \sqrt{(1-r)\sigma^2}$ (volatility of diffusion/ GBM process)

- $\mu_{Mer} = \gamma_{Mer} + \sigma_{Mer}^2 / 2$ (drift of GBM process)

</div>

Figure 5-4: Calibration of the Initial Parameter Values for Merton Model

5.7.3 Kou's Model

Kou's model has the same form as Merton's model:

$$X_t^{\text{Kou}} = \gamma_{\text{Kou}} t + \sigma_{\text{Kou}} W_t + \sum_{i=1}^{N_t} Y_i,$$

where

$$X_t^{\text{Kou}} = \ln\left(\frac{S_t}{S_0}\right), \quad \gamma_{\text{Kou}} = \mu_{\text{Kou}} - \sigma_{\text{Kou}}^2 / 2,$$

and $(N_t)_{t \geq 0}$ is a Poisson process. However, in this case, $(Y_i)_{i \geq 1}$ are i.i.d. random variables

such that $\Upsilon_i = \log(Y_i) \sim \text{DExp}(p, \lambda_+, \lambda_-)$ has an asymmetric double exponential

distribution as opposed to having a normal distribution. $p \in [0,1]$ is the probability of an

upward jump, while $\lambda_+ > 0$ and $\lambda_- > 0$ govern the decay of the tails for the distribution

of positive and negative jump sizes.

Similar to Merton's model, Kou's is also of the jump diffusion type, and the log-

uncertainty process above can also be represented as

$$X_t^{\text{Kou}} = X_t^{\text{K\_D}} + X_t^{\text{K\_J}} \tag{5.54}$$

where,

$X_t^{\text{K\_D}} = \gamma_{\text{Kou}} t + \sigma_{\text{Kou}} W_t$ is a Brownian motion (diffusion) process and

$X_t^{\text{K\_J}} = \sum_{i=1}^{N_t} Y_i$ is compound Poisson (jump) process, where $(Y_i)_{i \geq 1}$ is as defined

above.

From equation (5.54) and by independence:

$$\mu_{X_t^{\text{Kou}}} = \mu_{X_t^{\text{K\_D}}} + \mu_{X_t^{\text{K\_J}}}$$
$$\sigma^2_{X_t^{\text{Kou}}} = \sigma^2_{X_t^{\text{K\_D}}} + \sigma^2_{X_t^{\text{K\_J}}} \tag{5.55}$$

where

$$\mu_{X_t^{\text{Kou}}} = \mathrm{E}\left[X_t^{\text{Kou}}\right], \mu_{X_t^{\text{K\_D}}} = \mathrm{E}\left[X_t^{\text{K\_D}}\right], \mu_{X_t^{\text{K\_J}}} = \mathrm{E}\left[X_t^{\text{K\_J}}\right],$$
$$\sigma^2_{X_t^{\text{Kou}}} = \mathrm{var}\left(X_t^{\text{Kou}}\right), \sigma^2_{X_t^{\text{K\_D}}} = \mathrm{var}\left(X_t^{\text{K\_D}}\right), \text{ and } \sigma^2_{X_t^{\text{K\_J}}} = \mathrm{var}\left(X_t^{\text{K\_J}}\right).$$

$$\mu_{X_t^{\text{K\_D}}} = \gamma_{\text{Kou}} t \tag{5.56}$$

$$\mu_{X_t^{\text{K\_J}}} = \lambda t \, \mathrm{E}[Y] = \lambda t \left[\frac{p}{\lambda_+} - \frac{(1-p)}{\lambda_-}\right] \tag{5.57}$$

$$\sigma^2_{X_t^{\text{K\_D}}} = \sigma^2_{\text{Kou}} t \tag{5.58}$$

$$\sigma^2_{X_t^{\text{K\_J}}} = \lambda t \left[\frac{p}{\lambda_+^2} + \frac{(1-p)}{\lambda_-^2}\right] \tag{5.59}$$

From (5.57) and (5.59), one can obtain the following expressions for λ_+ and λ_+^2:

$$\lambda_+ = p \frac{\lambda \lambda_-}{\mu_{X_1^{\text{M\_J}}} \lambda_- + (1-p)\lambda} \tag{5.60}$$

$$\lambda_+^2 = p \frac{\lambda \lambda_-^2}{\sigma^2_{X_1^{\text{M\_J}}} \lambda_-^2 - (1-p)\lambda} \tag{5.61}$$

These produce the following quadratic equation:

$$\left(p\lambda\sigma^2_{X_1^{\text{K\_J}}} - \mu^2_{X_1^{\text{K\_J}}}\right)\lambda_-^2 - 2(1-p)\mu_{X_1^{\text{K\_J}}}\lambda\lambda_- - (1-p)\lambda^2 = 0 \tag{5.62}$$

The solution of (5.62) together with (5.60) yields the following explicit expressions for

λ_- and λ_+ in terms of the mean, $\mu_{X_t^{\text{K\_J}}}$, and variance, $\sigma^2_{X_t^{\text{K\_J}}}$, of the Kou jump process:

$$\lambda_- = \frac{\mu_{X_1^{K\_J}}\lambda(1-p)\pm\sqrt{\mu_{X_1^{K\_J}}{}^2\lambda^2(1-p)^2+\left(p\lambda\sigma_{X_1^{K\_J}}^2-\mu_{X_1^{K\_J}}^2\right)(1-p)\lambda^2}}{p\lambda\sigma_{X_1^{K\_J}}^2-\mu_{X_1^{K\_J}}^2} \tag{5.63}$$

$$\lambda_+ = p\,\frac{\lambda\lambda_-}{\mu_{X_1^{K\_J}}\lambda_-+(1-p)\lambda} \tag{5.64}$$

In calibrating Kou's model, one way of assigning values to the mean and the variance, in addition to setting the sum of moments of the diffusion and jump components of the uncertainty process to be the same as those of the geometric Brownian motion base model, is to also set these component moments to be exactly the same as their counterparts in Merton's model, i.e.,

$$\mu_{X_t^{K\_J}}=\mu_{X_t^{M\_J}}\ \text{and}\ \sigma_{X_t^{K\_J}}^2=\sigma_{X_t^{M\_J}}^2 \tag{5.65}$$

and

$$\mu_{X_t^{K\_D}}=\mu_{X_t^{M\_D}}\ \text{and}\ \sigma_{X_t^{K\_D}}^2=\sigma_{X_t^{M\_D}}^2 \tag{5.66}$$

This will enable us to compare results afterwards.

With equations (5.65) in mind, note that as a way of ensuring in Kou's model above that $\lambda_->0$, the term $\left(p\lambda\sigma_{X_1^{K\_J}}^2-\mu_{X_1^{K\_J}}^2\right)$ in Eq. (5.62) is forced to be strictly positive; this explains why we previously assigned the values λ and ρ in Merton's model such that

$$\left(\rho<\sqrt{\frac{p\cdot r\cdot\sigma^2}{\lambda}}\right).$$

At time $t=1$:

- the values $\mu_{X_1}=\gamma$ and $\sigma_{X_1}^2=\sigma^2$ from the base model are known,

- γ_{Mer} is given from Merton's model,

- the volatility due jumps takes a percentage *r* of that of the overall process variance

  (i.e. $\sigma^2_{X_1^{K\_J}} = \sigma^2_{X_1^{M\_J}} = r\sigma^2$ and $\sigma^2_{X_1^{K\_D}} = \sigma^2_{X_1^{M\_D}} = (1-r)\sigma^2$, $0 \leq r = r_{\mathrm{Kou}} = r_{\mathrm{Mer}} \leq 1$),

- λ is the same as that of Merton's model, and

- the probability of upward jump, *p* is given

Given the above, the parameters of the Kou model $\left(\mu_{\mathrm{Kou}}, \sigma_{\mathrm{Kou}}, p, \lambda_-, \lambda_+\right)$ can be calibrated

as shown in Figure 5-5 below:

Initial parameters for Kou model

- $t = 1$

- $\gamma, \sigma, \text{and } \sigma_{\varepsilon_1,\varepsilon_2}$ (from base model)

- $r_{Mer}, \lambda_{Mer} \text{ and } \gamma_{Mer}$ (from Merton model)

- $r = r_{Kou} = r_{Mer}, 0 \le r \le 1$

- $\mu_{X_1^{K\_J}} = \mu_{X_1^{M\_J}} = \gamma - \gamma_{Mer}$

- $\sigma^2_{X_1^{K\_J}} = \sigma^2_{X_1^{M\_J}} = r\sigma^2$

- $\lambda = \lambda_{Mer}$

- $p, 0 \le p \le 1$

- $\lambda_- = \dfrac{\mu_{X_1^{K\_J}}\lambda(1-p) \pm \sqrt{(1-p)\lambda^2\left(\mu_{X_1^{K\_J}}{}^2(1-p) + \left(p\lambda\sigma^2_{X_1^{K\_J}} - \mu^2_{X_1^{K\_J}}\right)\right)}}{p\lambda\sigma^2_{X_1^{K\_J}} - \mu^2_{X_1^{K\_J}}}, \ \lambda_- > 0$

- $\lambda_+ = p\dfrac{\lambda\lambda_-}{\mu_{X_1^{K\_J}}\lambda_- + (1-p)\lambda}, \ \lambda_+ > 0$

- $\sigma_{Kou} = \sigma_{X_1^{K\_D}} = \sqrt{(1-r)\sigma^2}$

- $\gamma_{Kou} = \gamma - \mu_{X_1^{K\_J}} = \gamma - \lambda\left[\dfrac{p}{\lambda_+} - \dfrac{(1-p)}{\lambda_-}\right]$

- $\gamma_{Kou} = \gamma - \lambda\rho$

- $\mu_{Kou} = \gamma_{Kou} + \sigma^2_{Kou}/2$

Figure 5-5: Calibration of the Initial Parameter Values for Kou Model

5.7.4 NIG Model

Having four parameters, $(\alpha, \beta, \mu, \delta)$, the negative inverse Gaussian model is of the infinite activity Lévy subclass; it contains no diffusion component. The model will be calibrated by simultaneously equating its first two moments, m_1 and m_2, with their counterparts in the base model, m_1^* and m_2^*, and solving for the two parameters α and β (μ and δ are assumed to be known). Details are as follows:

$$m_1 = \kappa_1 = \mu + \frac{\delta\beta}{\left(\alpha^2 - \beta^2\right)^{\frac{1}{2}}} = m_1^* \tag{5.67}$$

Let $L = \dfrac{m_1^* - \mu}{\delta}$, then $\dfrac{\beta}{\left(\alpha^2 - \beta^2\right)^{\frac{1}{2}}} = L$, $\alpha^2 - \beta^2 = \dfrac{\beta^2}{L^2}$, $\alpha^2 = \left(1 + \dfrac{1}{L^2}\right)\beta^2$, and

$$\frac{\alpha^2}{\alpha^2 - \beta^2} = 1 + L^2.$$

$$m_2 = \kappa_2 + \left(m_1\right)^2 = \frac{\delta\alpha^2}{\left(\alpha^2 - \beta^2\right)^{\frac{3}{2}}} + \left(\mu + \frac{\delta\beta}{\left(\alpha^2 - \beta^2\right)^{\frac{1}{2}}}\right)^2 = m_2^* \tag{5.68}$$

$$m_2 = \mu^2 + \frac{\delta}{\left(\alpha^2 - \beta^2\right)^{\frac{1}{2}}}\left(\frac{\delta\beta^2}{\left(\alpha^2 - \beta^2\right)^{\frac{1}{2}}} + 2\mu\beta + \frac{\alpha^2}{\alpha^2 - \beta^2}\right) = \mu^2 + \frac{\delta L}{\beta}\left(\delta L\beta + 2\mu\beta + L^2 + 1\right)$$

$$= \mu^2 + \delta L\left(\delta L + 2\mu\right) + \frac{\delta L}{\beta}\left(L^2 + 1\right) = m_2^*$$

Therefore, given μ and δ, $\quad \beta = \dfrac{\delta L\left(L^2+1\right)}{m_2{}^* - \mu^2 - \delta L\left(\delta L + 2\mu\right)}$ and $\alpha^2 = \left(1 + \dfrac{1}{L^2}\right)\beta^2$, where

$L = \dfrac{m_1{}^* - \mu}{\delta}$. The initial values for the parameters of the NIG model can be explicitly

calibrated as shown in Figure 5-6, below:

Initial parameters for NIG model

- Boundary conditions:

  $\alpha > 0$ (shape), $0 \le |\beta| < \alpha$ (skewness), $\mu \in \mathbb{R}$ (location), $\delta > 0$ (scale)

- $t = 1$

- γ and σ $\qquad\qquad$ (from base model)

- $m_1^* = \mathrm{E}[X] = \gamma$

- $m_2^* = \mathrm{E}[X^2] = \gamma^2 + \sigma^2$

- μ and δ are arbitrarily chosen such as above boundary conditions are met

- $L = \dfrac{m_1{}^* - \mu}{\delta}$

- $\beta = \dfrac{\delta L\left(L^2+1\right)}{m_2{}^* - \mu^2 - \delta L\left(\delta L + 2\mu\right)}$

- $\alpha = \beta\sqrt{\left(1 + \dfrac{1}{L^2}\right)}$
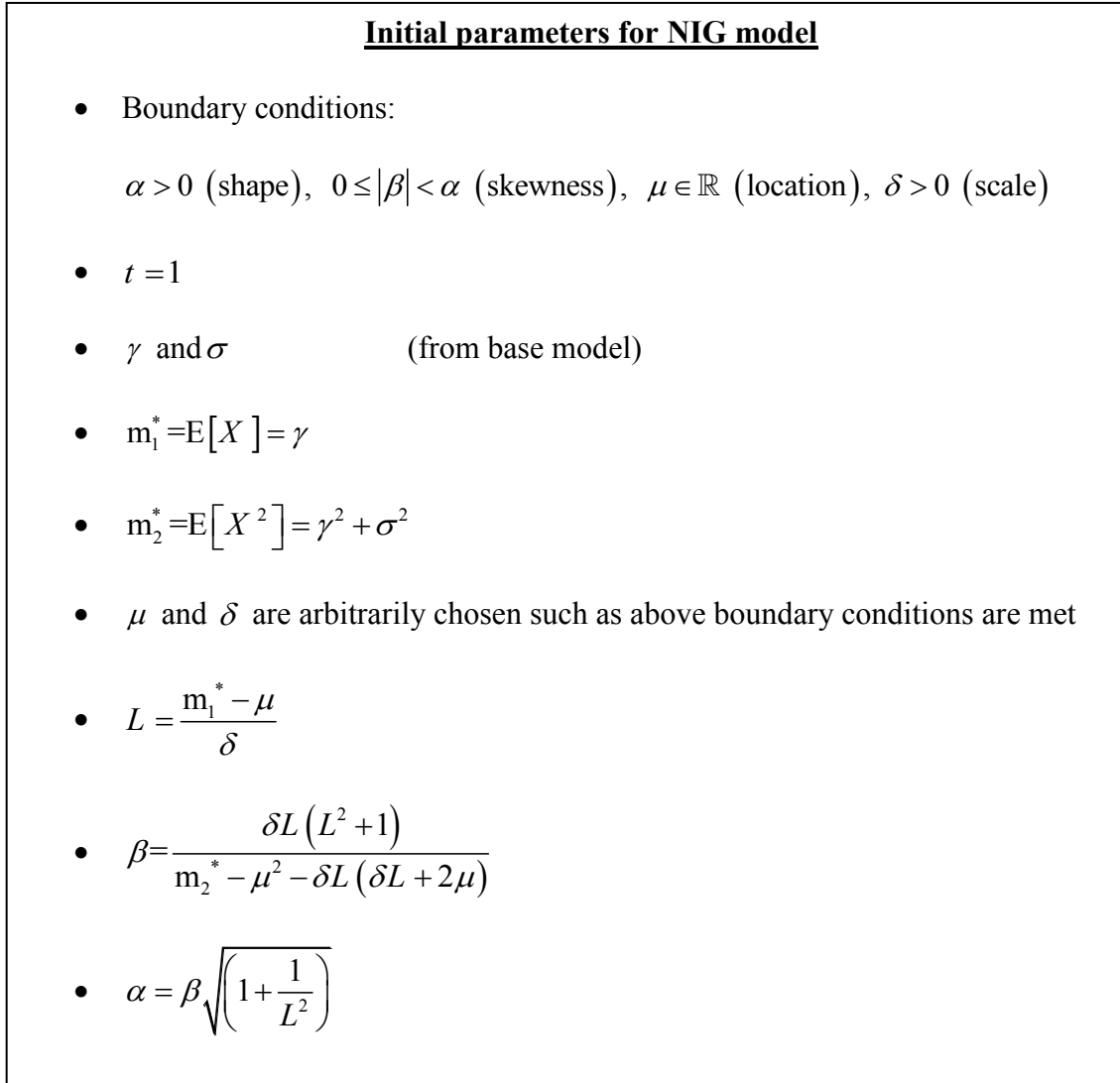
Figure 5-6: Calibration of the Initial Parameter Values for NIG Model

Note that unlike Merton and Kou models, where the uncertainties are correlated, the

uncertainties in the NIG case are assumed to be independent.

6   Model Implementations and Testing

The purpose of this chapter is to implement, test and analyze the core and proposed models. In the first section, we outline our version of the decision-making system algorithm by highlighting its key distinguishing features. Subsequently, in Section 6.2 we present the case study in which the testing of the models is implemented. To facilitate model comparability and establish a baseline, we calculate the moments of the base GBM model in Section 6.3, where we further show a sample detailed system output and reveal the simulation results of the GBM model as a baseline. Sections 6.4 through 6.6 unveil the calibration calculations and the simulation results for the proposed Merton, Kou, and NIG models. Analysis and discussion follow in Section 6.7 and final conclusions are communicated in Section 6.8.

6.1 *System Algorithm*

The algorithm developed by Zhao et al. (2004) is based on the least-squares Monte Carlo (LSMC) method originally proposed by Longstaff and Schwartz (2001) and extended to "solve a much more complex problem" (Zhao et al., 2004). The algorithm used in this paper is a modified version of the one developed by Zhao et al. (2004), as presented in Section 3.1.3. In an effort to make the decision making algorithm more realistic, several important changes are introduced to the algorithm that bear important consequences, as will be seen shortly. The aspects of similarity and disparity between the two algorithms are described below.

The embedded real options, the underlying uncertainties, and the multi-stage stochastic model for the development of the highway system are the same in our implementation as those presented in Zhao et al. (2004) (see Section 3.1) with the following exceptions:

1. In Zhao et al, 2004, the do-nothing is not considered as an option for the land purchase and the highway expansion decisions. However, in our implementation this option is explicitly exercised. As a result, there are 10 states and 10 possible decisions as opposed to the 9 and 8 in Zhao et al. (2004).

2. Unlike the implementation in Zhao et al. (2004), where in the simulation step the highway service quality index, I_t, is introduced as a Markov chain but subsequently evaluated deterministically, I_t in our implementation is evaluated stochastically as Markov process (see Section 3.1.3).

3. It is unclear exactly how the rehabilitation decision is made and what is its relation to the HSQI matrix in Zhao et al (2004). Some statements indicate that

154

the rehabilitation decision is not automatically deduced from HSQI matrix but rather as an independent option, although others have suggested otherwise. Below is a list of both positions.

a. **Rehabilitation decisions being independent from HSQI matrix**:

    i. The rehabilitation decision is introduced as an embedded American-style real option where "the focus will be on the exercise timing […]" (Ibid., p. 25).

    ii. Zhao et al., 2004, state that "for simplicity we have implicitly assumed that the uncertainties considered are independent of the DM's [decision maker's] decisions" (Ibid. p.26).

    iii. In the numerical examples (Ibid., p. 29), it is stated that

$$\text{when } I_t > 1, \ I_{t+1} = \begin{cases} I_t - 1 & p = 0.5 \\ I_t & p = 0.5 \end{cases} \tag{6.1}$$

$$\text{when } I_t = 1, \ I_{t+1} = 1 \tag{6.2}$$

    iv. Figure 1 on (Ibid., p. 29) displays a plot of the regression of $\pi_t(\cdot)$ when $I_t = 2$ and $h_t = 1$.

b. **Rehabilitation decisions being dependent on HSQI matrix**:

    i. As presented in conditions (3.9) and (3.10) in Section 3.1.3, "[t]he rehabilitation constraints state that when the highway is in the 'poor' condition, rehabilitation is mandatory. After the rehabilitation, the highway service level is upgraded to the 'excellent' condition". (Ibid., p. 27). This also seems to be inconsistent with (6.2) above.

ii. "[T]he maximum number of functions $\pi_t(\cdot)$ to be determined at time t to be 360 $(=72\times5)$" (Ibid., p. 29). Had the rehabilitation decision been considered an independent decision, the maximum number would instead have been the product of the number of states, the number of lane purchases and highway expansion decision options, the number of the highway service quality indices, and the two rehabilitation decision options: i.e. $9\times8\times5\times2=720$, or more accurately, $9\times8\times9=648$ given that rehabilitation would not be required when $I_t=5$.

4. In our implementation, the rehabilitation decision is mechanically controlled by the HSQI transition probability matrix. It is based on conditions (6.3) and the rehabilitation constraints (3.9) and (3.10) in Section 3.1.3. As such, the Highway Service Quality Index Transition Probability Matrix takes the following form:

$$
\begin{array}{c}
\begin{array}{ccccc} 5 & 4 & 3 & 2 & 1 \end{array} \\
\begin{array}{c} 5 \\ 4 \\ 3 \\ 2 \\ 1 \end{array}
\begin{bmatrix}
0.5 & 0.5 & 0 & 0 & 0 \\
0 & 0.5 & 0.5 & 0 & 0 \\
0 & 0 & 0.5 & 0.5 & 0 \\
0 & 0 & 0 & 0.5 & 0.5 \\
1 & 0 & 0 & 0 & 0
\end{bmatrix}
\end{array}
\tag{6.4}
$$

5. Using the adopted procedure, one can still allow for rehabilitation decisions to be randomly made at other states by modifying the HSQI matrix probabilities. Below is one example.

$$
\begin{array}{ccccc}
5 & 4 & 3 & 2 & 1 \\
\end{array}
$$

$$
\begin{array}{c}
5 \\ 4 \\ 3 \\ 2 \\ 1
\end{array}
\begin{bmatrix}
0.500 & 0.500 & 0 & 0 & 0 \\
0.200 & 0.400 & 0.400 & 0 & 0 \\
0.333 & 0 & 0.333 & 0.333 & 0 \\
0.400 & 0 & 0 & 0.300 & 0.300 \\
1 & 0 & 0 & 0 & 0
\end{bmatrix}
\tag{6.5}
$$

6. The regression using the functional form used in taking the form of (3.19) yields badly scaled matrices, inaccurate and inconsistent results, and relatively very negligible coefficient values for the higher order terms (Ibid.). For example, one sample set of coefficients (generated with 2000 iterations) presented below indicate that a_6 is 0.

$$\pi_t\left(\cdot\right)=a_1+a_2 P_t+a_3 Q_t+a_4 Q_t^2+a_5 Q_t^3+a_6 Q_t^4$$

1.0e+008 *

a_1=6.65996220563437

a_3=0.00243747654678

a_4=-0.00000050131797

a_5=0.00000000005314

a_6=-0.00000000000000

a_2=-0.00000088006731

7. Despite the previous observation, the functional form in (3.19) is still adopted:

$$\pi_t\left(\cdot\right)=a_1+a_2 P_t+a_3 Q_t+a_4 Q_t^2+a_5 Q_t^3+a_6 Q_t^4 \tag{6.6}$$

8. The multi-stage stochastic model adopted here uses the same general model framework but with some alterations:

   a. Boundary conditions at $t=T$:

   In addition to setting $\pi_T\left(X_T; u_T, v_T\right)=0, \forall u_T, v_T, X_T$ (i.e. expected system value for future states at $t=T+1$ is zero), the condition $c_T\left(u_T, v_T\right)=0, \forall u_T, v_T$ is also assumed in our implementation (i.e. given that no more decisions are to be considered at $t=T$, the costs should be zero as well).

   b. Conditional expectation:

   Given that $\pi_t\left(X_t; u_t, v_t\right)$ "can be viewed as conditional expectation of $\left(X_t, u_t, v_t\right)$" and "that there is a separate $\pi_t\left(\cdot\right)$ for each possible realization of $\left(u_t, v_t\right)$" (Zhao, 2003), then regression should take place before the maximization operator is applied in Step 2 of the algorithm in Section 3.1.3. Otherwise, regardless of the origin state, $\pi_t\left(\cdot\right)$ would have the same value for any state decision whose destination state is the same.

   c. Given that at $t=0$, there is only one data item, it is not possible to determine $\pi_{t=0}\left(\cdot\right)$ at $t=1$. Thus, discounting will be used instead.

   d. More details are available in the modified algorithm presented below.

9. Apart from the above, the principal change in this paper, which is the main thesis put forth, is the alteration of uncertainty model of X_t from the Brownian motion

to the Merton, Kou, and NIG models. Below is a description of the algorithm used in this dissertation.

Algorithm: Obtaining $\pi_{t-1}\left(X_{t-1};u_{t-1},v_{t-1}\right)$ with $\pi_t\left(X_t;u_t,v_t\right)$ known for all u_t,v_t from $t=T-1$ until $t=2$.

Data: u_{t-1} and v_{t-1} are given.

- Step 0:

    o Generate, based on the assumed uncertainty model, a random matrix

    X_t for all paths from $t=1$ to T and evaluate the transformed matrix $X_t^{"}$

    from $t=1$ to $T-1$ based on (6.6)

    o Set $t \leftarrow T$, $\pi_T\left(X_T;u_T,v_T\right)=0, \forall u_T,v_T,X_T$ and $c_T\left(u_T,v_T\right)=0, \ \forall u_T,v_T$

- Step 1: Evaluate $F\left(u_t,v_t;X_t\right)=f_t\left(v_t;X_t\right)+e^{-r}\pi_t\left(X_t;u_t,v_t\right)-c_t\left(u_t,v_t\right),\forall u_t,v_t$

- Step 2: Evaluate $F_t\left(v_t\right)=\max_{u_t}\left\{F\left(u_t;v_t\right)\right\},\forall v_t$

- Step 3: While $t \neq 1$, regress $F\left(u_t,v_t;X_t\right)$ on $X_{t-1}^{"}$ to obtain an individual

    $\pi_{t-1}\left(X_{t-1};u_{t-1},v_{t-1}\right) \forall u_{t-1},v_{t-1}$

- Step 4: while $t \neq 0$, update $t \leftarrow t-1$, then go to step 1

At $t=0$, by setting $u_0 =\bar{u}_0$, $v_0 =\tilde{v}_0$, and $X_0 =\tilde{X}_0$, the evaluation of (6.7) below gives the optimal decision that yields the maximal expected system profit, F^*.

$$F^* = f_{t=0}\left(v_0,X_0\right)+\max_{u_0}\left\{e^{-r}F\left(u_0,v_0;X_1\right)-c_0\left(u_0,v_0\right)\right\} \tag{6.7}$$

6.2   Case Study: Selecting Design Alternatives

The case study in which the proposed algorithm and uncertainty models are tested is the one used in Zhao et al. (2004) in selecting a design alternative during the design phase. In this phase, two decisions that need to be made when designing a new highway are the number of lanes to be built and the right-of-way that needs to be acquired.

As in Zhao et al. (2004), we apply the model to a 50-mile-long section of highway. Likewise, the planning horizon is 25 years and the initial traffic demand (Q_0) and land price (P_0) are 4,200 vehicles of ADT and $70,000 per acre, respectively. The interest rate is 0.08.

The tables presented below list the highway configuration options and system parameters used in Zhao et al. (2004) and adopted herein.

Number of Lanes	Width (ft)
2	150
4	150
6	175
8	200

Table 1: Available Right-of -Way and Corresponding Minimum Width

Parameter	Value
γ	$14,000
α	1000 vehicles
ℓ	$10,000 per acre per year
ω	12 ft
d	50 miles
c_n	$750,000
c_m	$200,000
T	25 years
β	0.7

Table 2: Test System Values

Note: According to Zhao et al. (2004), the above cost data are based on a highway cost survey by the Washington State Department of Transportation (2002).

In the following four sections we present the results of our implementations of this case study using the different uncertainty models: GBM, Merton, Kou and NIG. In each, the number of simulation iterations is 10,000 and the number of time steps is 25 years.

6.3 Geometric Brownian Motion Model

6.3.1 Moments of the Base Model

To enable the calibration of the proposed models, moments of the GBM are determined here.

The parameters used in the geometric Brownian motion for the uncertainties, $S_t = \begin{bmatrix} Q_t \\ P_t \end{bmatrix}$,

in Zhao et al. (2004) are $\mu = \begin{bmatrix} 0.05 \\ 0.1 \end{bmatrix}, \sigma = \begin{bmatrix} 0.2 \\ 0.2 \end{bmatrix}$, and $\varepsilon_{1,2} = \text{cov}(\varepsilon_1, \varepsilon_2) = 0.2$.

Therefore, as previously illustrated in Section 5.7.1, the uncertainty processes $X_{t=1}$,

$X_t \sim N(\gamma, \sigma^2)$, have these parameters $\gamma = \mu - \sigma^2/2 = \begin{bmatrix} 0.03 \\ 0.08 \end{bmatrix}$ and $\sigma = \begin{bmatrix} 0.2 \\ 0.2 \end{bmatrix}$.

Correspondingly, the first five moments of the base model $X \sim N(\gamma, \sigma^2)$ are as follows:

$$\text{E}[X] = \gamma = \begin{bmatrix} 0.03 \\ 0.08 \end{bmatrix}$$

$$\text{E}[X^2] = \gamma^2 + \sigma^2 = \begin{bmatrix} 0.0409 \\ 0.0464 \end{bmatrix}$$

$$\text{E}[X^3] = \gamma(\gamma^2 + 3\sigma^2) = \begin{bmatrix} 0.003627 \\ 0.010112 \end{bmatrix}$$

$$\text{E}[X^4] = \gamma^4 + 6\gamma^2\sigma^2 + 3\sigma^4 = \begin{bmatrix} 0.00501681 \\ 0.00637696 \end{bmatrix}$$

$$\text{E}[X^5] = \gamma(\gamma^4 + 10\gamma^2\sigma^2 + 15\sigma^4) = \begin{bmatrix} 0.0007308243 \\ 0.0021280768 \end{bmatrix}$$

The above moments will used later to calibrate the proposed models.

6.3.2 Sample Model Implementation

The calculation requirement of the decision-making problem at hand is immense. In an effort to depict our implementation of the system through tangible means, we exhibit in Appendix 4 a sample of a complete output of the GBM model algorithm for a hypothetical project in the planning phase; the planning horizon is 3 years, while the initial traffic demand and land price are 4,200 vehicles of ADT and $70,000, respectively. For conciseness, the core calculations are not displayed and the number of iterations (matrix rows) is confined to 3. However, given the differences in implementation noted earlier in Section 6.1, we illustrate in detail below how, in the regression core of the algorithm, the values of $\pi_{t-1}\left(X_{t-1};u_{t-1},v_{t-1}\right)$ are calculated and used for a sample state. The reader is encouraged to go through the material of Appendix 4 to become familiarized with the notation used and to refer back there as needed to verify the input and the results values.

Sample Illustrative Example of the Core Algorithm Results for a Sample State

At time step t=3, the regression of $\pi_{t-1}\left(X_{t-1};u_{t-1},v_{t-1}\right)$ uses the following values of the untransformed values of the two uncertainties, $S_{t=2}$ (or S below) that are generated for previous time step t=2:

```
S(:,2,1) =              S(:,2,2) =
  1.0e+003 *              1.0e+003 *
    5.3031                  92010
    3.7649                  94650
    3.6136                  66800
```

With $(6.6)^{40}$, these translate into the poorly scaled transformed matrix $X_{t=2}$ (or X_T below):

```
X_T(:,:,2) =
  1.0e+014 *
  0.00000000000001  0.00000000005303  0.00000028122870  0.00149138389829  7.90895795101062  0.00000000092010
  0.00000000000001  0.00000000003765  0.00000014174472  0.00053365469670  2.00915656762273  0.00000000094650
  0.00000000000001  0.00000000003614  0.00000013058105  0.00047186768083  1.70514105146377  0.00000000066800
```

As a result of this fact, the computation of $X(X'X)^{-1}X'$ transpires into an unreliable[41] result:

```
X*inv(X'*X)*X' =
                -0.527347    -0.6191752   -0.556429
                -0.4826184    0.83481309   -0.142078
                -0.0062542    0.13832138    1.1452568
```

Given that at the time step $t=3$, $\pi_3 = 0$ and $c_3 = 0$ $\forall u_t, v_t$, then

$F(u_3; v_3) = f_3(v_3; S_3)$ $\forall u_3$ [Note: f_t here is a function of the untransformed uncertainty matrix, S_t, not X_t]

Therefore, all three decisions, $u_{t=3} \in \{1, 2, 3\}$ that are feasible at state $v_{t=3} = 7$ have the same values. For example, $F(u_3; v_3)$ (or F_all_d below) takes the same values for all the decisions:

```
F_all_d42 =
                103440000    103440000    103440000
                103440000    103440000    103440000
                103440000    103440000    103440000
```

---

[40] Implemented as $\pi_t(\cdot) = a_1 + a_2 Q_t + a_3 Q_t^2 + a_4 Q_t^3 + a_5 Q_t^4 + a_6 P_t$

[41] The unreliability is reflected in the associative matrix multiplication property not holding in the computations involving X_t and in the different outcomes generated using different computing programs.

[42] Note: while the columns of F_all_d have to be the same at $t=T$, the rows here happened randomly to be identical.

164

and the value-to-go (or total value) of this state, $F_t\left(v_{t=3}\right) = \max\limits_{u_t=3}\left\{F\left(u_{t=3};v_{t=3}\right)\right\}$ (or F_i

below) is

F_i =
    103440000
    103440000
    103440000

Consequently, $\pi_2\left(X_2;u_2,v_2=7\right)\,\forall u_2$ (or F_hat_all_d $= X\left(X\,'X\,\right)^{-1}X\,'$F_all_d) is:

F_hat_all_d =
    1.00E+08*

-1.7615	-1.7615	-1.7615
0.2173	0.2173	0.2173
1.3213	1.3213	1.3213

At t=2, the value of state 7, $f_2\left(v_2=7;S_2\right)$ is:

f_t(:,7,2) =
    103440000
    115200000
    103440000

and the cost matrix of the decisions u_2 is:

c_PathDecStateTime(:,:,7,2) =

0	75000000	150000000
0	75000000	150000000
0	75000000	150000000

As a result of the costs of the decisions taking different values, the values of the state

would likewise be different under these decisions. For decisions u_2 at state $v_2=7$,

$F\left(u_2=3;v_2=7\right)$ (or F_all_d below) is:

F_all_d =

    1.00E+08*

        -0.5917   -1.3417   -2.0917

         1.3526   0.6026   -0.1474

         2.2541   1.5041   0.7541

and the value-to-go, $F_2(v_2) = \max_{u_2} \{F(u_2; v_2)\}$ is

F_i=

    1.00E+08

      -0.5917

       1.3526

       2.2541

corresponding to the 1st decision.

Using $S_{t=1}$, $X_{t=1}$ becomes:

X_T(:,:,1) =

 1.0e+014 *

 0.00000000000001 0.00000000003934 0.00000015473996 0.00060870056846 2.39444542614139 0.00000000069930

 0.00000000000001 0.00000000003998 0.00000015988002 0.00063928026997 2.55616215946005 0.00000000075180

 0.00000000000001 0.00000000003158 0.00000009975491 0.00031506589385 0.99510411912649 0.00000000074530

and

X*inv(X'*X)*X' =

        -1.0712 -2.1204 -1.3663

        -2.0396 -1.0722 -1.5655

        -1.7139 -1.7871   0.0795

Therefore, $\pi_1(X_1; u_1, v_1 = 7)$ becomes:

F_hat_all_d =

      1.00E+08*

        -5.3142   -1.8957   1.5228

        -3.7722   -0.2643   3.2437

        -1.2239   1.3422   3.9082

At $t=1$, the same process continues except that regression would no longer be performed

given that $S_{t=0}$ is constant (known).

The value at state $v_1 = 7$, $f_1(v_1;S_1)$ is:

f_t(:,7,1) =

   115200000
   115200000
   115200000

and the cost matrix of the decisions u_1 is:

c_PathDecStateTime(:,:,7,1) =

         0   75000000   150000000
         0   75000000   150000000
         0   75000000   150000000

Then $F(u_1;v_1 = 7)$ becomes:

F_all_d =

   1.00E+08*
    -3.7536   -1.3417   1.0577
    -2.3302   0.1580   2.6463
    0.0222   1.6410   3.2597

and the value-to-go, $F_1(v_1) = \max_{u_1} \{F(u_1;v_1)\}$ is

F_i=

  1.00E+08
    1.0577
    2.6463
    3.2597

corresponding to the 3rd decision.

At $t=0$, $v_{t=0} = 1$ and $f_0(v_0;S_0)$ (or f_to below) is:

f_to =

   0
   0
   0

The cost of decision $u_0 = 7$ is:

```
c_Path_vo_to (:,7) =
                1.00E+09
                    0.8500
                    0.8500
                    0.8500
```

Then $F\left(u_0 = 7; v_0 = 1\right)$ becomes:

```
Fo_all_d (:,7)=
            1.00E+08
                -7.5236
                -6.0572
                -5.4909
```

The evaluation of (6.7) for $\forall u_{t=0}$ at $v_{t=0} = 1$ yields the project value and the optimal

decision. The maximum expected project value is:

```
Expected_System_Value (7) =
                    1.00E+09
                        3.2667
```

corresponding to decision 1 (do-nothing).

6.3.3   GBM Model Simulation

Having shown above how the algorithm works in a trivial example, we now present the

results of our implementation of the algorithm to the case study in Zhao et al. (2004).

Below is a summary of the simulation output for the GBM model. The table presented

shows the average project values for all 10 states at each time step in the 25-year

planning horizon in reverse order. The highlighted values correspond to the states having

the maximum project values at each time step.

Time	1	2	3	4	5	6	7	8	9	10
		System State Value (1.0e+08 *)								
		Geometric Brownian Motion Model								
25	0	0.7891	0.9141	1.0391	0.8044	0.9294	**1.0544**	0.9207	1.0457	1.0175
24	0	1.4955	1.7359	1.9763	1.5038	1.7442	**1.9846**	1.7052	1.9455	1.8681
23	0	2.1243	2.5471	2.9698	1.5457	1.9684	**2.3911**	0.9754	1.3981	0.0219
22	0	2.7489	3.1941	3.6394	2.7438	3.189	**3.6342**	3.095	3.5402	3.3726
21	0	2.7489	3.1941	3.6394	2.7438	3.189	**3.6342**	3.095	3.5402	3.3726
20	0	3.8211	4.4409	5.0607	3.8107	4.4305	**5.0503**	4.2926	4.9124	4.6704
19	0	4.2971	4.9943	5.6914	4.2847	4.9818	**5.679**	4.8245	5.5216	5.2461
18	0	4.7379	5.5064	6.275	4.7247	5.4933	**6.2618**	5.3183	6.0868	5.7797
17	0	5.1449	5.9793	6.8138	5.1311	5.9656	**6.8**	5.7731	6.6075	6.2687
16	0	5.5159	6.4112	7.3065	5.4976	6.3929	**7.2882**	6.1809	7.0762	6.7051
15	0	5.8578	6.8093	7.7608	5.8363	6.7877	**7.7392**	6.5582	7.5097	7.1098
14	0	6.1733	7.1766	8.1799	6.1492	7.1525	**8.1559**	6.9077	7.911	7.4848
13	0	6.4672	7.5183	8.5695	6.4436	7.4948	**8.546**	7.2378	8.289	7.8401
12	0	6.7418	7.8372	8.9326	6.7225	7.8179	**8.9132**	7.5525	8.6479	8.1788
11	0	7.0017	8.1379	9.274	6.9914	8.1275	**9.2637**	7.8573	8.9935	8.5072
10	0	7.245	8.4188	9.5926	7.2455	8.4192	**9.593**	8.144	9.3178	8.8122
9	0	7.4675	8.6761	9.8846	7.4753	8.6838	**9.8924**	8.3993	9.6079	9.078
8	0	7.662	8.903	10.144	7.669	8.91	**10.15**	8.608	9.849	9.289
7	0	7.832	9.102	10.372	7.829	9.099	**10.369**	8.777	10.047	9.458
6	0	7.975	9.273	10.57	7.955	9.253	**10.55**	8.91	10.208	9.592
5	0	8.103	9.426	10.748	8.068	9.391	**10.714**	9.037	10.36	9.727
4	0	8.241	9.587	10.934	8.216	9.562	**10.908**	9.218	10.565	9.932
3	0	8.409	9.776	11.144	8.428	9.796	**11.163**	9.484	10.852	10.227
2	0	8.594	9.981	11.369	8.683	10.07	**11.458**	9.791	11.179	10.545
1	0	8.801	10.207	11.613	8.987	10.392	**11.798**	10.129	11.535	10.857
0	0	2.1243	2.5471	**2.9698**	1.5457	1.9684	2.3911	0.9754	1.3981	0.0219

Table 3: System State Values -GBM Model (10,000 iterations)

The maximum average state value at time 0 is 2.9698×10^8, corresponding to state 4.

This suggests that the most optimal decision is to acquire maximum width (200ft) of land

and build only two lanes.

6.4 Merton's model

Calibration

As illustrated in Figure 5-4 in Section 5.7.2, the initial parameters of the Merton model as represented in Eq. (5.16), namely $\mu_{Mer}, \sigma_{Mer}, \lambda, \rho, \delta$, can be obtained by matching the moments with respect to μ_{Mer} and σ_{Mer} as follows:

- $t = 1$,

- $\gamma = \begin{bmatrix} 0.03 \\ 0.08 \end{bmatrix}, \sigma = \begin{bmatrix} 0.2 \\ 0.2 \end{bmatrix}, \sigma_{\varepsilon_1, \varepsilon_2} = 0.2$ (given),

- $r = \begin{bmatrix} 0.5 \\ 0.5 \end{bmatrix}$ (by assumption), $0 \leq r \leq 1$,

- $\lambda = \lambda_{Mer} = \begin{bmatrix} 0.05 \\ 0.03 \end{bmatrix}$ (by assumption),

- $\rho = \begin{bmatrix} 0.4 \\ 0.5 \end{bmatrix}, \left(\rho < \begin{bmatrix} \sqrt{\dfrac{0.5 \cdot 0.5 \cdot 0.04}{0.05}} = 0.447 \\ \sqrt{\dfrac{0.5 \cdot 0.5 \cdot 0.04}{0.03}} = 0.577 \end{bmatrix} \right)$,

- $\delta = \sqrt{\dfrac{r\sigma^2}{\lambda} - \rho^2} = \begin{bmatrix} \sqrt{\dfrac{0.5 \cdot 0.04}{0.05} - 0.4^2} \\ \sqrt{\dfrac{0.5 \cdot 0.04}{0.03} - 0.5^2} \end{bmatrix} = \begin{bmatrix} \sqrt{6}/5 \\ \sqrt{5/12} \end{bmatrix}$,

- $\gamma_{Mer} = \gamma - \lambda\rho = \begin{bmatrix} 0.03 - 0.05 \cdot 0.4 \\ 0.08 - 0.03 \cdot 0.5 \end{bmatrix} = \begin{bmatrix} 0.010 \\ 0.065 \end{bmatrix}$,

- $\sigma_{Mer} = \sqrt{(1-r)\sigma^2} = \begin{bmatrix} \sqrt{0.5 \cdot 0.04} \\ \sqrt{0.5 \cdot 0.04} \end{bmatrix} = \begin{bmatrix} \sqrt{0.02} \\ \sqrt{0.02} \end{bmatrix}$, and

$$\mu_{Mer} = \gamma_{Mer} + \sigma^2_{Mer}/2 = \begin{bmatrix} 0.010+0.02/2 \\ 0.065+0.02/2 \end{bmatrix} = \begin{bmatrix} 0.020 \\ 0.075 \end{bmatrix}$$

Using the above initial parameters, parameter calibration is subsequently performed numerically by matching the first two, three, and four moments. The two tables below portray the calibration results of the Merton model parameters for the traffic demand and land price uncertainties, respectively.

	Base model GBM given	1st 2 mom. mat'ed. Merton calculation	**1st 2 mom. mat'ed. Merton calibration**	1st 3 mom. mat'ed. Merton calibration	1st 4 mom. mat'ed. Merton calibration
gama_GBM	0.03				
sigma_GBM	0.2				
r*		0.5			
lambda*		0.05	0.050000000	0.157173774	**-2.29020E-16**
rho*		0.4	0.400000001	0.001376479	0.121013564
delta		0.489897949	0.489897948	0.000060899	**-0.050458405**
gama_Mer		0.01	0.010000000	0.029783654	0.030000000
sigma_Mer		0.141421356	0.141421356	0.199999254	0.200000000
mu_Mer		0.02	0.020000000	0.049783504	0.050000000
c1=		0.03	0.03	0.03	0.03
c2=		0.04	0.04	0.04	0.04
c3=		0.0176	0.0176	4.12317E-10	-6.17547E-19
c4=		0.030436326	0.030436326	6.77356E-13	-1.20823E-20
m1=	0.03	0.03	0.03	0.03	0.03
m2=	0.0409	0.0409	0.0409	0.0409	0.0409
m3=	0.003627	0.021227	0.021227	0.003627	0.003627
m4=	0.00501681	0.037565136	0.037565136	0.00501681	0.00501681
* Assumed to be given initially		fval:	0	4.078833E-10	1.22663E-18

Row label (left side, rotated): Traffic Demand, Q - Merton

Table 4: Calibrated Parameters for Traffic Demand Uncertainty -Merton Model

		Base model GBM given	1st 2 mom. mat'ed. Merton calculation	**1st 2 mom. mat'ed. Merton calibration**	1st 3 mom. mat'ed. Merton calibration	1st 4 mom. mat'ed. Merton calibration
	gama_GBM	0.08				
	sigma_GBM	0.2				
	r*		0.5			
	lambda*		0.03	0.030000000	0.036888760	0.026112682
	rho*		0.5	0.500000000	0.001907359	0.000567222
	delta		0.645497224	0.645497224	**-0.000344301**	0.000078905
Land Price, P - Merton	gama_Mer		0.065	0.065000000	0.079929640	0.079985188
	sigma_Mer		0.141421356	0.141421356	0.199999653	0.199999979
	mu_Mer		0.075	0.075000000	0.099929571	0.099985184
	c1=		0.08	0.08	0.08	0.08
	c2=		0.04	0.04	0.04	0.04
	c3=		0.0225	0.0225	2.80994E-10	5.04217E-12
	c4=		0.044831146	0.044831146	-3.93312E-12	4.15022E-14
	m1=	0.08	0.08	0.08	0.08	0.08
	m2=	0.0464	0.0464	0.0464	0.0464	0.0464
	m3=	0.010112	0.032612	0.032612	0.010112	0.010112
	m4=	0.00637696	0.058408106	0.058408106	0.00637696	0.00637696
* Assumed to be given initially			fval:	0	2.719354E-10	5.04841E-12

Table 5: Calibrated Parameters for Land Price Uncertainty -Merton Model

For both uncertainties, matching the first two moments yields almost the same values for all the parameters as those assumed and calculated initially. Apart from the fact that when the first three and four moments are matched, some infeasible parameter values are obtained (i.e. λ and/or $\delta < 0$); the value of ρ for the other cases is so small that jumps are being effectively smoothed out (i.e., the model is forced back to GBM).

Based on these findings, one may reasonably conclude that to calibrate the Merton model parameters it would suffice to match only the first two moments after guesstimating the jump parameters, based on one's belief regarding the behaviour of jumps in the empirical data.

Model Implementation

The above calibrated parameters, obtained by matching the first two moments, are used to generate the traffic demand and land price uncertainties using the Merton model. The

simulated average project values obtained in the decision-making system using the

Merton model are presented in

Table 6 below. Again, the highlighted values correspond to the states having maximum

project values at each time step.

	System State Value (1.0e+08 *) Merton Model									
Time	1	2	3	4	5	6	7	8	9	10
25	0	0.7931	0.9181	1.0431	0.8255	0.9505	1.0755	0.9652	**1.0902**	1.0882
24	0	1.5033	1.7437	1.9841	1.5433	1.7837	2.0241	1.7894	**2.0297**	2.002
23	0	2.1597	2.5066	2.8535	2.2073	2.5542	**2.9012**	2.5518	2.8987	2.8473
22	0	2.7653	3.2105	3.6558	2.8197	3.265	**3.7102**	3.2539	3.6991	3.6242
21	0.0048	3.3278	3.8624	4.397	3.389	3.9236	**4.4582**	3.9042	4.4388	4.3406
20	0	3.8424	4.4622	5.082	3.9107	4.5305	**5.1503**	4.5035	5.1233	5.0037
19	0	4.3188	5.016	5.7131	4.3921	5.0893	**5.7864**	5.0541	5.7512	5.6097
18	0	4.7605	5.529	6.2976	4.8407	5.6093	**6.3778**	5.5679	6.3365	6.1743
17	0	5.1673	6.0018	6.8362	5.253	6.0874	**6.9219**	6.0377	6.8722	6.6876
16	0	5.5401	6.4354	7.3307	5.6279	6.5232	**7.4185**	6.4628	7.3581	7.1497
15	0	5.8829	6.8344	7.7859	5.9711	6.9226	**7.8741**	6.8501	7.8016	7.569
14	0	6.1979	7.2012	8.2045	6.2851	7.2884	**8.2917**	7.2032	8.2065	7.9493
13	0	6.4906	7.5418	8.593	6.5794	7.6305	**8.6817**	7.5348	8.586	8.307
12	0	6.7665	7.8619	8.9572	6.862	7.9574	**9.0527**	7.8559	8.9513	8.6545
11	0	7.0254	8.1615	9.2976	7.1312	8.2674	**9.4035**	8.1628	9.2989	8.9852
10	0	7.2689	8.4427	9.6165	7.388	8.5618	**9.7356**	8.4545	9.6283	9.2955
9	0	7.494	8.703	9.911	7.625	8.834	**10.042**	8.72	9.928	9.572
8	0	7.688	8.929	10.17	7.817	9.057	**10.298**	8.923	10.164	9.774
7	0	7.852	9.122	10.392	7.964	9.234	**10.504**	9.072	10.342	9.915
6	0	7.993	9.291	10.588	8.084	9.381	**10.679**	9.194	10.491	10.032
5	0	8.26	9.606	10.952	8.336	9.683	**11.029**	9.484	10.831	10.347
4	0	8.26	9.606	10.952	8.336	9.683	**11.029**	9.484	10.831	10.347
3	0	8.426	9.794	11.161	8.544	9.911	**11.279**	9.742	11.11	10.628
2	0	8.609	9.997	11.384	8.794	10.181	**11.569**	10.042	11.429	10.928
1	0	8.816	10.221	11.627	9.095	10.501	**11.907**	10.368	11.773	11.214
0	0	2.1378	2.5605	**2.9832**	1.646	2.0688	2.4915	1.1954	1.6181	0.352

Table 6: System State Values -Merton Model (10,000 iterations)

Using the Merton model to simulate the traffic demand and land price uncertainties, the

maximum average state value at time 0 is 2.9832×10^8, which corresponds to state 4.

This suggests that the most optimal decision is to acquire maximum width (200ft) of land

and build only 2 lanes.

6.5 Kou's model

Calibration

As illustrated in Figure 5-5 in Section 5.7.3, the initial parameters of the Kou model as represented in Eq. (5.16) $\left(\mu_{\text{Kou}}, \sigma_{\text{Kou}}, \lambda, p, \lambda_-, \lambda_+ \right)$ can be calibrated as follows:

- $t = 1$,

- $\gamma = \begin{bmatrix} 0.03 \\ 0.08 \end{bmatrix}, \sigma = \begin{bmatrix} 0.2 \\ 0.2 \end{bmatrix}, \sigma_{\varepsilon_1, \varepsilon_2} = 0.2$ (from base model)

- $r_{\text{Mer}} = \begin{bmatrix} 0.5 \\ 0.5 \end{bmatrix}, \lambda_{\text{Mer}} = \begin{bmatrix} 0.05 \\ 0.03 \end{bmatrix}$, and $\gamma_{\text{Mer}} = \begin{bmatrix} 0.010 \\ 0.065 \end{bmatrix}$ (from Merton model)

- $r = r_{\text{Kou}} = r_{\text{Mer}} = \begin{bmatrix} 0.5 \\ 0.5 \end{bmatrix}$ (by assumption)

- $\mu_{X_1^{K\_J}} = \mu_{X_1^{M\_J}} = \gamma - \gamma_{\text{Mer}} = \begin{bmatrix} 0.03 - 0.010 \\ 0.08 - 0.065 \end{bmatrix} = \begin{bmatrix} 0.020 \\ 0.015 \end{bmatrix}$

- $\sigma_{X_1^{K\_J}}^2 = \sigma_{X_1^{M\_J}}^2 = r\sigma^2 = \begin{bmatrix} 0.5 \times 0.04 \\ 0.5 \times 0.04 \end{bmatrix} = \begin{bmatrix} 0.02 \\ 0.02 \end{bmatrix}$

- $\lambda = \lambda_{\text{Kou}} = \lambda_{\text{Mer}} = \begin{bmatrix} 0.05 \\ 0.03 \end{bmatrix}$ (by assumption)

- $p = \begin{bmatrix} 0.5 \\ 0.5 \end{bmatrix}$ (by assumption)

- $\lambda_- = \dfrac{\mu_{X_1^{K\_J}} \lambda (1-p) \pm \sqrt{(1-p)\lambda^2 \left(\mu_{X_1^{K\_J}}{}^2 (1-p) + \left(p\lambda\sigma_{X_1^{K\_J}}^2 - \mu_{X_1^{K\_J}}^2 \right) \right)}}{p\lambda\sigma_{X_1^{K\_J}}^2 - \mu_{X_1^{K\_J}}^2}$, $\lambda_- > 0$

$\lambda_- = \begin{bmatrix} 11.124 \\ 6.873 \end{bmatrix}$

- $$\lambda_+ = p \frac{\lambda \lambda_-}{\mu_{X_1^{K\_J}} \lambda_- + (1-p)\lambda} = \begin{bmatrix} 1.124 \\ 0.873 \end{bmatrix}, \ \lambda_+ > 0$$

$$\lambda_+ = \begin{bmatrix} 1.124 \\ 0.873 \end{bmatrix}$$

- $$\sigma_{Kou} = \sigma_{X_1^{K\_D}} = \sqrt{(1-r)\sigma^2} = \begin{bmatrix} \sqrt{0.5 \cdot 0.04} \\ \sqrt{0.5 \cdot 0.04} \end{bmatrix} = \begin{bmatrix} \sqrt{0.02} \\ \sqrt{0.02} \end{bmatrix}$$

- $$\gamma_{Kou} = \gamma - \mu_{X_1^{K\_J}} = \gamma - \lambda\left[\frac{p}{\lambda_+} - \frac{(1-p)}{\lambda_-}\right] = \begin{bmatrix} 0.010 \\ 0.065 \end{bmatrix}$$

- $$\mu_{Kou} = \gamma_{Kou} + \sigma^2_{Kou}/2 = \begin{bmatrix} 0.010 + 0.02/2 \\ 0.065 + 0.02/2 \end{bmatrix} = \begin{bmatrix} 0.020 \\ 0.075 \end{bmatrix}$$

Again, using the above initial values, parameter calibration for the Kou model is subsequently performed numerically by matching the first two, three, four, and five moments. The tables below portray the calibration results of the Kou model parameters for the traffic demand and land price uncertainties, respectively.

		Base model GBM given	1st 2 mom. mat'ed. Kou calculation	1st 2 mom. mat'ed. Kou calibration	1st 3 mom. mat'ed. Kou calibration	1st 4 mom. mat'ed. Kou calibration	1st 5 mom. mat'ed. Kou calibration
	gama_GBM	0.03					
	sigma_GBM	0.2					
	mu_j		0.02				
	r		0.5				
	sigma²_j		0.02				
	lambda*		0.05	0.040293586	2.89840E-17	-4.99230E-16	1.58650E-16
	p*		0.5	0.444662747	0.381919537	0.236589282	0.201817928
	lambda_minus			11.12372436	11.98442029	6.701078843	6.282359572	0.002614807
	lambda_plus			1.123724357	1.254063855	1.654956499	6.282359572	4.484019040
	gama_Kou			0.01	0.017579939	0.030000000	0.030000000	0.029999885
	sigma_Kou			0.141421356	0.169596811	0.200000000	0.200000000	0.200001275
	mu_Kou			0.02	0.031961478	0.050000000	0.05	0.05000014
	c1=			0.03	0.03	0.03	0.03	0.029999885
	c2=			0.04	0.040311594	0.04	0.04	0.04000051
	c3=			0.0176	0.00907164	2.3826E-18	1.06071E-18	-7.0831E-09
	c4=			0.01568	0.007245245	1.48454E-18	-3.20486E-19	2.70884E-06
	c5=			0.013952	0.005776458	8.9033E-19	2.68751E-20	-0.001035963
	m1=		0.03	0.03	0.030000000	0.030000000	0.030000000	0.029999885
	m2=		0.0409	0.0409	0.041211594	0.040900000	0.040900000	0.040900503
	m3=		0.003627	0.021227	0.012726683	0.003627000	0.003627000	0.003627025
	m4=		0.00501681	0.02280881	0.013427408	0.005016810	0.005016810	0.005019642
	m5=		0.000730824	0.025427953	0.012477559	0.001767153	0.001767153	0.000731631

column label at left, rotated: Traffic Demand, Q - Kou

* Assumed to be given initially   fval: 0   2.16840E-18   8.67362E-19   2.63729E-06

Table 7: Calibrated Parameters for Traffic Demand Uncertainty -Kou Model

Land Price, P - Kou	Base model GBM given	1st 2 mom. mat'ed. Kou calculation	**1st 2 mom. mat'ed. Kou calibration**	1st 3 mom. mat'ed. Kou calibration	1st 4 mom. mat'ed. Kou calibration	1st 5 mom. mat'ed. Kou calibration
gama_GBM	0.08					
sigma_GBM	0.2					
mu_j		0.015				
r		0.5				
$sigma^2\_j$		0.02				
lambda*		**0.03**	0.030448786	**1.849100E-16**	-2.34180E-15	0.069674461
p*		**0.5**	0.499161010	0.301320051	0.068368862	**-5.83680E-15**
lambda_minus		6.872983346	7.171128945	8.775615795	6.338434529	23.61848977
lambda_plus		0.872983346	0.907691309	2.117482896	3.051165251	0.002509577
gama_Kou		0.065	0.065382064	0.080000000	0.080000000	0.082950825
sigma_Kou		0.141421356	0.147814695	0.200000000	0.200000000	0.200321622
mu_Kou		0.075	0.076306656	0.100000000	0.1	0.103015201
c1=		0.08	0.08	0.08	0.08	0.080000829
c2=		0.04	0.040593093	0.04	0.04	0.040253654
c3=		0.0225	0.020282035	5.67736E-18	2.93086E-18	-5.31404E-06
c4=		0.025833333	0.022395964	2.79324E-18	-3.19899E-18	-1.0029E-05
c5=		0.029583333	0.024666390	1.30636E-18	-3.92204E-19	-0.004085518
m1=	0.08	0.080000000	0.080000000	0.080000000	0.080000000	0.080000829
m2=	0.0464	0.046400000	0.046993093	0.046400000	0.046400000	0.046653787
m3=	0.010112	0.032612000	0.030536378	0.010112000	0.010112000	0.010167679
m4=	0.00637696	0.039410293	0.035429348	0.006376960	0.006376960	0.006436075
m5=	0.002128077	0.058016647	0.050832093	0.006219981	0.006219981	0.002195123
* Assumed to be given initially		fval:	0	3.46945E-18	2.45327E-18	1.25561E-05

Table 8: Calibrated Parameters for Land Price Uncertainty -Kou Model

As presented in tables above, the calibrated parameter values of Kou model for the two uncertainties exhibit similar patterns to those of the Merton model: matching moments beyond the second one result in jumps disappearing; this occurs by $\lambda \approx 0$ in all cases except for the fifth moment of the land price uncertainty, where the combination of the calibrated values of $p = 0^-$ and λ_- leads to only negative jumps of relatively small sizes (ignoring the fact that $p < 0$). However, unlike the calibration in Merton's case, the values calibrated are somewhat different from those assumed and calculated initially. Therefore, numeric calibration may offer a better fit.

Model Implementation

With parameters obtained by matching the first two moments, the traffic demand and land price uncertainties are generated in the decision-making system using the Kou model. The simulated average project values obtained are presented in Table 9 below.

The highlighted values correspond to the states having maximum project values at each time step.

| | | System State Value (1.0e+08 *) | | | | | | | | |
| | | | | | Kou Model | | | | | |
		1	2	3	4	5	6	7	8	9	10
	25	0	0.7909	0.9159	1.0409	0.8115	0.9365	**1.0615**	0.9351	1.0601	1.0397
	24	0	1.5003	1.7407	1.9811	1.5193	1.7597	**2.0001**	1.7357	1.9761	1.9145
	23	0	1.5003	1.7407	1.9811	1.5193	1.7597	**2.0001**	1.7357	1.9761	1.9145
	22	0.0038	2.7588	3.2035	3.6482	2.7746	3.2192	**3.6639**	3.1504	3.5951	3.454
	21	**114.46**	32.42	18.4	4.39	32.44	18.42	4.4	18.33	4.31	4.13
	20	**187.34**	51.29	28.18	5.07	51.31	28.2	5.09	28.09	4.98	4.77
	19	**330.88**	87.81	46.76	5.7	87.82	46.77	5.72	46.65	5.59	5.35
	18	**452.4**	118.76	62.52	6.29	118.77	62.54	6.3	62.4	6.16	5.89
	17	**109.95**	33.44	20.13	6.82	33.45	20.14	6.84	19.99	6.68	6.38
	16	0.2602	5.6015	6.4603	7.3192	5.6168	6.4757	**7.3345**	6.3032	7.1621	6.8308
	15	0.2526	5.9343	6.8537	7.7731	5.9463	6.8657	**7.7851**	6.6767	7.5961	7.2366
	14	**29.59**	13.585	10.889	8.193	13.597	10.901	8.205	10.699	8.003	7.618
Time	13	**21.749**	11.918	10.251	8.583	11.931	10.263	8.595	10.049	8.381	7.973
	12	**16.853**	10.97	9.958	8.947	10.988	9.977	8.965	9.755	8.744	8.316
	11	**16.075**	11.035	10.162	9.288	11.064	10.191	9.317	9.964	9.091	8.645
	10	**11.512**	10.138	9.873	9.607	10.178	9.913	9.647	9.681	9.415	8.948
	9	**10.483**	10.104	10.002	9.9	10.153	10.051	9.949	9.809	9.707	9.216
	8	8.81	9.883	10.022	10.161	9.932	10.071	**10.21**	9.813	9.952	9.432
	7	7.266	9.662	10.024	10.386	9.698	10.059	**10.421**	9.778	10.14	9.586
	6	5.902	9.462	10.022	10.581	9.477	10.037	**10.597**	9.733	10.293	9.711
	5	0	8.113	9.436	**10.758**	8.112	9.435	10.757	9.118	10.441	9.842
	4	0	8.253	9.6	10.946	8.262	9.608	**10.955**	9.304	10.65	10.054
	3	0	8.42	9.788	11.156	8.474	9.842	**11.209**	9.571	10.939	10.349
	2	0	8.605	9.993	11.38	8.728	10.116	**11.503**	9.879	11.266	10.663
	1	0	8.812	10.217	11.623	9.033	10.439	**11.845**	10.212	11.618	10.966
	0	0	2.1342	2.5569	**2.9796**	1.5885	2.0112	2.4339	1.0521	1.4748	0.1225

Table 9: System State Values -Kou Model (10,000 iterations)

Using the Kou model to simulate the traffic demand and land price uncertainties, the maximum average state value at time 0 is \$2.9796 $\times 10^8$, again corresponding to state 4 with the right of way width of 200 ft to be acquired and two lanes to be constructed.

6.6 Negative inverse Gaussian Model

Calibration

As illustrated in Figure 5-6 in Section 5.7.4, the initial parameters of the NIG model as presented in Eq. (5.16) $(\alpha,\ \beta,\ \mu,\ \delta)$ can be calibrated as follows:

- Boundary conditions:

$\alpha > 0$ (shape), $0 \le |\beta| < \alpha$ (skewness), $\mu \in \mathbb{R}$ (location), $\delta > 0$ (scale)

- $t = 1$

- $\gamma = \gamma^{Geo} = \begin{bmatrix} 0.03 \\ 0.08 \end{bmatrix}$ and $\sigma = \sigma_{Geo} = \begin{bmatrix} 0.2 \\ 0.2 \end{bmatrix}$ (from base model)

- $m_1^* = \mathrm{E}[X] = \gamma^{Geo} = \begin{bmatrix} 0.03 \\ 0.08 \end{bmatrix}$

- $m_2^* = \mathrm{E}[X^2] = \gamma^{Geo\,2} + \sigma_{Geo}{}^2 = \begin{bmatrix} 0.03^2 + 0.2^2 = 0.0409 \\ 0.08^2 + 0.2^2 = 0.0464 \end{bmatrix}$

- Let $\mu = \begin{bmatrix} 0.01 \\ 0.05 \end{bmatrix}$ and $\delta = \begin{bmatrix} 1 \\ 1 \end{bmatrix}$

- $L = \dfrac{m_1^* - \mu}{\delta} = \begin{bmatrix} 0.02 \\ 0.03 \end{bmatrix}$

- $\beta = \dfrac{\delta L \left(L^2 + 1 \right)}{m_2^* - \mu^2 - \delta L \left(\delta L + 2\mu \right)} = \begin{bmatrix} 0.500200 \\ 0.750675 \end{bmatrix}$

- $\alpha = \beta \sqrt{\left(1 + \dfrac{1}{L^2} \right)} = \begin{bmatrix} 25.029984 \\ 25.042474 \end{bmatrix}$

The tables below respectively show the calibration results of the NIG model parameters for the traffic demand and land price uncertainties, based on the above initial values.

178

	Base model GBM given	1st 2 mom. mat'ed. NIG calculation	**1st 2 mom. mat'ed. NIG calibration**	1st 3 mom. mat'ed. NIG calibration	1st 4 mom. mat'ed. NIG calibration	1st 5 mom. mat'ed. NIG calibration
mu*		0.01	0.01008	0.03	**145612.5589**	**-21817455.83**
delta*		1	1.00338	1.73805	**4614711.325**	**1494930630**
alpha		25.02998402	25.0994	43.45125	**115540125.6**	**37458666460**
beta		0.5002	0.49815	0	**-3643937.717**	**546624548.9**
gama		25.02498551	25.0944561	43.45125	**115482649.5**	**37454677872**
gama_GBM	0.03					
sigma_GBM	0.2					
m1=	0.03	0.029988024	0.029998094	0.03	0.030000633	0.029937647
m2=	0.0409	0.04087531	0.040899772	0.0409	0.040900038	0.040817819
m3=	0.003627	0.003719163	0.003721682	0.003627	0.003627078	0.003612304
m4=	0.00501681	0.000191885	0.000190932	6.35589E-05	9.04283E-18	8.54631E-23
m5=	0.000730824	0.001082361	0.001083426	0.001024166	0.001014656	0.001008435
* Assumed to be given initially		fval:	0	0	3.70189E-11	0.001031026

(Row label for the block: Traffic Demand, Q - NIG)

Table 10: Calibrated Parameters for Traffic Demand Uncertainty -NIG Model

	Base model GBM given	1st 2 mom. mat'ed. NIG calculation	**1st 2 mom. mat'ed. NIG calibration**	1st 3 mom. mat'ed. NIG calibration	1st 4 mom. mat'ed. NIG calibration	1st 5 mom. mat'ed. NIG calibration
mu		0.05	0.04994	0.08	**-330333.875**	**-58489112.47**
delta		1	1.00296	5.53324	**8160232.654**	**2107494042**
alpha		25.04247404	25.10769	138.331	**204507477.2**	**53797811877**
beta		0.750675	0.75224	-3.61E-13	**8271881.76**	**1492471685**
gama		25.03122037	25.09641871	138.331	**204340118.9**	**53777105640**
gama_GBM	0.08					
sigma_GBM	0.2					
m1=	0.08	0.079989549	0.080002721	0.08	0.080002757	0.0797076
m2=	0.0464	0.046384368	0.046400609	0.0464	0.046400442	0.045572915
m3=	0.010112	0.010250915	0.010255743	0.010112	0.010112384	0.00988471
m4=	0.00637696	0.000192315	0.000191384	6.27108E-06	2.89746E-18	4.08412E-23
m5=	0.002128077	0.003804094	0.003806736	0.003671705	0.003669406	0.003528794

(Row label for the block: Land Price, P - NIG)

Table 11: Calibrated Parameters for Land Price Uncertainty -NIG Model

The NIG model, being of the infinite activity class, does not contain a diffusion component; therefore, a different calibration pattern is revealed here. The parameters values obtained by matching the first two and three moments both resulted in different and feasible values. This is not the case for the higher moments, however.

In the case of two moments being matched, the values generated are very close to those obtained manually. This is different for the case where three moments are matched; where β is or is close to 0.

For the sake of consistency with the other models, we shall use the parameter values for the two matched moments' case.

Table 12 below presents the simulation results for the system state values using the NIG model.

| | System State Value (1.0e+08 *) | | | | | | | | | |
| | Negative Inverse Guassian Model | | | | | | | | | |
	1	2	3	4	5	6	7	8	9	10
25	0	0.7933	0.9183	1.0433	0.8246	0.9496	1.0746	0.9647	**1.0897**	1.0895
24	0	1.5035	1.7439	1.9842	1.5408	1.7812	2.0216	1.7871	**2.0275**	2.004
23	0	2.1584	2.5053	2.8522	2.2007	2.5476	**2.8945**	2.5439	2.8908	2.8437
22	0	2.762	3.2073	3.6525	2.8083	3.2535	**3.6988**	3.2403	3.6856	3.6153
21	0	3.3218	3.8578	4.3938	3.3743	3.9103	**4.4463**	3.8903	4.4263	4.3357
20	0	3.8382	4.458	5.0778	3.8956	4.5154	**5.1352**	4.4884	5.1082	4.9978
19	0	4.317	5.0142	5.7113	4.3813	5.0784	**5.7756**	5.0457	5.7428	5.6142
18	0	4.7582	5.5268	6.2953	4.8278	5.5964	**6.3649**	5.5566	6.3251	6.1772
17	0	5.1646	5.9991	6.8336	5.238	6.0725	**6.907**	6.0241	6.8586	6.6904
16	0	5.5371	6.4324	7.3277	5.6118	6.5071	**7.4024**	6.4484	7.3437	7.154
15	0	5.8787	6.8302	7.7817	5.9525	6.904	**7.8555**	6.8339	7.7854	7.5731
14	0	6.1932	7.1966	8.1999	6.2662	7.2695	**8.2728**	7.1886	8.1919	7.9581
13	0	6.4878	7.539	8.5901	6.5643	7.6155	**8.6667**	7.5277	8.5789	8.3272
12	0	6.765	7.8603	8.9557	6.8494	7.9448	**9.0401**	7.8539	8.9493	8.6823
11	0	7.0245	8.1606	9.2968	7.1185	8.2546	**9.3908**	8.1619	9.2981	9.0152
10	0	7.2684	8.4422	9.616	7.3751	8.5488	**9.7226**	8.4549	9.6287	9.3302
9	0	7.491	8.7	9.909	7.607	8.815	**10.024**	8.715	9.924	9.603
8	0	7.685	8.926	10.166	7.797	9.038	**10.278**	8.92	10.161	9.81
7	0	7.85	9.12	10.39	7.947	9.218	**10.488**	9.076	10.346	9.96
6	0	7.991	9.288	10.586	8.067	9.364	**10.662**	9.195	10.493	10.076
5	0	8.12	9.443	10.766	8.178	9.501	**10.824**	9.315	10.637	10.199
4	0	8.259	9.605	10.951	8.322	9.668	**11.014**	9.485	10.832	10.388
3	0	8.425	9.793	11.16	8.529	9.896	**11.264**	9.741	11.109	10.667
2	0	8.609	9.997	11.384	8.778	10.166	**11.553**	10.039	11.426	10.968
1	0	8.815	10.221	11.627	9.078	10.483	**11.889**	10.366	11.771	11.258
0	0	2.1376	2.5603	**2.9831**	1.6298	2.0525	2.4752	1.1936	1.6163	0.3921

(Time is the row axis label on the left.)

Table 12: System State Values -NIG Model (10,000 iterations)

The maximum average state value at time 0 is 2.9831×10^8, belonging to state 4 with the right of way width of 200ft to be acquired and two lanes to be constructed.

6.7 Results, Analysis and Discussion

6.7.1 Do-nothing Option

The no-action option is introduced explicitly as a decision in our implementation. Over the project duration, this option was predominantly the highest valued option within all decision states.

6.7.2 Calibration

As expected, in the calibration processes for the Merton and Kou models, where higher moments are matched to those of the GBM model, the jump components of the processes disappear. This is not the case for the NIG model, being of the infinite activity type.

6.7.3 Algorithm Final Decisions

The final outcomes of the algorithm in terms of optimality decisions, as summarized in Table 13 below, are essentially the same for all four models. It should be recognized, however, that while the optimal decisions at time 0 are all identical in nature and close in magnitude, the dynamics of the uncertainty processes over time that lead to these decisions at time 0 are significantly different and can lead to different interim decisions, as seen clearly in the Kou model (Table 9). There, the fluctuations of the optimal states are more frequent when compared to the other models. Moreover, the variations of the actual state values in the Kou model are so large that they assume values that are, at one point, up to two orders of magnitude higher.

	Average State Decision Values at t=0 ($ 1.0e+08 *)								
	1	2	3	4	5	6	7	8	9	10
GBM	0	2.1243	2.5471	**2.9698**	1.5457	1.9684	2.3911	0.9754	1.3981	0.0219
Merton	0	2.1378	2.5605	**2.9832**	1.646	2.0688	2.4915	1.1954	1.6181	0.352
Kou	0	2.1342	2.5569	**2.9796**	1.5885	2.0112	2.4339	1.0521	1.4748	0.1225
NIG	0	2.1376	2.5603	**2.9831**	1.6298	2.0525	2.4752	1.1936	1.6163	0.3921

Table 13: Average State Decision Values for All Models at *t*=0 (10,0000 iterations)

Other vivid illustrations that speak to the same effect of the varying uncertainty dynamics are presented below; the figures portray the generated project uncertainty values and their corresponding regression plots for all four models for state 10 at time 2.
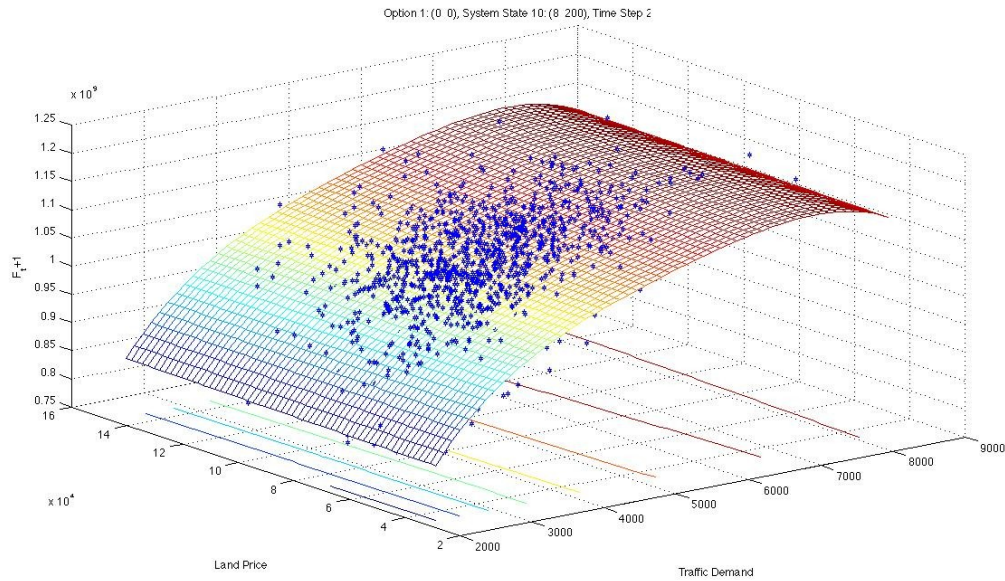

Figure 6-1: Project Values and Regression Plot for State 10 at time 2 –GBM Model (2,000 iterations)
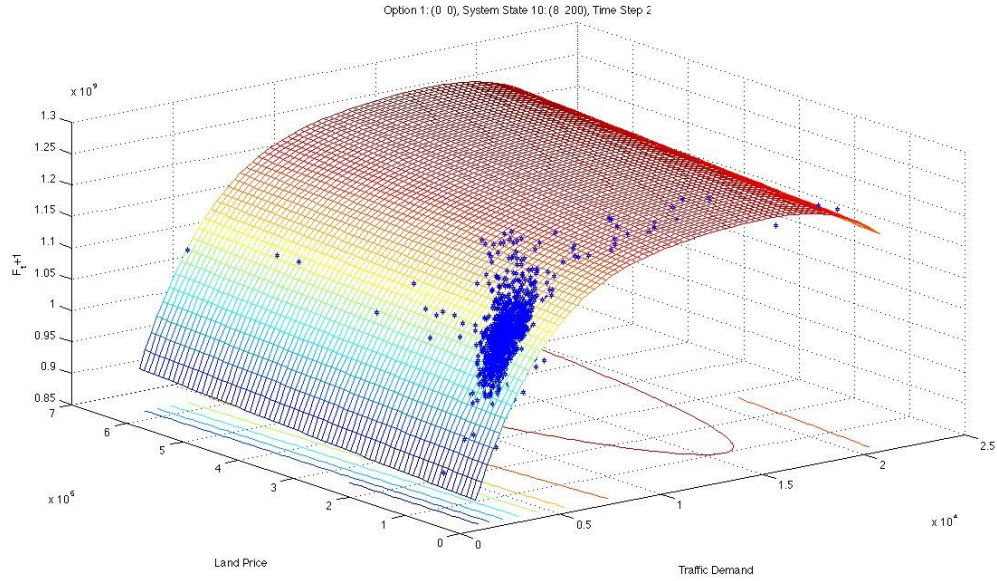
**Figure 6-2: Project Values and Regression Plot for State 10 at time 2 –Merton Model (2,000 iterations)**
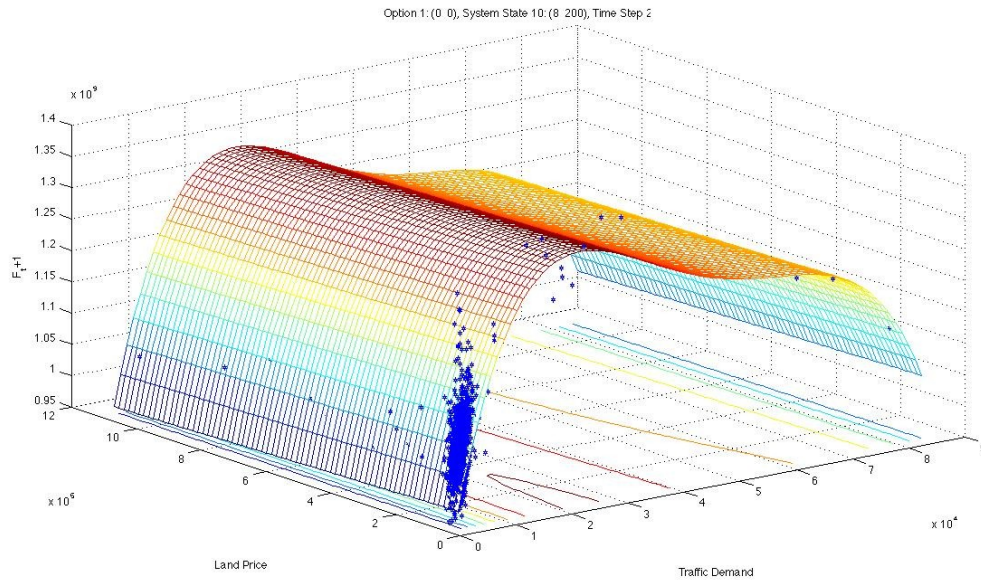
**Figure 6-3: Project Values and Regression Plot for State 10 at time 2 –Kou Model (2,000 iterations)**

183
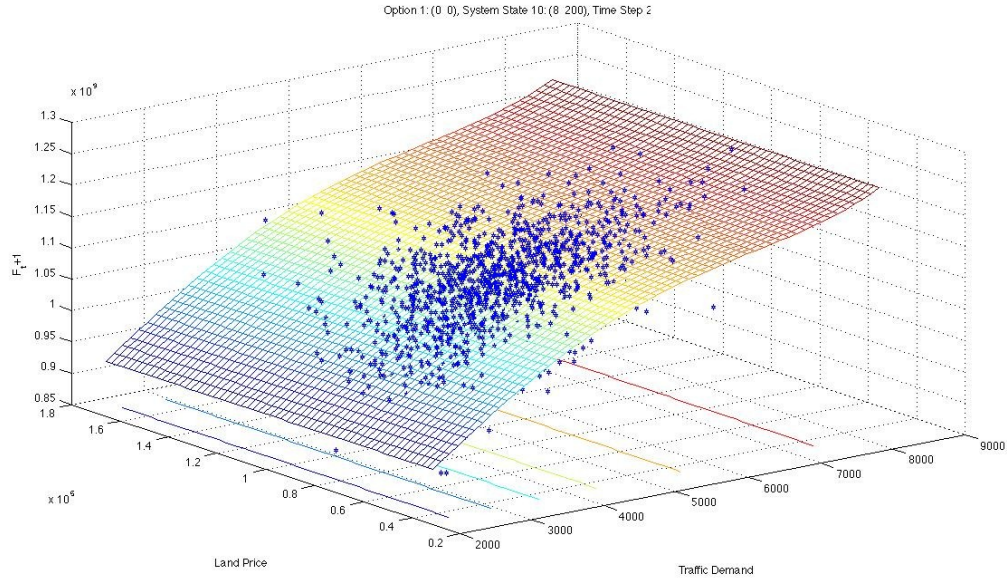
Figure 6-4: Project Values and Regression Plot for State 10 at time 2 –NIG Model (2,000 iterations)

Moreover, while close at state 4, the values of other states are not necessarily similar among the different models. As an illustration, below presents the percentage change of the values of all possible future states for the three proposed models as compared to the base GBM model.

	Percentage Change Relative to GBM Model (%)								
	2	3	4	5	6	7	8	9	10
Merton	0.64	0.53	0.45	6.49	5.10	4.20	22.55	15.74	1507.31
Kou	0.47	0.38	0.33	2.77	2.17	1.79	7.86	5.49	459.36
NIG	0.63	0.52	0.45	5.44	4.27	3.52	22.37	15.61	1690.41

Table 14: Percentage Change of State Decision Values Relative to GBM Model (10,000 iterations)

6.7.4   Continuous Time Jumps and the Highway Deterioration-Rehabilitation Processes

Earlier in Section 6.1, we stated how the deterioration process and the rehabilitation decisions are modeled in our algorithm. As a result of the approach used, jumps other than those lead by the underlying traffic demand and land price processes can still occur in a given iteration per unit time due to either a unit deterioration in the highway quality or a decision to rehabilitate. With the assumed highway quality index transition matrix in equation (6.4), there are three possibilities for the discrete time jumps: a no jump scenario, a jump due to a deterioration of one index unit, or another due to an upgrade from an index 1 to 5 (when applicable). Consequently, three project value surfaces may arise. In this case, the regression surface would be an average surface of all the possible scenarios occurring at this particular decision state. Below are illustrations at the different independent decisions available at the decision state 4 for the four models.
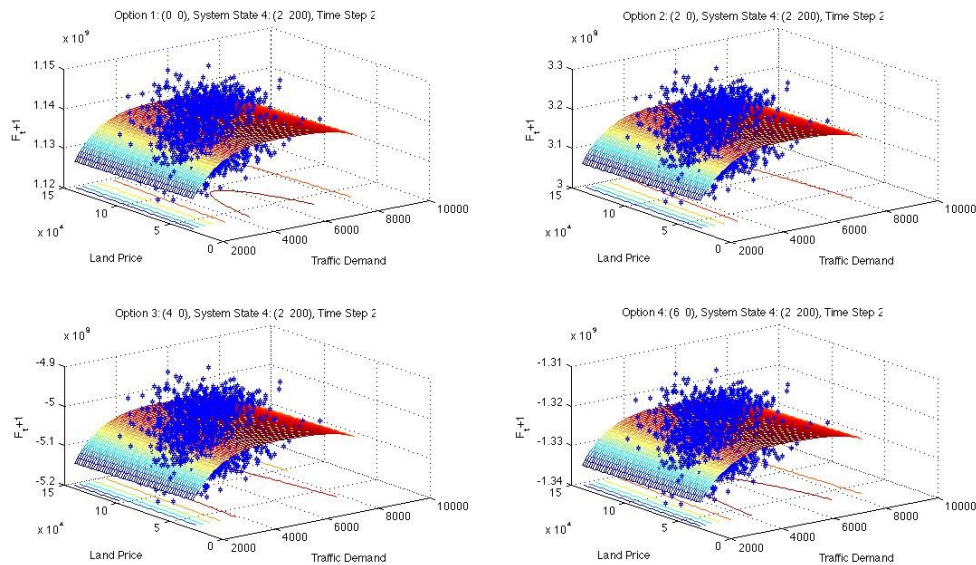
Figure 6-5: Project Values and Regression Plot for State 4 at time 2 –GBM Model (2,000 iterations)

185
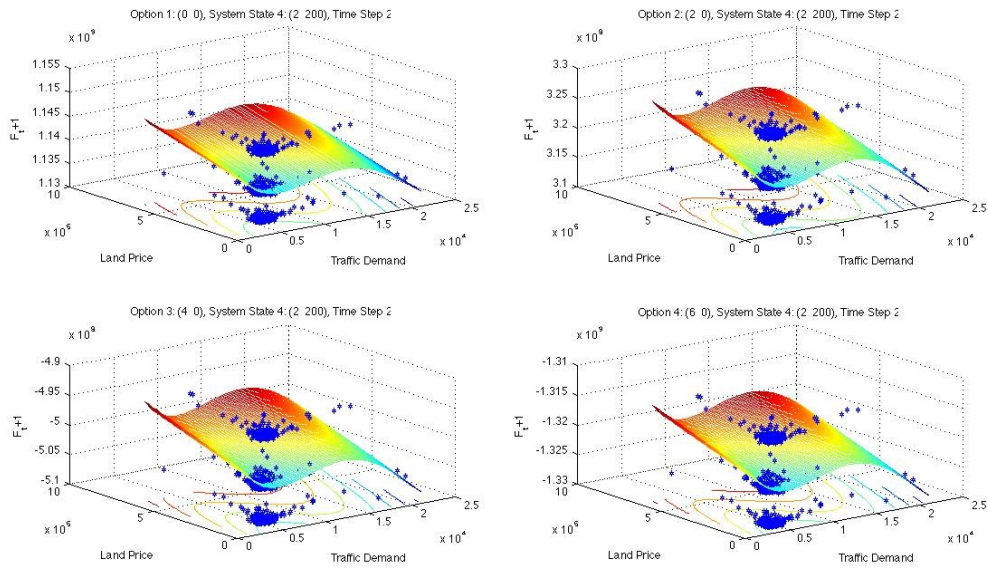
Figure 6-6: Project Values and Regression Plot for State 4 at time 2 –Merton Model (2,000 iterations)
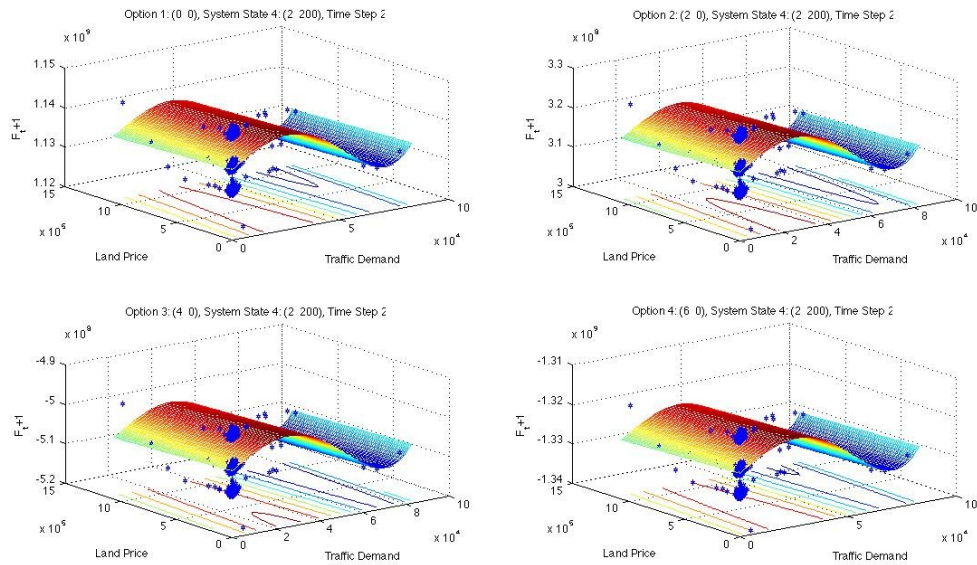
**Figure 6-7: Project Values and Regression Plot for State 4 at time 2 –Kou Model (2,000 iterations)**
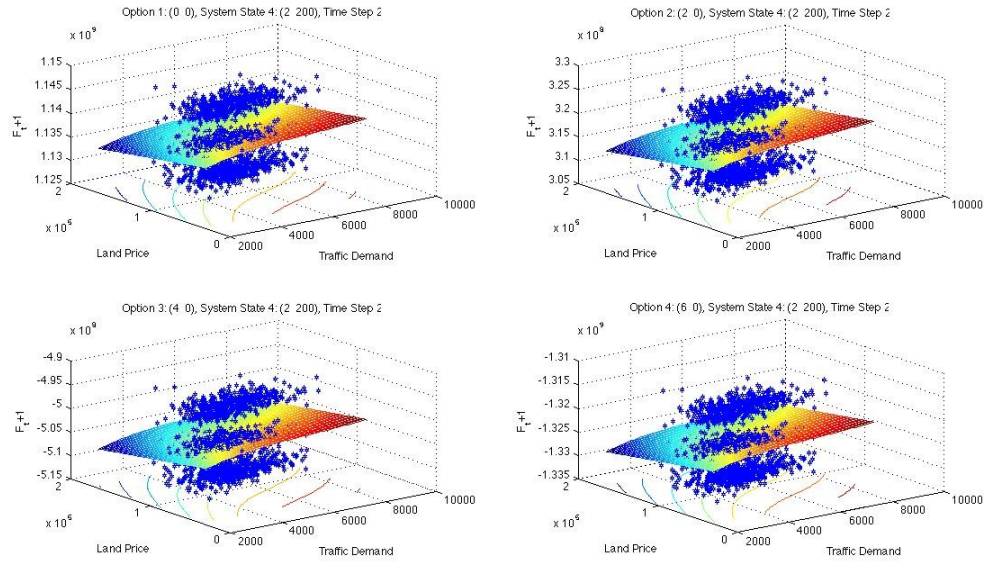
Figure 6-8: Project Values and Regression Plot for State 4 at time 2 –NIG Model (2,000 iterations)

Indeed, three surfaces are clearly visible in all four models. Furthermore, if the above assertion is accurate, then one would also expect to have a single surface of values if deterioration and rehabilitation of the highway were not possible. One easy way to investigate this is to modify the highway quality transition matrix to reflect this situation, as shown below:

$$
\begin{array}{c}
\begin{array}{ccccc} 5 & 4 & 3 & 2 & 1 \end{array} \\
\begin{array}{c} 5 \\ 4 \\ 3 \\ 2 \\ 1 \end{array}
\begin{bmatrix}
1 & 0 & 0 & 0 & 0 \\
0 & 1 & 0 & 0 & 0 \\
0 & 0 & 1 & 0 & 0 \\
0 & 0 & 0 & 1 & 0 \\
0 & 0 & 0 & 0 & 1
\end{bmatrix}
\end{array}
\qquad (6.8)
$$

In the above case, HSQI remains constant throughout the entire project duration. Likewise, if the last row of the original HSQI transition matrix were to be modified as shown in matrix (6.9) below, an additional value surface, reflecting the possibility of highway remaining at index 1, should emerge as well.

$$
\begin{array}{c}
\begin{array}{ccccc} 5 & 4 & 3 & 2 & 1 \end{array} \\
\begin{array}{c} 5 \\ 4 \\ 3 \\ 2 \\ 1 \end{array}
\begin{bmatrix}
0.5 & 0.5 & 0 & 0 & 0 \\
0 & 0.5 & 0.5 & 0 & 0 \\
0 & 0 & 0.5 & 0.5 & 0 \\
0 & 0 & 0 & 0.5 & 0.5 \\
0.5 & 0 & 0 & 0 & 0.5
\end{bmatrix}
\end{array}
\qquad (6.9)
$$

Implemented in the Kou model, the regression plots in Figure 6-9 and Figure 6-10 below are for state 4, using a hypothetical initial HSQI value of 3 and the above transition matrices (6.8) and (6.9) above, respectively. Both sets of figures reveal the expected patterns.
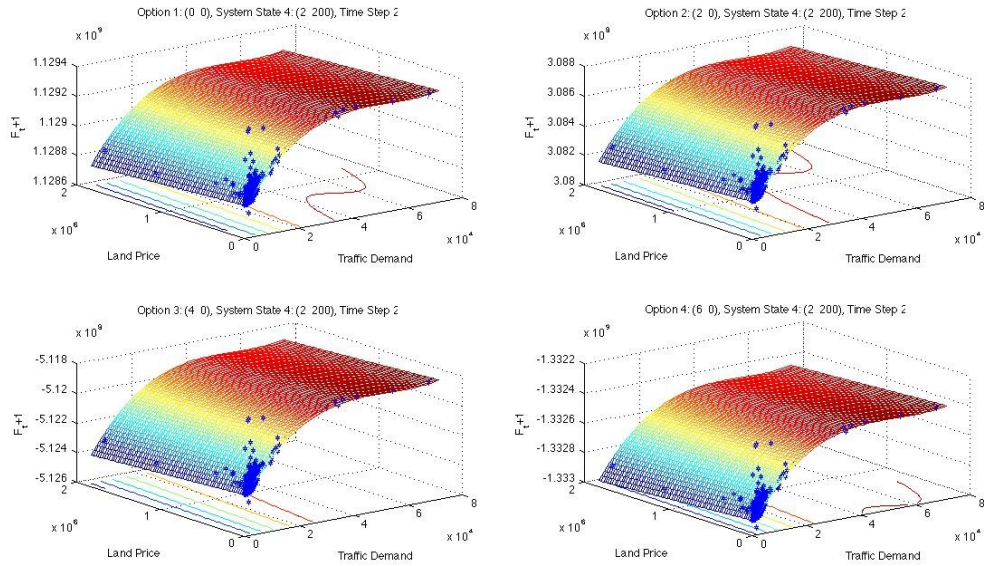
Figure 6-9: Project Values and Regression Plot for State 4 at time 2 with HSQI Matrix (6.8)– Kou Model (2,000 iterations)
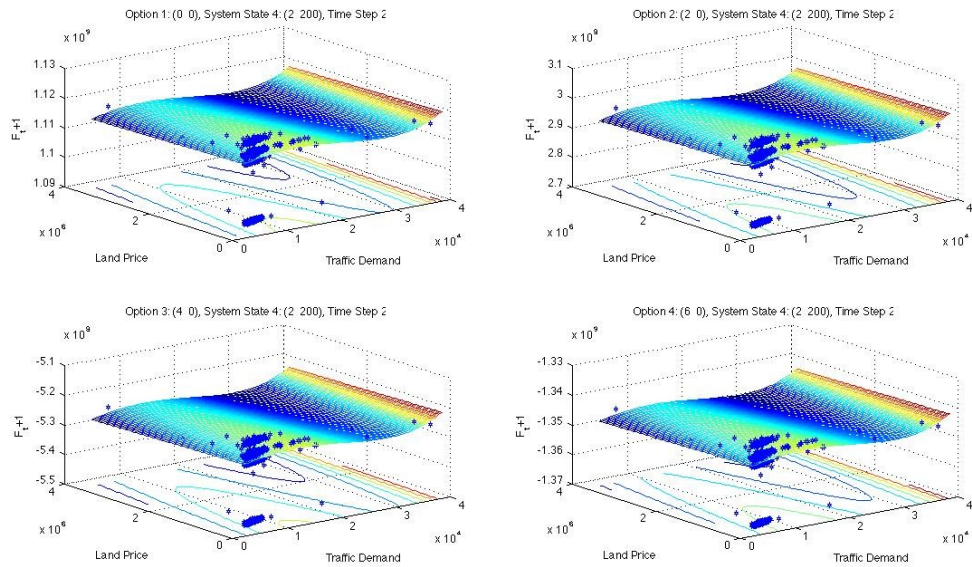
Figure 6-10: Project Values and Regression Plot for State 4 at time 2 with HSQI Matrix (6.9) Kou Model (2,000 iterations)

In general, one can see in the above figures that for a given decision state, the land price

and traffic demand uncertainties define the uncertainty surface pattern that tend to be

replicated up or down, depending on the configuration of highway service quality index

transition matrix. These value surfaces are easily visible due to the high impact of the

discrete jumps and their high probabilities in comparison with those of the continuous time uncertainties. On the other hand, when the continuous time jumps do occur (at the extremities), the situation reverses; the exact magnitude of the impact of the continuous-time jumps becomes less clear due to their low frequency and scattering among the different HSQI variable states (discrete jumps). This may lead to inaccurate regression surfaces being generated at the extremities, as seen when comparing the shapes of the regression surfaces in Figure 6-7 and Figure 6-9 above.

6.7.5 Highway Service Quality Index and the Algorithm Decisions

From the shape of the regression plots presented in Figure 6-1 to Figure 6-4, it can be seen that the state decision value is more sensitive to the traffic demand uncertainty than to that of the land price. Moreover, Figure 6-5 to Figure 6-8 show that jumps in the HSQI variable overshadows those of the continuous time uncertainties.

We have seen earlier that alterations of the continuous time models do not ultimately produce any significant effect in terms of the final outcomes of the decision algorithm. The question that would naturally arise is: can an alteration in the discrete time uncertainty model produce a different outcome?

We will investigate the potentials of this possibility through a simple modification of the HSQI transition matrix in the Kou model. The table below, presenting average state values at $t=0$, shows that alterations in the highway service quality index variable can have a more profound impact on values and decisions than the continuous time uncertainties.

Average State Decision Values at *t*=0 ($ 1.0e+08 *) -Kou Model											
HSQI		State Number									
Matrix	at *t*=0	1	2	3	4	5	6	7	8	9	10
6.5	**5**	0.4648	2.4345	2.7985	**3.1626**	1.9765	2.3405	2.7046	1.265	1.629	0.0485
6.9	**5**	0	2.0774	2.5001	**2.9228**	1.4893	1.912	2.3347	0.9405	1.3632	0.0245
6.8	**5**	0.1088	3.4445	3.8527	4.2609	3.808	4.2162	**4.6243**	3.4333	3.8414	2.4438
6.8	**3**	0.0473	1.976	2.3924	**2.8088**	1.3735	1.7899	2.2064	1.0758	1.4923	0.5491
6.8	**1**	0	1.2384	1.6611	**2.0838**	-0.0606	0.3621	0.7848	-0.9424	-0.5197	-1.8375

Table 15: Average State Decision Values for Kou Model at t=0 using Different HSQI Matrices (5,000 iterations)

6.8   Conclusions

It was shown that in our decision-making system that the optimal decision and the project value outcomes were both indifferent in all of the proposed models.

Earlier, evidence of heavy-tail behaviour was established on quantitative and qualitative grounds. The underlying uncertainty models proposed, while significantly different, all satisfy this empirical reality and thus in theory should be more precise than the GBM model. Had more data been available, parameter estimation, as opposed to calibration, could have been attempted and consequently may have yielded different outcomes. Moreover, our treatment of the HSQI variable, a non-deterministic variable to which the decision-making algorithm was shown to be sensitive, may also have had an impact on the final outcome. The sensitivity demonstrated in our implementation signifies that perhaps more emphasis should be devoted to enhancing the modeling of the HSQI variable in the mathematical representation and with respect to correlation with other variables.

Regardless of the final outcomes of the proposed Merton, Kou, and NIG models, the ultimate conclusion is that it is possible to extend the uncertainty models far beyond that of the geometric Brownian motion to a much larger and flexible parametric family of models (Lévy processes); a set of models that is not only capable of producing distributions that are heavy-tailed, but also skewed and/or having smile-shaped implied volatilities. Thus, it can offer a more accurate depiction of the empirical observations. This could be a significant advancement in the modeling of continuous-time uncertainties, not only in our implementation or in the real options framework, but also in

other types of decision-making systems, as well as anywhere else where there is evidence of jumps and where geometric Brownian motion is unjustifiably used.

Lastly, in our realm of decision-making in highway systems, this mathematical advancement represents only a humble contribution as this advancement furthers only one aspect of a node (the uncertainty factor) in the nested complexities on the path towards optimality, as discussed earlier in Chapter 2.

7 Conclusions

7.1 *Summary*

In this thesis, we started by emphasizing the value of transportation and the need for developing transportation systems. Presenting the complexity of current transportation systems, we showed the relative importance of the highway system and listed some constraints that need to be met when developing efficient transportation systems. More specifically, we reiterated the ultimate goal of ensuring that the transportation system is convenient, reliable, and economical to the commuters; economical and sustainable to the government in construction, operation, and maintenance; and balanced with respect to the benefits to the public at large and the potential private distresses to the local residents.

Developing efficient systems demands rigorous analysis and sound decisions. While the benefits of making optimal decisions are tremendous, so are the costs of making wrong decisions. It is noteworthy to reiterate here that the emphasis in these costs is not on those associated with the physical erection or expansion of the system, but rather the costs pertaining to making non-optimal decisions. To portray some aspects of these costs, we provided an elaborate and detailed list of factors, which included the size, the cost, the profitability, the human, the environmental, the irreversibility and the time factors. One other cost item mentioned that a decision-maker may fail to recognize is the opportunity cost. In the context of non-optimal decisions, we introduced the concept of opportunity cost of wrong decisions to be the forgone value that would have been realized (during the same time period) from investing in the second-highest-valued option, the sum of the

original amount of investment, any remedial expenses, and the money value of wasted time or delay.

Subsequently, we presented a few real life cases illustrating the real possibility of errors in decisions on mega-scales. We claimed that inaction is not a viable option and the path to making optimal decisions is not trivial. To realize optimality, three challenges facing the development of an optimal decision-making system were identified to be the choice of decisions, underlying uncertainties, and optimization technique.

In the context of our implementation, the first and last challenges were essentially dealt with in accordance with the treatment in Zhao et al. (2004). On the contrary, the treatment of the second challenge relating to the underlying uncertainties presented a significant diversion from Zhao et al. (2004). In the analysis, it was stated that not only are uncertainties numberless, they are highly correlated, have unknown stochastic dynamics, and consequently require vigorous data analysis and tedious data collection efforts to model.

We then examined extensively some of the most important uncertainties. In particular, we asserted that in modeling the total highway development cost process, the land acquisition cost, being possibly manifolds that of construction, supersedes the latter in importance. Also, because the land acquisition cost is in fact the expropriation price paid to landowners, in which the land price is only one component, modeling it solely as land price process involves a significant degree of underestimation.

We also stated that within the highway construction cost (modeled as a constant), which still represents a significant amount, the material cost represents a sizeable part; modeling the volatile material price process may be useful in better capturing the dynamics of the expansion and rehabilitation cost processes and, ultimately, that of the highway development cost process. Other important uncertainties presented were oil price, traffic demand, and highway service quality index.

Despite the above, we maintained Zhao et al.'s (2004) choice and definitions of the uncertainties yet, nonetheless, questioned the validity of the geometric Brownian motion assumption. In testing this assumption, real data on traffic demand and land acquisition costs needed to be collected. We explored some venues where highway traffic volume as well as both unit land price and total land acquisition cost data could be obtained in Canada. The ultimate outcome of this quest was that data could be obtained, but in statistically insignificant numbers.

Using the data collected a simple graphical test, Quantile-Quantile plot, was employed to investigate the normality of the log-ratios of the sampled uncertainty increments. The plots revealed significant deviation from normality that, while indicating unanimously that the data came from heavy-tailed distributions, failed to identify any unique distributional pattern. This supported the hypothesis that jumps could be a plausible contributing element in this heavy-tail behaviour. Aside from the logical rationale, when tested statistically the calculated low probabilities of the extreme values of the sampled increments supported this theory.

When it came to the probability theory, the varied distributions and the established existence of jumps justified the proposal of Lévy processes. Being a very wide and flexible class of jump models that, apart from being the only possible extension to the geometric Brownian motion, Lévy processes offer a very wide range of jump models that are capable of generating distributions that are heavy-tailed, skewed, and/or having smile-shaped implied volatilities.

From the list of Lévy processes, the Merton and Kou models from the finite activity subclass, as well as the negative inverse Gaussian model from the infinite activity subclass, were chosen to be implemented and tested. All of these models assume different sets of parameters.

The scarcity of data mentioned previously prohibited parameter estimation and left parameter calibration to be the only feasible alternative. Calibration was performed based on the method of moments, where the first two moments of the proposed models were matched numerically with those of the geometric Brownian motion model applied by Zhao et al. (2004) in the Selecting Design Alternatives case study.

In testing the proposed models, the above calibrated parameters were applied to the same case study settings, but using our own modified version of the decision-making algorithm of Zhao et al. The key differences in our decision-making algorithm included: the do-nothing being considered explicitly as an option; the highway service quality index

197

(HSQI) being simulated randomly as a Markov chain, where the rehabilitation decision is being made mechanically using the HSQI transition probability matrix; and in calculating the expected future state value, $\pi_t(\cdot)$, the regression is performed before the maximization operator is being applied in Step 2 of the algorithm in Zhao et al. (2004). Last but not least, the thesis put forth the introduction of Lévy processes as an alternative class of models to the GBM model.

Upon implementation of the base GBM model and the proposed Merton, Kou, and NIG models, it was found that the optimal decisions (states) and the project values were both indifferent in all four of the models. This was not necessarily the case for the other states. Moreover, the dynamics of the proposed jump processes over time were also shown to be different and that they can yield different interim decisions.

Because of the way the deterioration process and the rehabilitation decisions are modeled in the decision-making system, jumps other than those lead by the underlying traffic demand and land price processes could still occur due to either a unit deterioration in the highway quality or a decision to rehabilitate. Therefore, depending on the setting of the HSQI matrix, several state value surfaces could arise where the regression surface would represent the average state surface. This also revealed the relatively high sensitivity of project value to the HSQI variable; a fact that signified that perhaps more emphasis should be devoted to enhancing the modeling of the HSQI variable in the mathematical representation, as well as with respect to correlation with other variables.

Despite the above findings, the implementation performed proved that, with the proposed class of Lévy processes, it is possible to extend the uncertainty models far beyond that of

the geometric Brownian motion to a much larger and flexible parametric family of models; a set of models that is not only capable of producing distributions that are heavy-tailed, but also skewed and/or having smile-shaped implied volatilities. Thus, it can offer a more accurate depiction of the empirical observations. This could be a significant advancement in the modeling of continuous-time uncertainties, not only in our decision-making system or other real options applications, but also in other types of decision-making systems, as well as anywhere else where there is evidence of jumps and where geometric Brownian motion is unjustifiably used.

7.2   Future Research

Future extensions of this research can be carried out to address the following aspects:

1. Including factors such as safety and environmental implication into the analysis.

2. Exploring the impact of incorporating the expropriation cost into the land price uncertainty, the construction cost as a variable where material cost variability is incorporated, and other factors (such as fuel price) into the analysis.

3. Advancing the discrete state and time uncertainty model for the highway service quality index factor.

4. Extending the analysis to include Lévy jump processes other than Merton, Kou, and negative inverse Gaussian models.

5. Calibrating the different models based on one of the jump models as opposed to the diffusion model.

6. Acquiring more data to improve testing of the normality of the uncertainties and to allow for parameter estimation as opposed to calibration; sources of data listed in this literature can be valuable for this undertaking.

7. Experimenting with different functional forms in the regression of $\pi_t(\cdot)$.

8. Determining the value of the HSQI variable deterministically as opposed to randomly, whereby it remains constant in the regression.

References

407 ETR. (n.d.). 407 ETR financial information. Retrieved from
http://www.407etr.com/About/investors.htm

Amram, M. & Kulatilaka, N. (1999) Real options: Managing strategic investment in an uncertain world. Cambridge, MA: Harvard Business School Press.

Boyle, T. (2007, September 7). Airport fight takes off again; Pickering airport opponents dust off protest signs as Ottawa asks GTAA to assess need for facility. The Toronto Star, A08.

Branswell, B. (1997, September 8). White elephant. Maclean's, 24.

Buechner, W.R. (2005). Value of transportation construction put in place May 2005. Washington, DC: The American Road and Transportation Builders Association (ARTBA). Retrieved from
http://www.artba.org/economics_research/TCMIR/mvtcppr/monthly_value.htm

Canadian Environmental Assessment, Statutes of Canada 1992, c. 37.
http://laws.justice.gc.ca/en/ShowFullDoc/cs/C-15.2///en

CBC News. (2004, April 28). Mirabel looks for new role–again. Retrieved from
http://www.cbc.ca/story/canada/national/2004/04/28/miracle040428.html

CBC News. (2006, December 18). Expropriated Mirabel land to be returned. Retrieved from http://www.cbc.ca/canada/montreal/story/2006/12/18/qc-mirabel20061218.html

Clibbon, P.B. (1975). Structure and dynamics of land use. Montréal: Les Presses del'Université de Montréal.

Colliers International. (2006). Greater Toronto industrial land sales report. Retrieved from
http://www.colliersteams.com/prod/ccgrd.nsf/publish/08cadbc3df222b50852571810064e796/$file/q106+industrial+land+sales+rpt.pdf

Comprehensive Study List Regulations, SOR/94-638.
http://laws.justice.gc.ca/en/ShowFullDoc/cr/SOR-94-638///en

Construction Industry Institute. (1989). Management of project risks and uncertainties. Austin, TX: author.

Cont, R. & Tankov, P. (2004). Financial modelling with jump processes. Boca Raton, FL: Chapman & Hall.

Delean, P. (2006). Mirabel may take off as theme park. The Montreal Gazette. Retrieved from http://www.canada.com/montrealgazette/news/story.html?id=33ac544a-148d-4ffa-a57c-1d9be2258646&k=46021

Dumfries, C. (2002). Sources of historical data for appraisal reports. Appraisal Institute of Canada. Retrieved from http://www.aicanada.ca/e/articles/sources_of_historical_data_for_appraisal_reports.cfm

Expropriation Act, Revised Statutes of Canada 1985, c. E-21. Retrieved from http://laws.justice.gc.ca/en/ShowFullDoc/cs/E-21///en

Farmers will get more for lands taken for airport. (1978, January 10). The Globe and Mail.

Ford, D.N., Lander, D.M., & Voyer, J.J. (2002). A real options approach to valuing strategic flexibility in uncertain construction projects. Construction Management and Economics, 20(4), 343-351.

Garvin, M.J. (2005). Real options analysis: Can it improve infrastructure development decisions?. Paper presented at ASCE Construction Research Congress, April 5-7, in San Diego, CA.

Government of Ontario. (2006, March 31). Province and 407 ETR agree to better deal for drivers. Retrieved from http://ogov.newswire.ca/ontario/GPOE/2006/03/31/c1204.html?lmatch=&lang=_e.html

Government of Ontario. (2007). Electronic land registration. Retrieved from http://www.gov.on.ca/ont/portal/!ut/p/.cmd/cs/.ce/7_0_A/.s/7_0_GTS/_s.7_0_A/7_0_GTS/_l/en?docid=STEL02_165314

Kalemanova, A., & Werner. (2006). A short note on efficient implementation of the Normal Inverse Gaussian distribution. München, Germany: Risklab. Retrieved from http://www.mathfinance.ma.tum.de/papers/KalemanovaWerner_NoteOnImplementation.pdf

InvestorWords.com (2010, January 30). *Opportunity cost, definition*. Retrieved from http://www.investorwords.com/3470/opportunity_cost.html

Koole, J. (2006). York region's VIVA. Toronto Transit. Retrieved from http://transit.toronto.on.ca/gotransit/2111.shtml

Kou, S.G. (2002). A jump diffusion model for option pricing. Management Science, 48(8), 1086-1101.

Kou, S.G. & Hui Wang. (2004). Option pricing under a double exponential jump diffusion model. Management Science, 50 (9), 1178-1192.

Krauss, C. (2004, October 3). End of era near in Montreal for white-elephant airport. The New York Times. Retrieved from http://query.nytimes.com/gst/fullpage.html?res=9406E6D91038F930A35753C1A96 29C8B63&sec=&spon=&pagewanted=print

Leatherdale, L. (2005, January 9). 'The 99-Year Fleece'; Let's take back the 407, our highway by rights. The Toronto Sun, 43.

Lem, S. (2007, September 15). Flight turbulence; The proposed Pickering airport: 35 years later, the debate takes off again. The Toronto Sun, 26.

Longstaff, Francis and Eduardo S. Schwartz. 2001. Valuing American options by simulation: A simple least-squares approach. The Review of Financial Studies, 14 (1), 113-147.

Marathe, R.R., & Ryan, S.M. (2005). On the validity of the geometric Brownian motion assumption. Engineering Economist, 50(2), 59-193.

Marshall, S. (2006). The expressways of Toronto (built and unbuilt). Toronto Transit. Retrieved from http://transit.toronto.on.ca/spare/0019.shtml

Merton, R.C. (1976). Option pricing when underlying stock returns are discontinuous. Journal of Financial Economics, 3 (2), 125–144.

Mirabel airport opened. (1975, October 11). Facts on File World News Digest.

Mirabel may unite opposition parties. (2004, November 20). The Record, D16.

Mylvaganam, C, & Sandford B. (2005, January 14). Better ways to privatize. The Toronto Star. A21.

Mylvaganam, C. & Sandford, B. (2004). "If you build it…": Business, government and Ontario's electronic toll highway. Toronto, ON: University of Toronto Press.

Ng, F. & Björnsson, H. (2004). Using Real Option and decision analysis to evaluate investments in the architecture, construction and engineering industry. Construction Management and Economics, 22(5), 471-482.

Ontario. Legislative Assembly. (1998, October 21). Debates and proceedings. Retrieved from http://www.ontla.on.ca/web/house-proceedings/house_detail.do?Date=1998-10-21&Parl=36&Sess=2&locale=en

Ontario Ministry of Finance. (2007). Public accounts 2006-2007 annual report and financial statement. Retrieved from http://www.fin.gov.on.ca/english/budget/paccts/2007/07_ar.pdf

Ontario Ministry of Transportation. (2005). Northern Ontario highways strategy. Retrieved from http://www.mto.gov.on.ca/english/pubs/nohs.htm

Ontario Ministry of Transportation. (2006). Provincial highways traffic volumes 1988-2003. Retrieved from http://www.mto.gov.on.ca/english/pubs/trafficvolumes.htm

Papapantoleon, A. (2005). An introduction to Lévy Processes with finance in view [Lecture notes], University of Leipzig, Leipzig, Germany. Retrieved from http://www.math.uni-leipzig.de/~tschmidt/Papapantoleon_IntroductiontoLévy.pdf

Rasmus, S., Asmussen, S., & Wiktorsson, M. (2004). Pricing of some exotic options with NIG-Lévy input. In M. Bubak (Ed.), Computational Science - ICCS 2004, Proceedings Lecture Notes in Computer Science (Vol. 4, p. 795-802). Berlin, Germany: Springer-Verlag. Retrieved from http://www.springerlink.com/content/e4n2agv49nu9kt9c/fulltext.pdf

Requiem for an airport. (2004, September 18). Toronto Star, H1.

Ribeiro, C., & Webber, N. 2003. A Monte Carlo Method for the Normal Inverse Gaussian Option Valuation Model using an Inverse Gaussian Bridge. Paper presented at the 9th International Conference of Computing in Economics and Finance, July 11-13, Seattle, Washington. Retrieved from http://depts.washington.edu/sce2003/Papers/05.pdf

Rydberg, T.H. (1997). The normal inverse Gaussian Lévy Process: Simulation and approximation. Communications in Statistics: Stochastic Models, 13(4), 887-910.

Simon, B. (1996, February 20). Montreal's plans come down to earth: Prospects for the city's white elephant Mirabel airport. Financial Times, 4.

Stentoft, L. (2001). Assessing the least square Monte-Carlo approach to American Option Valuation. CAF Working Paper Series, No. 90, University of Aarhus.

Stentoft, L. (2004). Assessing the least square Monte-Carlo approach to American option valuation. Review of Derivatives Research, 7(2), 129-168.

Teranet, Inc. 2006. The land professional's information resource. Retrieved from http://www.teranet.ca/products/geowarehouse.html

The Canada Line. (n.d.). About the Canada Line, financing. Retrieved from http://www.canadaline.ca/aboutFinancing.asp

Translink. (n.d.a) 2005 - 2007 three-year plan & ten-year outlook. Retrieved from http://www.translink.bc.ca/Plans_Projects/10YearPlan/default.asp

Translink. (n.d.b) Vision, mission & values. Retrieved from http://www.translink.bc.ca/About_TransLink/VisionMissionValues/default.asp

Transport Canada. (n.d.). Chronology of the decisions concerning Mirabel Airport. Retrieved from http://www.tc.gc.ca/mediaroom/backgrounders/b06-a005e.htm

Transport Canada. (2005). The Confederation Bridge, a partnership for progress. Retrieved from http://www.tc.gc.ca/pol/en/Report/brochure/confederation_bridge.htm

Weisstein, E.W. (2008). Modified Bessel Function of the second kind. MathWorld - A Wolfram Web Resource. Retrieved from http://mathworld.wolfram.com/ModifiedBesselFunctionoftheSecondKind.html

Zhao, T. (2003). Valuing facility expansion and layout: A real options approach. Unpublished doctoral dissertation, University of Maryland at College Park.

Zhao, T., Sundararajan, S.K., & Tseng, C. (2004). Highway development decision-making under uncertainty: A real options approach. Journal of Infrastructure Systems 10 (1), 23-32.

Appendix 1

Sample FTMS Traffic Volume Counts
(QEW-Burlington spring 2001)

FTMS - COMPASS DATA							
W.B. EXPRESS		BETWEEN THIRD LINE & BRONTE ROAD					
QEWDE0180DWS		LHRS - 10130	ICMS - 235				
QEWDE0180DWS	**Mon**	**Tue**	**Wed**	**Thu**	**Fri**	*** SAT ***	*** SUN ***
Hour Ending	23/04/2001	24/04/2001	25/04/2001	26/04/2001	27/04/2001	28/04/2001	29/04/2001
1:00:00	1179	1276	1586	1466	1611	2195	2125
2:00:00	15	955	975	986	1015	1523	1379
3:00:00	540	513	552	570	663	858	1011
4:00:00	375	414	471	436	547	658	687
5:00:00	727	434	428	487	540	466	394
6:00:00	1326	887	812	918	930	610	417
7:00:00	3134	2397	2465	2404	2433	1301	810
8:00:00	4495	4461	4473	4566	4429	2387	1502
9:00:00	4950	5171	4893	5058	5031	3555	2129
10:00:00	4041	4206	4303	4711	4438	4401	3408
11:00:00	3990	3930	4192	4323	4563	4934	4288
12:00:00	4360	4111	4402	4588	4730	5455	5048
13:00:00	4463	4351	4535	4496	5120	5376	5373
14:00:00	4606	4689	4868	5220	5481	5156	5394
15:00:00	5017	5131	5267	5850	5344	4353	5033
16:00:00	5361	5607	5518	4894	5077	5443	5158
17:00:00	5081	5006	4782	4550	4525	5257	5060
18:00:00	5301	4801	4813	4578	4769	5384	5043
19:00:00	4813	5558	4906	5885	5216	5337	4707
20:00:00	4162	4487	4105	4085	5152	3976	4039
21:00:00	3335	3372	4085	3634	4363	3025	3710
22:00:00	2848	3181	3452	3325	3820	2840	3291
23:00:00	2276	2515	2900	2871	3489	2965	2395
0:00:00	1966	2228	2536	2236	3251	2758	1567
24HR TOT	78361	79681	81319	82137	86537	80213	73968
A.M. TOT	29132	28755	29552	30513	30930	28343	23198
P.M. TOT	49229	50926	51767	51624	55607	51870	50770
NOON-NOON		77984	80478	82280	82554	83950	75068
	ADT =	**80317**			**AWD=**	**81607**	

FTMS - COMPASS DATA							
E.B. EXPRESS		BETWEEN THIRD LINE & BRONTE ROAD					
QEWDE0180DES		LHRS - 10130	ICMS - 235				
QEWDE0180DES	**Mon**	**Tue**	**Wed**	**Thu**	**Fri**	*** SAT ***	*** SUN ***
Hour Ending	16/04/2001	17/04/2001	18/04/2001	19/04/2001	20/04/2001	21/04/2001	22/04/2001
1:00:00	1022	809	815	765	843	1205	1700
2:00:00	781	510	504	439	555	860	1248
3:00:00	690	428	414	459	499	800	1146
4:00:00	648	493	489	558	542	637	758
5:00:00	1740	945	924	1006	987	629	556
6:00:00	3912	3923	4120	4062	3895	1144	709
7:00:00	4930	5340	5515	5543	5591	2028	1249
8:00:00	5614	5392	5601	5796	5778	2728	1435
9:00:00	5429	5443	5511	5864	6055	3594	1889
10:00:00	5052	5376	5344	5616	5435	4018	2651
11:00:00	5108	4876	4917	4929	4970	4422	3604
12:00:00	5178	4797	4706	4920	5151	4875	4426
13:00:00	5091	4623	4714	5137	4889	5002	4680
14:00:00	5068	4549	4610	4680	4967	4916	4957
15:00:00	5113	4932	5084	5112	5163	4800	4827
16:00:00	5018	4885	5374	4871	4141	4806	4907
17:00:00	5265	5182	5203	4809	4596	4934	5095
18:00:00	3861	5053	4775	4554	4853	4937	5415
19:00:00	4173	4170	4357	4141	4630	4420	4849
20:00:00	3396	3009	3063	3246	3666	3515	4348
21:00:00	2848	2367	2516	2680	2923	2873	3956
22:00:00	2585	2401	2420	2577	2702	2659	3249
23:00:00	2134	1942	2050	2287	2206	2579	2453
0:00:00	1367	1323	1265	1340	1858	2733	1344
24HR TOT	86023	82768	84291	85391	86895	75114	71451
A.M. TOT	40104	38332	38860	39957	40301	26940	21371
P.M. TOT	45919	44436	45431	45434	46594	48174	50080
NOON-NOON		84251	83296	85388	85735	73534	69545
	ADT =	**81705**			**AWD=**	**85074**	

Appendix 2

Sample Average Traffic Volume Counts
(QEW-1988-2003 Traffic Volumes Production Page 18 of 736)

Highway	Location Description	Dist	Year	Patt Type	AADT	SADT	SAWDT	WADT	AR
			2001	C	158000	178500	178500	142200	2.3
			2002	C	152400	170700	172000	137100	2.6
			2003	C	157100	176000	177500	141400	3.2
QEW	HWY 25-BRONTE RD-IC111-OAKVILLE	2.1	1988	C	95500	106000	106000	85900	1.7
			1989	C	98750	109600	110600	88800	1.2
			1990	C	102700	113900	113900	92400	1.0
			1991	C	104200	114600	115600	94800	0.8
			1992	C	107700	116300	119500	99100	1.2
			1993	C	110900	119800	123100	103100	1.2
			1994	C	114200	124500	127900	102800	1.2
			1995	C	116800	126100	130800	107500	0.9
			1996	C	119700	134700	136500	107900	0.8
			1997	C	122600	137900	139800	110500	1.1
			1998	C	125500	141200	141700	113100	0.8
			1999	C	136100	153800	153700	122600	0.7
			2000	C	141300	159000	159500	127300	0.8
			2001	C	151100	170700	170700	136000	0.4
			2002	C	151600	169800	171100	136400	0.6
			2003	C	156800	175600	177200	141100	0.7
QEW	THIRD LINE IC 113	3.1	1990	C	102700	113900	113900	92400	0.7
			1991	C	105000	115500	116600	95600	0.6
			1992	C	108100	116700	120000	99500	0.6
			1993	C	115000	124200	127700	107000	0.7
			1994	C	114300	124600	128000	102900	0.7
			1995	C	117300	126700	131400	107900	0.8
			1996	C	120300	135300	137100	108400	0.8
			1997	C	123200	138600	140400	111000	1.0
			1998	C	126200	142000	142500	113700	0.7
			1999	C	144400	163200	163000	130100	0.7
			2000	SC	147500	156800	172900	130200	0.7
			2001	SC	150700	161200	176300	132600	0.5
			2002	SC	153800	163200	180100	135600	0.6
			2003	SC	157000	164900	183700	138200	0.7
QEW	DORVAL DR-KERR ST-IC116	2.1	1988	C	112000	124300	124300	100700	1.5
			1989	C	115800	128500	129600	104200	1.0
			1990	C	120400	133600	133600	108300	0.9
			1991	C	121850	134000	135200	110800	0.9
			1992	C	123800	133700	137400	115100	1.0
			1993	C	130000	140400	144300	119600	1.0
			1994	C	131500	143300	147300	118400	0.8
			1995	C	134500	145300	150600	123700	0.9

Appendix 3

Q-Q Plots of Semi-annual Farmland Prices for the Other Provinces
(1996-2005)
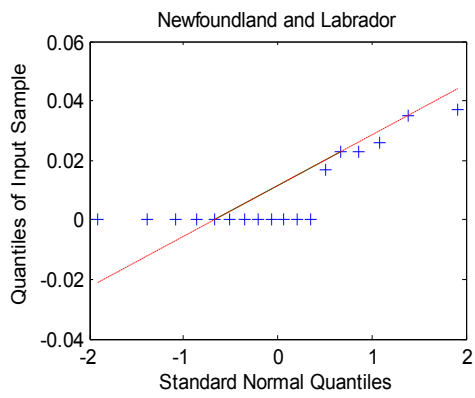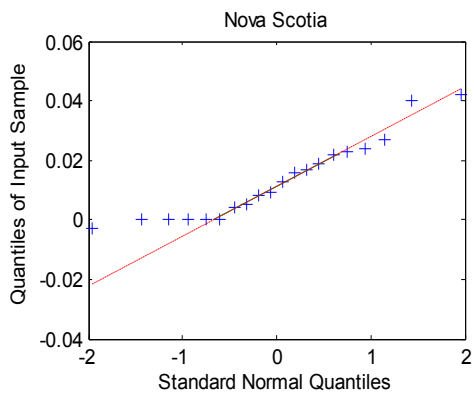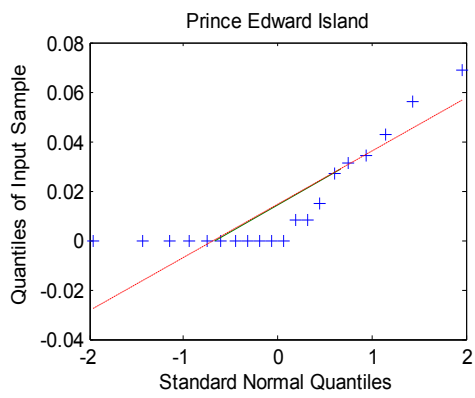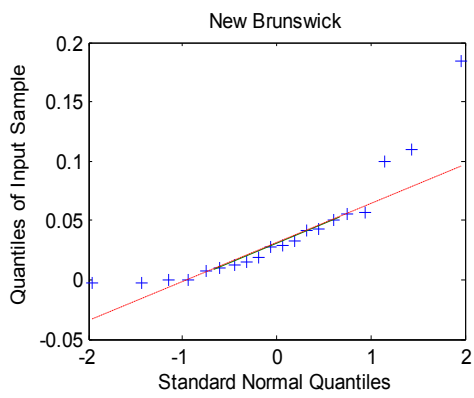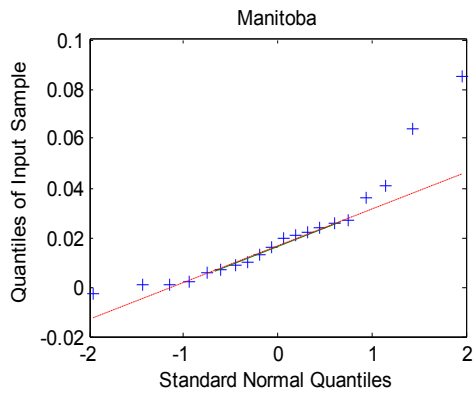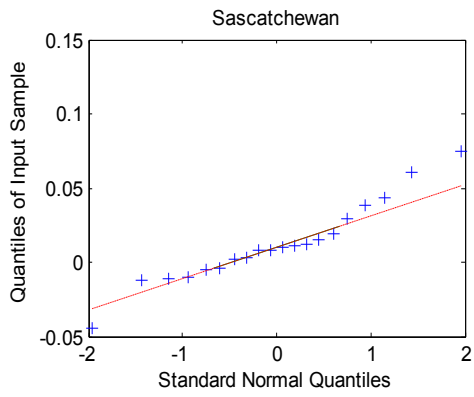
Appendix 4

Sample Output of the Decision-making System

```
NLane =              MinWidth=
     2                  150
     4                  150
     6                  175
     8                  200


Uncertainty =        Mean =              Volatility =           Corr_Mat =
  'Trafic_Demand'     0.03                 0.2               1.0000    0.2000
  'Land_Price'        0.08                 0.2               0.2000    1.0000


NUncer =             NPaths =            NtSteps=              Expir =
     2                  3                   3                    3


Inter =              no =                wo =
   0.08                0                   0


Qo =                 Po =                Io =
   4200               70000                5


gama =               alpha =             I =                   Omega =
   14000              1000                10000                 12


dis =                c_n =               c_m =                 beta =
    50                750000              200000                0.7


NU =                 NP =                NT =                  T =                        tStep =
     2                  3                   3                    3                           1


So =                 ir =                mu =                  Sigma =
   4200               0.08                0.03                  0.2
   70000                                  0.08                  0.2
```

All the possible design alternatives given the input number of lanes and lane minimum widths
```
v =
  0    0
  2  150
  2  175
  2  200
  4  150
  4  175
  4  200
  6  175
  6  200
  8  200
```

All the possible future states, v_t(n,w,k) for the state k:
```
v_t(:,:,1)=       v_t(:,:,2)=       v_t(:,:,3)=       v_t(:,:,4)=       v_t(:,:,5)=
  0    0            2 150             2 175             2 200             4 150
  2 150             2 175             2 200             4 200             4 175
  2 175             2 200             4 175             6 200             4 200
  2 200             4 150             4 200             8 200             6 175
```

4 150	4 175	6 175	0 0	6 200
4 175	4 200	6 200	0 0	8 200
4 200	6 175	8 200	0 0	0 0
6 175	6 200	0 0	0 0	0 0
6 200	8 200	0 0	0 0	0 0
8 200	0 0	0 0	0 0	0 0

v_t(:,:,6) =	v_t(:,:,7) =	v_t(:,:,8) =	v_t(:,:,9) =	v_t(:,:,10)=
4 175	4 200	6 175	6 200	8 200
4 200	6 200	6 200	8 200	0 0
6 175	8 200	8 200	0 0	0 0
6 200	0 0	0 0	0 0	0 0
8 200	0 0	0 0	0 0	0 0
0 0	0 0	0 0	0 0	0 0
0 0	0 0	0 0	0 0	0 0
0 0	0 0	0 0	0 0	0 0
0 0	0 0	0 0	0 0	0 0
0 0	0 0	0 0	0 0	0 0

All the possible decision alternatives, u_t(Dn, Dw, k) for the state k:

u_t(:,:,1)=	u_t(:,:,2)=	u_t(:,:,3)=	u_t(:,:,4)=	u_t(:,:,5)=
0 0	0 0	0 0	0 0	0 0
2 150	0 25	0 25	2 0	0 25
2 175	0 50	2 0	4 0	0 50
2 200	2 0	2 25	6 0	2 25
4 150	2 25	4 0	0 0	2 50
4 175	2 50	4 25	0 0	4 50
4 200	4 25	6 25	0 0	0 0
6 175	4 50	0 0	0 0	0 0
6 200	6 50	0 0	0 0	0 0
8 200	0 0	0 0	0 0	0 0

u_t(:,:,6) =	u_t(:,:,7) =	u_t(:,:,8) =	u_t(:,:,9) =	u_t(:,:,10) =
0 0	0 0	0 0	0 0	0 0
0 25	2 0	0 25	2 0	0 0
2 0	4 0	2 25	0 0	0 0
2 25	0 0	0 0	0 0	0 0
4 25	0 0	0 0	0 0	0 0
0 0	0 0	0 0	0 0	0 0
0 0	0 0	0 0	0 0	0 0
0 0	0 0	0 0	0 0	0 0
0 0	0 0	0 0	0 0	0 0
0 0	0 0	0 0	0 0	0 0

ND =
 10 9 7 4 6 5 3 3 2 1
ND is a vector of which the ith element is the number of possible decisions for design state i

The initial design state configuration of the highway, vo(no, wo), is:
vo =
 0 0

The initial highway system design state index number, isi, is:
isi =

     1

The vo_th corresponding possible future system state indecies, fsi, are:
fsi =
   1   2   3   4   5   6   7   8   9   10

The vo_th corresponding possible future system state configurations, fsc(n,w), are:
fsc =
   0   0
   2   150
   2   175
   2   200
   4   150
   4   175
   4   200
   6   175
   6   200
   8   200

The vo_th corresponding possible future system state decisions, fsd(Dn,Dw), are:
fsd =
   0   0
   2   150
   2   175
   2   200
   4   150
   4   175
   4   200
   6   175
   6   200
   8   200

The vo_th corresponding possible previous system state indices, psi, are:
psi =

     1

The vo_th corresponding possible previous system state configurations, psc(n,w), are:
psc =
   0   0

DecisionMap(Origin State, Option No, Destination State)
DecisionMap =
   1   1   1
   1   2   2
   1   3   3
   1   4   4
   1   5   5
   1   6   6
   1   7   7
   1   8   8

```
 1    9    9
 1   10   10
 2    1    2
 2    2    3
 2    3    4
 2    4    5
 2    5    6
 2    6    7
 2    7    8
 2    8    9
 2    9   10
 3    1    3
 3    2    4
 3    3    6
 3    4    7
 3    5    8
 3    6    9
 3    7   10
 4    1    4
 4    2    7
 4    3    9
 4    4   10
 5    1    5
 5    2    6
 5    3    7
 5    4    8
 5    5    9
 5    6   10
 6    1    6
 6    2    7
 6    3    8
 6    4    9
 6    5   10
 7    1    7
 7    2    9
 7    3   10
 8    1    8
 8    2    9
 8    3   10
 9    1    9
 9    2   10
10    1   10
```

S(i: path no, j: time step no, k: uncertainty no.)

S(:,:,1) =

  1.0e+003 *

3.9337	5.3031	5.5884
3.9985	3.7649	3.9880
3.1584	3.6136	2.9837

S(:,:,2) =

  1.0e+003 *

69930	92010	85190
75180	94650	125440
74530	66800	66390

Highway Service Quality Index probability transition matrix, P(I_t, I_t+1)

P =

```
0.5000   0.5000      0        0        0
   0     0.5000   0.5000      0        0
   0        0     0.5000   0.5000      0
   0        0        0     0.5000   0.5000
1.0000      0        0        0        0
```
P is the Highway Service Quality Index transition matrix from time t in t+1, where the index, I_t, goes from 5 to 1: [5,4,3,2,1]

I_to =

    5

I_to is the initial highway service quality index at time 0, as input by user

I_t =

   4   3   3
   4   4   3
   4   3   3

I_t is a matrix of the simulated (based on matrix P) highway servicce quality indecies, for all paths (rows of the matrix, I_t), from time step 1 till NT

ho =

    0
    0
    0

ho is a vector of the initial rehabilitation decisions, for all paths (rows), deduced from matrix P: taken when HSQI, I_t, increases in the next time step

h =

   0   0   0
   0   0   0
   0   0   0

h is a matrix of rehabilitation decisions from time steps 1 till NT, calculated as ho

x_I_to =

    1

x_I_to is weighting factor (at t=0) of the highway revenue in terms of the highway service quality index

x_I_t =

   0.7000   0.4900   0.4900
   0.7000   0.7000   0.4900
   0.7000   0.4900   0.4900

x_I_t is a matrix of weighting factors (for t >0) of the highway revenue in terms of the highway service quality index

NFS =

    10

f_t (Path, State, time)= Revenue from traffic flow + Revenue from land use. It depends on system state and uncertainty values (Decision independent.)
f_to (Path, Vo, t=0)
f_to =

    0
    0
    0

f_t(:,:,1) =

```
      0   82600000   95100000   107600000   90200000   102700000   115200000   106571800
119071800   107071800
      0   82600000   95100000   107600000   90200000   102700000   115200000   107479000
119979000   107979000
      0   82600000   95100000   107600000   90200000   102700000   115200000   95717600
108217600   96217600
```

f_t(:,:,2) =

```
      0   76720000   89220000   101720000   78440000   90940000   103440000   92660000
105160000   106880000
      0   82600000   95100000   107600000   90200000   102700000   115200000   104208600
116708600   104708600
      0   76720000   89220000   101720000   78440000   90940000   103440000   92660000
105160000   102590400
```

f_t(:,:,3) =

```
      0   76720000   89220000   101720000   78440000   90940000   103440000   92660000
105160000   106880000
      0   76720000   89220000   101720000   78440000   90940000   103440000   92660000
105160000   106880000
      0   76720000   89220000   101720000   78440000   90940000   103440000   92660000
105160000   93771800
```

c_PathDecStateTime (Path, Dec, State, Time)= expansion cost + acquisition cost for right of way + cost for rehabilitation. Costs depend on system states and uncertainty values
c_Path_vo_to =

```
 1.0e+009 *
      0    0.6000    0.6875    0.7750    0.6750    0.7625    0.8500    0.8375    0.9250    1.0000
      0    0.6000    0.6875    0.7750    0.6750    0.7625    0.8500    0.8375    0.9250    1.0000
      0    0.6000    0.6875    0.7750    0.6750    0.7625    0.8500    0.8375    0.9250    1.0000
```

c_PathDecStateTime(:,:,1,1) =

```
 1.0e+009 *
      0    0.5995    0.6869    0.7743    0.6745    0.7619    0.8493    0.8369    0.9243    0.9993
      0    0.6389    0.7328    0.8268    0.7138    0.8078    0.9018    0.8828    0.9768    1.0518
      0    0.6340    0.7271    0.8203    0.7090    0.8021    0.8953    0.8771    0.9703    1.0453
```

c_PathDecStateTime(:,:,2,1) =

```
      0   87412500   174825000   75000000   162412500   249825000   237412500   324825000
399825000          0
      0   93975000   187950000   75000000   168975000   262950000   243975000   337950000
412950000          0
      0   93162500   186325000   75000000   168162500   261325000   243162500   336325000
411325000          0
```

c_PathDecStateTime(:,:,3,1) =

```
      0   87412500   75000000   162412500   150000000   237412500   312412500    0    0    0
      0   93975000   75000000   168975000   150000000   243975000   318975000    0    0    0
      0   93162500   75000000   168162500   150000000   243162500   318162500    0    0    0
```

c_PathDecStateTime(:,:,4,1) =

```
      0   75000000   150000000   225000000    0    0    0    0    0    0
      0   75000000   150000000   225000000    0    0    0    0    0    0
      0   75000000   150000000   225000000    0    0    0    0    0    0
```

c_PathDecStateTime(:,:,5,1) =

0	87412500	174825000	162412500	249825000	324825000	0	0	0	0
0	93975000	187950000	168975000	262950000	337950000	0	0	0	0
0	93162500	186325000	168162500	261325000	336325000	0	0	0	0

c_PathDecStateTime(:,:,6,1) =

0	87412500	75000000	162412500	237412500	0	0	0	0	0
0	93975000	75000000	168975000	243975000	0	0	0	0	0
0	93162500	75000000	168162500	243162500	0	0	0	0	0

c_PathDecStateTime(:,:,7,1) =

0	75000000	150000000	0	0	0	0	0	0	0
0	75000000	150000000	0	0	0	0	0	0	0
0	75000000	150000000	0	0	0	0	0	0	0

c_PathDecStateTime(:,:,8,1) =

0	87412500	162412500	0	0	0	0	0	0	0
0	93975000	168975000	0	0	0	0	0	0	0
0	93162500	168162500	0	0	0	0	0	0	0

c_PathDecStateTime(:,:,9,1) =

0	75000000	0	0	0	0	0	0	0	0
0	75000000	0	0	0	0	0	0	0	0
0	75000000	0	0	0	0	0	0	0	0

c_PathDecStateTime(:,:,10,1) =

0	0	0	0	0	0	0	0	0	0
0	0	0	0	0	0	0	0	0	0
0	0	0	0	0	0	0	0	0	0

c_PathDecStateTime(:,:,1,2) =

1.0e+009 *

0	0.7651	0.8801	0.9951	0.8401	0.9551	1.0701	1.0301	1.1451	1.2201
0	0.7849	0.9032	1.0215	0.8599	0.9782	1.0965	1.0532	1.1715	1.2465
0	0.5760	0.6595	0.7430	0.6510	0.7345	0.8180	0.8095	0.8930	0.9680

c_PathDecStateTime(:,:,2,2) =

0	115012500	230025000	75000000	190012500	305025000	265012500	380025000	455025000	0
0	118312500	236625000	75000000	193312500	311625000	268312500	386625000	461625000	0
0	83500000	167000000	75000000	158500000	242000000	233500000	317000000	392000000	0

c_PathDecStateTime(:,:,3,2) =

0	115012500	75000000	190012500	150000000	265012500	340012500	0	0	0
0	118312500	75000000	193312500	150000000	268312500	343312500	0	0	0
0	83500000	75000000	158500000	150000000	233500000	308500000	0	0	0

c_PathDecStateTime(:,:,4,2) =

0	75000000	150000000	225000000	0	0	0	0	0	0
0	75000000	150000000	225000000	0	0	0	0	0	0
0	75000000	150000000	225000000	0	0	0	0	0	0

c_PathDecStateTime(:,:,5,2) =

0	115012500	230025000	190012500	305025000	380025000	0	0	0	0
0	118312500	236625000	193312500	311625000	386625000	0	0	0	0
0	83500000	167000000	158500000	242000000	317000000	0	0	0	0

c_PathDecStateTime(:,:,6,2) =

0	115012500	75000000	190012500	265012500	0	0	0	0	0
0	118312500	75000000	193312500	268312500	0	0	0	0	0
0	83500000	75000000	158500000	233500000	0	0	0	0	0

c_PathDecStateTime(:,:,7,2) =

0	75000000	150000000	0	0	0	0	0	0	0
0	75000000	150000000	0	0	0	0	0	0	0
0	75000000	150000000	0	0	0	0	0	0	0

c_PathDecStateTime(:,:,8,2) =

0	115012500	190012500	0	0	0	0	0	0	0
0	118312500	193312500	0	0	0	0	0	0	0
0	83500000	158500000	0	0	0	0	0	0	0

c_PathDecStateTime(:,:,9,2) =

0	75000000	0	0	0	0	0	0	0	0
0	75000000	0	0	0	0	0	0	0	0
0	75000000	0	0	0	0	0	0	0	0

c_PathDecStateTime(:,:,:,3) =

     0
     0
     0

lambda =

0	1	2	3	4	0
0	0	0	0	0	1

X_T(:,:,1) =
 1.0e+014 *

0.00000000000001	0.00000000003934	0.00000015473996	0.00060870056846	2.39444542614139
0.00000000069930				
0.00000000000001	0.00000000003998	0.00000015988002	0.00063928026997	2.55616215946005
0.00000000075180				
0.00000000000001	0.00000000003158	0.00000009975491	0.00031506589385	0.99510411912649
0.00000000074530				

X_T(:,:,2) =
 1.0e+014 *

0.00000000000001	0.00000000005303	0.00000028122870	0.00149138389829	7.90895795101062
0.00000000092010				
0.00000000000001	0.00000000003765	0.00000014174472	0.00053365469670	2.00915656762273
0.00000000094650				
0.00000000000001	0.00000000003614	0.00000013058105	0.00047186768083	1.70514105146377
0.00000000066800				

X_T is a matrix of transformed independent uncertainty values for all the time steps from NT-1 upto 1,

defining the functional form to be used in the regression

_____

InitialState =

                                                1

PossibleFutState =
   1   2   3   4   5   6   7   8   9   10
TimeStep =

                                                3

pi_t(:,:,:,1) = 0

   𝔼

pi_t(:,:,1,2) =
   0   0   0   0   0   0   0   0   0   0
   0   0   0   0   0   0   0   0   0   0
   0   0   0   0   0   0   0   0   0   0

pi_t(:,:,2,2) =
  1.0e+008 *
  -1.3065 -1.3065 -1.3065 -1.3065 -1.3065 -1.3065 -1.3065 -1.3065 -1.3065   0
   0.1612   0.1612   0.1612   0.1612   0.1612   0.1612   0.1612   0.1612   0.1612   0
   0.9800   0.9800   0.9800   0.9800   0.9800   0.9800   0.9800   0.9800   0.9800   0

pi_t(:,:,3,2) =
  1.0e+008 *
  -1.5194 -1.5194 -1.5194 -1.5194 -1.5194 -1.5194 -1.5194   0   0   0
   0.1875   0.1875   0.1875   0.1875   0.1875   0.1875   0.1875   0   0   0
   1.1396   1.1396   1.1396   1.1396   1.1396   1.1396   1.1396   0   0   0

pi_t(:,:,4,2) =
  1.0e+008 *
  -1.7322 -1.7322 -1.7322 -1.7322   0   0   0   0   0   0
   0.2137   0.2137   0.2137   0.2137   0   0   0   0   0   0
   1.2993   1.2993   1.2993   1.2993   0   0   0   0   0   0

pi_t(:,:,5,2) =
  1.0e+008 *
  -1.3358 -1.3358 -1.3358 -1.3358 -1.3358 -1.3358   0   0   0   0
   0.1648   0.1648   0.1648   0.1648   0.1648   0.1648   0   0   0   0
   1.0019   1.0019   1.0019   1.0019   1.0019   1.0019   0   0   0   0

pi_t(:,:,6,2) =
  1.0e+008 *
  -1.5487 -1.5487 -1.5487 -1.5487 -1.5487   0   0   0   0   0
   0.1911   0.1911   0.1911   0.1911   0.1911   0   0   0   0   0
   1.1616   1.1616   1.1616   1.1616   1.1616   0   0   0   0   0

pi_t(:,:,7,2) =
  1.0e+008 *
  -1.7615 -1.7615 -1.7615   0   0   0   0   0   0   0
   0.2173   0.2173   0.2173   0   0   0   0   0   0   0

```
  1.3213   1.3213   1.3213      0       0       0       0       0       0       0
```

pi_t(:,:,8,2) =
 1.0e+008 *
```
 -1.5780  -1.5780  -1.5780      0       0       0       0       0       0       0
  0.1947   0.1947   0.1947      0       0       0       0       0       0       0
  1.1836   1.1836   1.1836      0       0       0       0       0       0       0
```

pi_t(:,:,9,2) =
 1.0e+008 *
```
 -1.7908  -1.7908      0       0       0       0       0       0       0       0
  0.2210   0.2210      0       0       0       0       0       0       0       0
  1.3432   1.3432      0       0       0       0       0       0       0       0
```

pi_t(:,:,10,2) =
 1.0e+008 *
```
 -1.7472      0       0       0       0       0       0       0       0       0
  0.2432      0       0       0       0       0       0       0       0       0
  1.2151      0       0       0       0       0       0       0       0       0
```

pi_t(:,:,:,3) = 0

F_i =
```
        0  76720000  89220000  101720000  78440000  90940000  103440000  92660000  105160000
 106880000
        0  76720000  89220000  101720000  78440000  90940000  103440000  92660000  105160000
 106880000
        0  76720000  89220000  101720000  78440000  90940000  103440000  92660000  105160000
  93771800
```

EF_i =
```
        0  76720000  89220000  101720000  78440000  90940000  103440000  92660000  105160000
 102510600
```

MaxState =
         9

TimeStep =
         2

pi_t(:,:,1,1) =
 1.0e+009 *
```
        0   3.2708   3.7590   4.2472   3.6127   4.1009   4.5890   4.4427   4.9309   5.2727
        0   3.3037   3.7959   4.2880   3.6545   4.1467   4.6388   4.4975   4.9896   5.3404
        0   2.6681   3.0700   3.4719   2.9247   3.3266   3.7285   3.5832   3.9851   4.2417
```

pi_t(:,:,2,1) =
 1.0e+009 *
```
 -0.3881   0.1000   0.5882  -0.0463   0.4419   0.9301   0.7837   1.2719   1.6138      0
 -0.2767   0.2154   0.7076   0.0741   0.5662   1.0584   0.9170   1.4092   1.7600      0
 -0.0857   0.3162   0.7181   0.1709   0.5728   0.9747   0.8294   1.2313   1.4879      0
```

pi_t(:,:,3,1) =

  1.0e+009 *

  -0.4493   0.0388   -0.1075   0.3807   0.2344   0.7225   1.0644   0   0   0
  -0.3208   0.1714   0.0300   0.5222   0.3808   0.8729   1.2237   0   0   0
  -0.0979   0.3040   0.1587   0.5606   0.4153   0.8172   1.0738   0   0   0

pi_t(:,:,4,1) =

  1.0e+008 *

  -5.1053   -1.6868   1.7317   5.1502   0   0   0   0   0   0
  -3.6486   -0.1406   3.3674   6.8753   0   0   0   0   0   0
  -1.1019   1.4641   4.0302   6.5962   0   0   0   0   0   0

pi_t(:,:,5,1) =

  1.0e+009 *

  -0.4090   0.0792   0.5673   0.4210   0.9092   1.2510   0   0   0   0
  -0.2891   0.2031   0.6952   0.5538   1.0460   1.3968   0   0   0   0
  -0.0979   0.3040   0.7059   0.5606   0.9625   1.2191   0   0   0   0

pi_t(:,:,6,1) =

  1.0e+008 *

  -4.7021   0.1795   -1.2836   3.5980   7.0165   0   0   0   0   0
  -3.3316   1.5899   0.1763   5.0979   8.6058   0   0   0   0   0
  -1.1014   2.9177   1.4647   5.4838   8.0498   0   0   0   0   0

pi_t(:,:,7,1) =

  1.0e+008 *

  -5.3142   -1.8957   1.5228   0   0   0   0   0   0   0
  -3.7722   -0.2643   3.2437   0   0   0   0   0   0   0
  -1.2239   1.3422   3.9082   0   0   0   0   0   0   0

pi_t(:,:,8,1) =

  1.0e+008 *

  -4.7818   0.0998   3.5183   0   0   0   0   0   0   0
  -3.3900   1.5315   5.0395   0   0   0   0   0   0   0
  -1.1145   2.9046   5.4707   0   0   0   0   0   0   0

pi_t(:,:,9,1) =

  1.0e+008 *

  -5.3939   -1.9754   0   0   0   0   0   0   0   0
  -3.8306   -0.3226   0   0   0   0   0   0   0   0
  -1.2370   1.3291   0   0   0   0   0   0   0   0

pi_t(:,:,10,1) =

  1.0e+008 *

  -5.0478   0   0   0   0   0   0   0   0   0
  -3.6158   0   0   0   0   0   0   0   0   0
  -1.1692   0   0   0   0   0   0   0   0   0

$$\vdots$$

F_i =
 1.0e+008 *
      0   -0.4389   -0.5104   -0.5819   -0.4487   -0.5202   -0.5917   -0.5300   -0.6015   -0.5440
      0   0.9748   1.1241   1.2733   1.0541   1.2034   1.3526   1.2218   1.3711   1.2716
      0   1.6718   1.9442   2.2166   1.7093   1.9817   2.2541   2.0192   2.2916   2.1476

EF_i =
 1.0e+008 *
      0   0.7359   0.8526   0.9693   0.7716   0.8883   1.0050   0.9036   1.0204   0.9584

MaxState =
          9

TimeStep =
          1

F_i =
 1.0e+009 *
   3.8680   1.1725   0.7652   0.3580   0.9202   0.5130   0.1058   0.2689   -0.1383   -0.3589
   3.8780   1.2943   0.9058   0.5173   1.0417   0.6531   0.2646   0.4037   0.0152   -0.2258
   2.8703   1.0448   0.7682   0.4915   0.8793   0.6026   0.3260   0.4326   0.1559   -0.0117

EF_i =
 1.0e+009 *
   3.5388   1.1705   0.8131   0.4556   0.9470   0.5896   0.2321   0.3684   0.0109   -0.1988

MaxState =
          1

++++++++++++++++++++++++++++++++++

TimeStep =
          0

fdsi_s =
   1   2   3   4   5   6   7   8   9   10

ND_s =
         10

Expected_System_Value =
 1.0e+009 *
   3.2667   0.4805   0.0631   -0.3544   0.1992   -0.2182   -0.6357   -0.4974   -0.9149   -1.1835

value =
        3.27E+09

Next_Optimal_State =
   0   0

Next_Optimal_Decision =

    0   0